

12-2016

## ORGAN SPECIFIC VASCULAR RESPONSE TO FIBROSIS AFFECTS BREAST CANCER METASTATIC ORGANOTROPISM

Eliot S. Fletcher

Eliot S. Fletcher

Follow this and additional works at: [https://digitalcommons.library.tmc.edu/utgsbs\\_dissertations](https://digitalcommons.library.tmc.edu/utgsbs_dissertations)

 Part of the [Medicine and Health Sciences Commons](#)

### Recommended Citation

Fletcher, Eliot S. and Fletcher, Eliot S., "ORGAN SPECIFIC VASCULAR RESPONSE TO FIBROSIS AFFECTS BREAST CANCER METASTATIC ORGANOTROPISM" (2016). *The University of Texas MD Anderson Cancer Center UTHealth Graduate School of Biomedical Sciences Dissertations and Theses (Open Access)*. 723. [https://digitalcommons.library.tmc.edu/utgsbs\\_dissertations/723](https://digitalcommons.library.tmc.edu/utgsbs_dissertations/723)

This Dissertation (PhD) is brought to you for free and open access by the The University of Texas MD Anderson Cancer Center UTHealth Graduate School of Biomedical Sciences at DigitalCommons@TMC. It has been accepted for inclusion in The University of Texas MD Anderson Cancer Center UTHealth Graduate School of Biomedical Sciences Dissertations and Theses (Open Access) by an authorized administrator of DigitalCommons@TMC. For more information, please contact [digitalcommons@library.tmc.edu](mailto:digitalcommons@library.tmc.edu).

ORGAN SPECIFIC VASCULAR RESPONSE TO FIBROSIS  
AFFECTS BREAST CANCER METASTATIC ORGANOTROPISM

by

Eliot Sananikone Fletcher, MPH

APPROVED:

-----  
Raghu Kalluri, MD. Ph.D.  
Advisory Professor

-----  
Valerie LeBleu, Ph.D.

-----  
Laura Berretta, Ph.D.

-----  
Jonathan Kurie, Ph.D.

-----  
Menasche Bar-Eli, Ph.D.

APPROVED:

-----  
Dean, The University of Texas  
Graduate School of Biomedical Sciences at Houston

ORGAN SPECIFIC VASCULAR RESPONSE TO FIBROSIS  
AFFECTS BREAST CANCER METASTATIC ORGANOTROPISM

A

THESIS

Presented to the Faculty of  
The University of Texas  
Health Science Center at Houston  
and  
The University of Texas  
MD Anderson Cancer Center  
Graduate School of Biomedical Sciences  
in Partial Fulfillment

of the Requirements

for the Degree of

DOCTOR OF PHILOSOPHY

By

Eliot Sananikone Fletcher, BA, MPH  
Houston, Texas

Date of Graduation (December, 2016)

## Dedication

First and foremost, this thesis work is dedicated to my wife Michelle, without whom I would not have been able to complete this research. Her support and push has helped me overcome my struggles throughout my PhD and her encouragement and passion for medicine has driven my fervor for my research. Discussing her clinical observations in neurological disorders and my research with her late into the night has helped me piece together varying findings into the thesis before you. This would not have been possible without her.

I also dedicate this to my family who has supported me through the process. My father, a professor of Archaeology, continually telling me this is a hard process, but to never quit and keep slogging forward. My mother, whose success in the financial industry through drive, attention to detail, and hard work always asking me the right questions to keep me thinking about progressing forward. Also to my stepfather and stepmother, who have also pushed me to ever better myself.

Finally, I dedicate this to the men and women of the Armed Forces. Serving alongside them has been one of the greatest honors of my life. Their motivation and perseverance through situations, which most people cannot comprehend, is a constant driving force in my life. Even after being awake for days performing triage work, they still had the motivation to help me study for medical classes in a tent with no air-conditioning and poor water conditions. To my NCOIC, who has defied all the odds, survived hell, and taught me about leadership.

## Acknowledgements

Throughout my PhD work Dr. Raghu Kalluri has always had my back and I have never doubted it. From the first time we had a beer together, to the day he said it was time to write my thesis, I have always known that he knew what I was working on, how it was progressing, and what more I needed to do. Despite his persisted joking that he had nothing but free time, it was always clear that he was working hard to improve the student bodies research and professional experience, the lab, his students and post docs. It was never in question that he had his ear to the ground when it came to his students and his lab. As a student, this belief in your commander and mentor is invaluable. Especially given that he had an ability to know how to balance mentorship and autonomy. While unable to initially see his goal, much like an irate teen, it has become clear to me closer to the end that by allowing me to develop with significant autonomy he has helped me develop my passions and drive from within. To be my own scientist. But he would ensure to step-in when it was clear that I was stuck, or had found myself in a rut. His mentorship has provided me more than just a scientific guidance, it has also taught me how I need to go about succeeding in life goals. To achieve greatness.

If Dr. Kalluri has been my commander, then Dr. Valerie LeBleu would be the best drill instructor that I have ever had. I have learnt an invaluable amount of from Dr. LeBleu, from a balance of speed and attention to detail, surgical techniques, and scientific methods. Most importantly, I have learned from Dr. LeBleu two key things, the first being that there is a work ethic that is required in science that goes above and beyond just doing the job. Her dedication to this field is beyond anything I have ever seen and I endeavor to be half as hard working as she is. The second is her absolute love for the sciences. Her drive and passion for science are seemingly unparalleled. There is a look that Dr. LeBleu gets when

you are talking a new hypothesis with her, the kind of excitement that is usually reserved for someone who just tried ice cream for the first time. Easily some of the most enjoyable times I have had in the lab have been performing surgery or developing new hypothesis with Dr. LeBleu.

My advisory committee has been a constant source of information and support for me. Dr. Menasche Bar-Eli has taken time to talk with me after journal clubs and committee meetings to provide me with feedback on ways to improve. He has supported me at the academic level when I was struggling with classes and has always been in my corner. Dr. Jonathan Kurie has persistently asked me questions relating to the clinical relevance of my work, to keep me grounded in the reality of why we do basic science. Given his research and knowledge in metastatic research his guidance has been a huge support for my progression. Dr. Laura Beretta has also been a fundamental part of my progression as a scientist. Her questions and recommendations during committee meetings have allowed me to formulate new developments in my research and ultimately reach the goal of where I am today.

Finally, the students and post docs of the Kalluri and LeBleu lab have been my family for the past few years. Dr. Jiha Kim has on many occasions discussed with me vascular research and is in large part a reason I want to keep studying vascular biology. Dr. Julienne Carstens, Dr. Pedro Correa de Sampaio, Dr. Sara Lovisa all have helped me become a better scientist through discussion on histology, the kidney, and my research. They have all helped me up when I've fallen. I cannot thank any of them enough.

ORGAN SPECIFIC VASCULAR RESPONSE TO ANGIOPOIETIN 2 AFFECTS  
BREAST CANCER METASTATIC ORGANOTROPISM

Eliot Sananikone Fletcher, MPH, Ph.D.\*

Advisory Professor: Raghu Kalluri, MD, Ph.D.

The solid tumor microenvironment, pre-metastatic niche, and fibrotic environment are known to have significant biochemical and biomechanical similarities to the fibrotic environment. All have significantly increased levels of factors such as TGF $\beta$ , HIF1 $\alpha$ , TNF $\alpha$ , PDGF, VEGF, FGF, interleukins and other growth factors that are known to be pro-tumorigenic. Clinical and basic science research has shown that fibrosis presents an environment that favors tumor growth, such as hepatocellular carcinoma being commonly preceded by liver cirrhosis, or bleomycin induced lung fibrosis enhancing pulmonary metastasis in mouse models of breast cancer. In addition to the evidence indicating that fibrosis enhances primary tumor growth and metastasis it is also well characterized that primary tumor metastasis has specific organotropism, for example breast cancer commonly spreads to the lungs, brain, bone, liver and lymph nodes. However, whether non-organotropic fibrosis can redirect metastasis to the damaged organ has not been investigated.

To elucidate the fibrotic effect on tumor organotropism we induced fibrosis in the organotropic lungs and in the non-organotropic kidney of two mouse models of breast cancer, the 4T1 murine cancer cell line model and the genetic MMTV-PyMt model, both of which are known to metastasize. Using histopathology,

microarrays, gene expression by polymerase chain reaction, ELISA, chemokine array, and in vitro experiments we demonstrate that despite the pro-tumorigenic environment, kidney fibrosis does not redirect metastasis to the non-organotropic damaged organ. However, mice with kidney fibrosis had increased metastasis to their lungs. Furthermore, we found that kidney fibrosis increases the circulating levels of the pro-angiogenic factor Angiopoietin 2 that increased vascular permeability of the lungs, but not the kidneys. In fact, while fibrotic lungs showed decreased expression of endothelial tight gap junction protein Claudin-5, the fibrotic kidneys had an elevated expression of Claudin-5.

Our findings suggest that despite the similarities between fibrosis, the tumor microenvironment and the pre-metastatic niche, that while it can enhance tropic metastatic disease, it cannot redirect organotropism indicating that other factors must be involved in directing organotropism. Here we report that tumor organotropism may be a result of organ specific vascular responses to excess circulating factors and increased fibrotic factors. These findings indicate that organotropism is directly related to and as a result of organ specific vascular alterations.



## Table of Contents

Dedication_____	iii
Acknowledgements_____	iv
Abstract_____	vi
Chapter 1 Background and Significance_____	1
Metastatic Disease_____	2
Organotropism_____	6
Mouse Models for Metastasis and Organotropism_____	11
Vascular System_____	13
Angiogenesis and Angiopoietins_____	24
Tight Junctions_____	29
Wound Healing, Cancer and Fibrosis_____	33
Chapter 2 Material and Methods_____	39
Results_____	51
Chapter 3: Kidney and lung fibrosis express similar pro-tumorigenic factors_____	52
Histopathological characterization of cutaneous wound, lung fibrosis and kidney fibrosis shows increased collagen deposition and $\alpha$ SMA+_____	54
Fibrotic environments show sustained increased chronic expression of pro-tumorigenic factors_____	56
Chapter 4: The effect of organotropic and non-organotropic fibrosis on breast cancer metastasis_____	59
The effect of cutaneous skin wound on breast cancer metastasis_____	59
The effects of lung fibrosis on breast cancer metastasis_____	62
The effects of kidney fibrosis on breast cancer metastasis_____	64

Chapter 5: Kidney fibrosis increases the circulating levels of cytokines known to affect vasculature_____	68
Chronically elevated circulating cytokines during kidney fibrosis_____	68
Chapter 6: Circulating Angiopoietin -2 alters vasculature in organ specific manner___	75
Differential Vascular permeability responses in the lungs and kidneys of mice treated with Angiopoietin 2_____	76
Lung and kidney endothelial response to Angiopoietin 2 treatment in vitro_____	81
Organ specific tight junction response to Angiopoietin 2 treatment_____	84
Chapter 7: Anti-Angiopoietin 2 rescues the metastatic enhancement effects of kidney fibrosis_____	88
Summary of Results _____	91
Chapter 8: Summary and Discussion_____	92
The Unusual Suspects; Organotropism is not determined by previously published factors complicit in the pre-metastatic niche_____	93
The seed grows where you want, you just have to put it there_____	94
It is all tight junctions all the time_____	98
Multiple factors affecting organotropism_____	100
References_____	101

## List of Figures

Figure 1: Schematic of the metastatic cascade_____	5
Figure 2: National Cancer Institute's list of organotropic sites_____	6
Figure 3: Schematic representation of A) continuous B) fenestrated and C) sinusoidal capillaries_____	15
Figure 4: The structural and molecular connections between pericytes and Endothelial cells_____	17
Figure 5: Pericyte markers in murine research_____	18
Figure 6: Vasculature and blood of the kidney_____	22
Figure 7: Vasculature of the Lung_____	23
Figure 8: The three methods of angiogenetic growth_____	25
Figure 9: Factors affecting angiogenesis as determined from in vitro studies_____	26
Figure 10: Representation of Tie 2 receptor and Angiopoietin structure_____	28
Figure 11: Electron Microscope Image of endothelial cells tight junction_____	29
Figure 12: Representation of transmembrane proteins interactions and binding to proteins of the Tight Junction complex _____	30
Figure 13: Representation of the location of the Claudin tight junction proteins along the kidney nephron_____	31
Figure 14: Diagrammatic comparison between the wound healing process and the process of tumor growth and invasion_____	35
Figure 15: Table showing the cytokines implicated in both wound healing and in the cancer growth and development_____	36
Figure 16: Histology of fibrosis in skin, lung and kidney_____	55
Figure 17: Increase in expression of genes associated with pre-metastatic_____	57
Figure 18: Fold Change expression for genes associated with the pre-metastatic niche_____	58
Figure 19: Metastatic Analysis in Cutaneous Wound_____	60,61
Figure 20: Metastatic Analysis in Fibrosis Lung_____	62,63
Figure 21: Metastatic Analysis in Fibrosis Kidney_____	65,66

Figure 22: Metastasis did not spread to the kidneys despite the fibrotic environment_____	67
Figure 23: Heat Map of genes differentially expressed in healthy kidneys versus fibrotic kidneys_____	69
Figure 24: Gene Ontogeny and KEGG analysis from DAVID_____	70
Figure 25: Vascular Adhesion Related Genes and Cytokine array in multiple models of fibrosis_____	72
Figure 26: Quantitative Analysis of Serum Cytokine Array_____	73,74
Figure 27: Increased serum and fibrotic kidney expression of Angiopoietin 2_____	75
Figure 28: Increased dextran leakage in lungs of mice treated with Angiopoietin 2_____	77
Figure 29: No dextran leakage in kidneys of mice treated with Angiopoietin 2_____	78,79
Figure 30: Increased edema and lung damage in lung fibrosis and lungs of mice with kidney fibrosis and Angiopoietin 2_____	80
Figure 31: ZO-1 delocalized in lung endothelial cells, but not renal endothelial cells when treated with Angiopoietin 2 in vitro_____	83
Figure 32: Lung and kidney fibrosis show different expression of tight junction proteins_____	87
Figure 33: Recombinant Angiopoietin 2 and Anti-Angiopoietin 2 Antibody _____ in Tumor Bearing mice	89

Chapter 1  
Background and Significance

## **Metastatic disease**

Metastatic disease is the leading cause of mortality in patients diagnosed with cancer (Patrick Mehlen and Alain Puisieux 2006, Li and King 2012). It is estimated that metastatic disease is responsible for 90% of human cancer deaths (Li and King 2012). In 2016 1,685,210 people were diagnosed with cancer in the United States alone, 595,690 died from that diagnosis (National Institute of Health). Therefore 536,121 people died due to metastatic disease in the United States in 2016. Globally, 7.38 million people died from metastatic disease in 2012 (World Health Organization). Although metastatic disease occurs in almost all cancer types including the hematological cancers, breast cancer metastasis is one of the more readily researched and characterized pathologies. According to the National Cancer Institute there are 246,660 new cases of female and male breast cancer a year and 40,450 deaths (National Institute of Health). With modern preventative measures such as early mammography it is possible to detect primary breast tumors before they become malignant. Early detection measures with breast cancer allow for the surgical removal of breast cancer tissue either by resection or in more advanced cases mastectomy. While resection and mastectomy have scarification outcomes, these can be fixed by plastic surgery and loss of breast tissue does not place life threatening burden on the patient. However, if breast cancer cells metastasize to organs required for the sustainment of the organism this can impose a life threatening diagnosis, meaning that 100% of breast cancer deaths are due to metastasis. Thus the early detection of breast cancer since the late 1990s has significantly reduced the numbers of breast cancer related mortalities. However, metastasis from breast cancer and other cancer diagnosis remains the primary cause of cancer patient mortality (Bleyer and Welch 2013).

The process of metastasis follows a defined route based around fundamental anatomy and the location of the primary tumor (**Figure 1**) (Fidler 2003). Based on Kundson's Two hit hypothesis (Knudson 2000), two genetic mutations are required to occur in a cell that prompts the uncontrolled proliferation of that cell. The loss of a tumor suppressor and the gain of an oncogene are deemed sufficient to begin neoplastic formation. Initial formation of hyperplastic tissue begins the process of further genomic mutation which in turn begets even more genetic mutations (genomic instability), leading to dysplasia and cancer *in situ* (Gordon 2010). The increase in mutations acts as a Darwinian survival mechanism allowing the strongest tumor cells to survive and uncontrollably propagate (Pepper and Maley 2009). Most commonly this occurs in epithelial tissue which is separated from the surrounding stroma and vasculature by a basement membrane. Approximately 80-90% of tumors are epithelial in origin, the hematologic cancers make up 8%, and cancer of the connective tissue is around 1-2% of cancer diagnosis (National Cancer Institute). All three types of cancer are known to undergo metastasis. As the tumor continues to progress it can begin to invade through the basement membrane by secreting matrix metalloproteinases that can degrade extracellular matrix proteins (Peinado and Lyden 2011). Once the basement membrane has been breached cells from the primary tumor may cross the endothelial cell wall into the circulation via paracellular transendothelial migration, also known as intravasation (Junqueira and Avraham 2011).

In addition to degrading basement membrane via the secretion of matrix metalloproteinases, tumors also secrete significant angiogenic factors such as vascular endothelial growth factor (VEGF), angiopoietins, transforming growth factor  $\beta$  (TGF $\beta$ ), tumor necrosis factor  $\alpha$  (TNF $\alpha$ ), epidermal growth factor (EGF) and many others (Nishida and Kojiro 2006). This continued secretion of proangiogenic factors induces the growth of new

vasculature within and around the tumor. However, unlike healthy organ vasculature, tumor vasculature is dysregulated and malformed often leading to leaky vessels, poor perfusion, and diminished immune cell trafficking (Siemann 2011, Keskin and Kalluri 2013). Tumor vascular dysregulation increases the hypoxic environment of the tumor and perpetuates the survival of tumor cells that will be more likely to survive in austere conditions such as the circulatory system. It also presents a route for tumor cells to more easily enter the circulation and travel to distant organ sites (Siemann 2011).

Once tumor cells enter the circulation they are known as circulating tumor cells. Within the circulation these cells have to survive stresses that epithelial cells are not typically exposed to such as high shear stress from blood flow (Joosse and Pantel 2014). The malignant epithelial cells have to undergo a number of changes prior to entering the circulation that increases their capacity to survive. For example, healthy epithelial cells require attachments to adjacent cells via tight gap junctions, adherent junctions and/or desmosomes. The loss of these connections can result in apoptosis or autophagy due to anoikis (Gilmore 2005). Most cells within the body require cell-cell attachments to maintain survival signals with the exception of hematological cells such as red blood cells and immune cells. However, tumorigenic cells have typically undergone a process known as epithelial-to-mesenchymal transition that allows them survive in the absence of cell contact (Frisch and Cieply 2013).

If the tumor cell is able to survive the circulatory stresses it must then adhere to the luminal side of the endothelial cells, and again transport across the endothelial barrier by paracellular transendothelial migration in a process called extravasation (Li and King 2012, Boelte and Ling 2010). If a circulating tumor cell is able to extravasate into the parenchymal space of an organ that disseminated cancer cell may either lay dormant or begin



proliferating into a metastasis. Whether dormant or proliferative, disseminated cancer cells must undergo a mesenchymal-to-epithelial transition (the reverse of EMT) and anchor themselves to the organ in which they have extravasated (Gunasinghe and Hugo 2012). Under the correct circumstances, growth factors etc. these cells may develop into life threatening metastatic disease. Given the multi-step process of the metastatic cascade it is a highly inefficient process with less than 0.01% of circulating tumor cells shed from the primary tumor ultimately able of developing a distant organ metastasis (Fidler 1970, Fidler 2003).

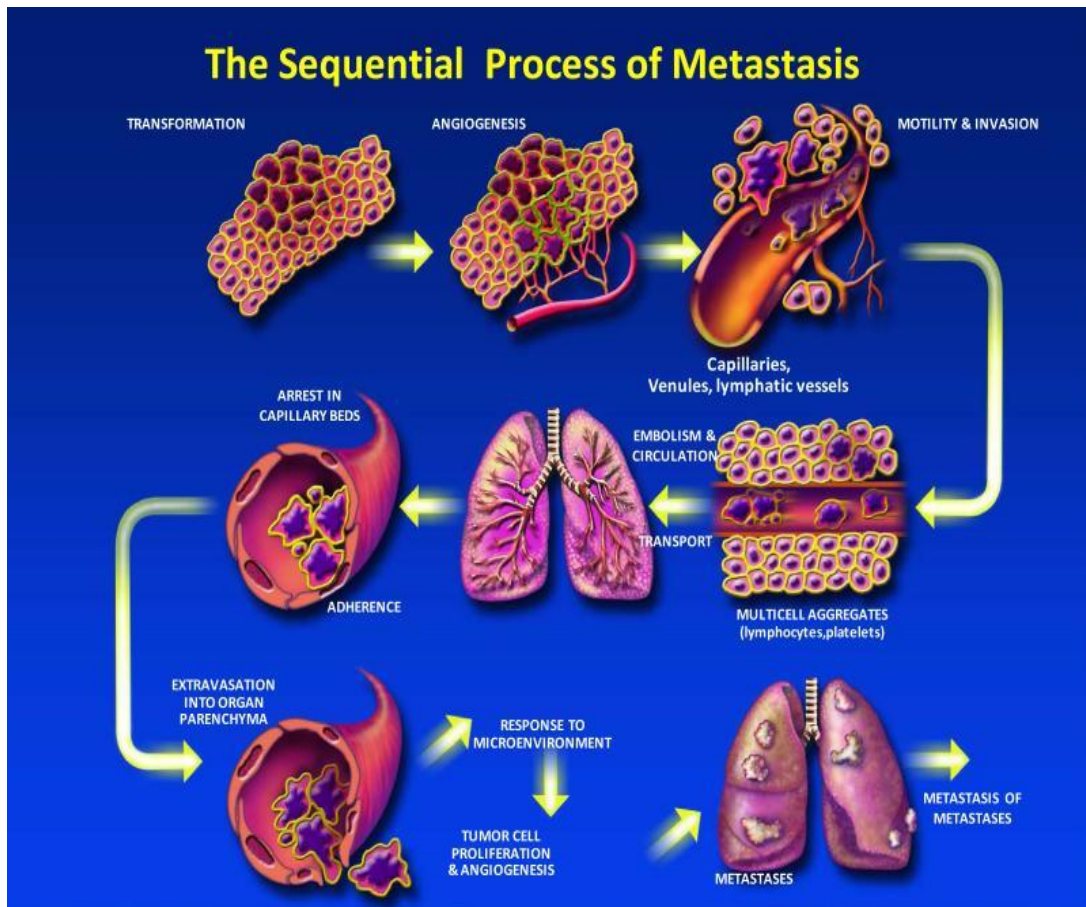


Figure 1: Schematic of the Metastatic Cascade. The process of metastasis consists of multiple stages each considered rate limiting. (Arshad, F., L. Wang, C. Sy, S. Avraham and H. K. Avraham (2010). "Blood-brain barrier integrity and breast cancer metastasis to the brain." *Patholog Res Int* **2011**: 920509). This is an open access article distributed under the Creative Commons Attribution License, which permits unrestricted use, distribution, and reproduction in any medium, provided the original work is properly cited.

## Organotropism

Metastatic organotropism is the propensity for tumors of a specific origin to spread to specific organs (National Cancer Institute). Based on basic science research, clinical reports, and pathology reports the National Cancer Institute reports the following likely metastatic organotropic organs for their primary cancer type (National Cancer Institute):

Cancer type	Main sites of metastasis*
<u>Bladder</u>	Bone, liver, lung
<u>Breast</u>	Bone, brain, liver, lung
<u>Colorectal</u>	Liver, lung, <u>peritoneum</u>
<u>Kidney</u>	<u>Adrenal gland</u> , bone, brain, liver, lung
<u>Lung</u>	Adrenal gland, bone, brain, liver, other lung
<u>Melanoma</u>	Bone, brain, liver, lung, skin/muscle
<u>Ovary</u>	Liver, lung, peritoneum
<u>Pancreas</u>	Liver, lung, peritoneum
<u>Prostate</u>	Adrenal gland, bone, liver, lung
<u>Stomach</u>	Liver, lung, peritoneum
<u>Thyroid</u>	Bone, liver, lung
<u>Uterus</u>	Bone, liver, lung, peritoneum, vagina

Figure 2: National Cancer Institute's list of sites that cancer most commonly spread to from the primary tumor. (National Cancer Institute. About Cancer. (n.d.). Retrieved August 07, 2016, from <http://www.cancer.gov/about-cancer>)

In 1889 Dr. Steven Paget proposed that certain primary tumors had specific metastatic tropism for specific organs, dubbed the seed-and-soil hypothesis. Paget stated that tumors of specific origin release circulating tumor cells, the seeds, which can only grow in a certain organ, the soil, based on the homeostatic factors found there. By performing autopsies on patients he observed a non-random spread from primary tumors to specific organs and deduced that this specific tumor organotropism was due to his seed-and-soil hypothesis (Paget 1889).

In the early 1900s a pathologist named Dr. Irving Zeidman found that circulating tumor cells of specific tumor types had different morphological appearance and that certain morphologies permitted the crossing of the endothelial capillary barrier leading to metastatic growth (Ewing 1928). The observation that differing tumors release circulating tumor cells with different morphologies led to the seed-and-soil hypothesis in that certain morphologies would be more likely to form emboli and more easily cross the endothelial barrier and extravasate. These were not homogenous populations of circulating tumor cells however and some cells did not appear to have the morphological attributes that would allow them to cross the endothelial barrier (Ewing 1928). This observation was one of the first examples of tumor heterogeneity and would be followed up with significant research over the next hundred years showing that tumors are not clonal populations deriving from a single dysplastic cell.

Tumor heterogeneity is defined by the fact that tumors do not generally consist of clonal cells derived from a parent cell with X number of mutations, but rather a number of different neoplastic cells with varying mutations conferring differing Darwinian survival advantages (Marusyk and Polyak 2010). Based on the different pressures placed on the cancer cells in the primary tumor such as hypoxia, excess lactic acid content, changes in pH, different mutations will confer survival advantages that if left untreated will eventually form into the ability to metastasize (Pepper and Maley 2009). Within a tumor different areas are subject to different pressures, and within each organ these pressures are different, and within an individual patient these pressures are further diverse. This multi-level difference in selective pressures results in cancer in each patient being different from that of another patient, even with a similar diagnosis. In large part this is the basis for today's research into more focused genetic therapies to target driver mutations. The heterogeneity of tumors

further indicates that the cells that are able to metastasize are also heterogeneous in nature, meaning that not all cells that metastasize are clonal either (Nowell 1976). However, research has shown that despite heterogeneous emboli in the circulation the metastatic tumors of melanoma were in fact clonally derived from a single parent cell (Talmadge 1982). This is additional evidence that only certain cells derived from the primary tumor have the ability to survive and proliferate after leaving the primary tumor. This tumor heterogeneity was further evidence that the cells able to enter the circulation had conferred survival mechanisms that allowed them to propagate in specific environments, and thus added weight to the seed-and-soil hypothesis. When all this evidence is amalgamated the seed-and-soil hypothesis can be simply stated as cancer that can “metastasize to locations that are biochemically and physiologically favorable for implantation and growth (Ramakrishna 2013).”

In 1980 Dr. Isiah Fidler published a seminal paper supporting the seed-and-soil hypothesis (Fidler 1982). After having worked with Dr. Irving Zeidman, Dr. Fidler performed experiments in which he injected B16-F10 cells intravenously, subcutaneously or intramuscular and observed their metastatic spread. The B16-F10 tumor cell line is a melanoma line that underwent serial transplantation to isolate a highly metastatic form of murine melanoma. Using both parabiosis and [125I]-5-iodo-2'-deoxyuridine cancer cell labelling experiments Dr. Fidler observed that despite circulating tumor cells being able to reach both the kidneys and the lungs, they would only form metastasis in the lungs (Fidler 1970). This led the authors to conclude that metastasis did indeed follow the seed-and-soil hypothesis given the presence of cancer cells in the kidney, but their inability to proliferate due to an unfavorable environment.

Prior to the seed-and-soil papers published in the mid-1900s, the predominant theory of metastasis was put forth by Dr. James Ewing. In the 1930s Dr. Ewing submitted an alternative hypothesis to seed-and-soil pertaining to metastatic disease in that cancer cells spread to specific organs due predominantly to the mechanistic nature of the vascular system (Ewing 1928). The vascular hypothesis asserted that once a cancer cell was able to enter the circulation it would pass through the arteries into arterioles and then capillaries and extravasate into parenchymal spaces. The organ that the cancer cell was able to extravasate to was immaterial of the primary tumor but due to the nature of vasculature and where the cancer cell happened to extravasate. The evidence for this was based primarily on research showing that metastatic cells predominantly formed emboli in the capillaries of metastatic organs, while similar emboli were found in the arterioles of organs that did not form metastasis (Ewing 1928). Ewing proposed that the circulatory framework and hemodynamics were responsible for the spread of cancer cells from their primary tumor. For example, breast cancer was likely to spread to the lungs because of its proximity to vena cava and the pulmonary arteries.

Recent studies using zebra fish models to visualize extravasation have also shown that vascular mechanics are essential for the process of metastasis. Two studies (Stoletov 2010, Kanada 2014), one by Stoletov et al. in 2010 and Kanada et al. in 2014 showed that when cancer cells were injected into zebrafish they could visualize the formation of emboli in the arterioles and capillaries. The researchers opted to use zebrafish due to the ease of visualization of their vasculature as compared to other animal models with non-opaque dermal layers. They also show that the endothelium played an active role in the crossing of the cancer cells across the vascular barrier and that when VEGF was depleted the cancer cells were unable to intravasate, but could still extravasate.

In addition to work in Zebrafish, significant gene research has focused on organotropism, predominantly in breast cancer mouse models. Dr. Joan Massagué compared the gene expression of human and mouse primary breast tumors in metastasis to the bone, lung and brain and identified a number of genes that are associated with organ specific metastasis. In their 2009 paper (Bos and Massagué 2009) they identified genes that were associated with increased metastatic spread to the brain. The brain possesses a particularly stable blood-brain barrier that is highly selective for permeabilization, none the less metastatic cells have developed a means by which to cross this barrier, while many chemotherapeutic drugs are unable to permeate the blood-brain barrier (Kreuter 2002). It is worth noting that a significant number of the genes found in these three different studies are overlapping, indicating that they may in fact not explain the organotropism of metastasis. The modern study of organotropism has focused primarily on researching the gene expression differences between different organs with metastatic disease and has not focused on the non-organotropic organs or vascular signatures.

Both Paget's and Ewing's hypothesis offer explanations for the organotropic properties of metastatic disease, and much like the nature versus nurture argument it is most likely that both contribute to the spread of the disease. Since Paget and Ewing significant research has been done on the vasculature indicating that there is in fact organ specific differences. Although less well studied, organ specific vasculature may in fact marry Paget's and Ewing's hypothesis as tumors of specific origin may affect organ specific vasculature differently. The result would be different responses in vascular dysregulation in varying organs and could contribute to the explanation for cancer tropism.

## Mouse Models for Metastasis and Organotropism

To continue the study of metastatic disease varying models have been designed to faithfully replicate human metastasis. To date the most accurate models of metastasis are found in mice that have transgenic induction of a tumor or are injected with a human or mouse metastatic cancer cell line. The majority of transgenic cancer models can accurately recreate primary tumor progression, but have been less successful at modelling metastasis showing significantly decreased penetrance than in the human counterparts (Francia 2011). Human derived cell lines necessitate injection into mice that are devoid of an active immune system (NOD/SCID mice) so as to ensure that the tumors are not rejected, and thus decreases the replication of the human model. This is especially important given recent research showing the involvement of the immune system in tumor progression. There are a number of mouse derived cancer cell lines that metastasize and this allows the orthotopic or intravenous injection of mice with fully functioning immune systems that are known to metastasize (Francia 2011). Although mice do differ from humans, the orthotopic injection of mouse derived cancer cell lines does recapitulate the human model and is often used today in the lab. Two such cell lines are the melanoma B16-F10 (Hart and Fidler 1980) and the mammary fat pad 4T1 (Aslakson 1992, Pulasaki 2001) cell line to model breast cancer. The B16-F10 cell was isolated by Dr. Fidler from a spontaneous melanoma that derived in Black-6 mice and was serially transplanted from metastasis to produce a highly metastatic line. The 4T1 cell line was similarly derived from a spontaneous tumor, this one formed in the mammary fat pad of a BALBc mouse and was selected from numerous cells in the primary tumor that showed high metastatic potential. There are also cell lines derived from this same tumor that show less metastatic potential such as the 67NR cell line highlighting the heterogeneous nature of tumors. As mentioned before Dr. Fidler utilized the B16-F10



cell line to determine the organotropism of melanoma to the bone, brain, liver, and lungs. Similarly, the 4T1 cell line when injected orthotopically has shown metastasis to the bone, brain, liver, lung as does breast cancer in human patients. Numerous publications have highlighted the spread of the B16-F10 and 4T1 tumor cell lines to their organotropic sites providing weight to Paget's seed-and-soil hypothesis.

More recent publications however have highlighted the capabilities of multiple mouse cancer cell lines including B16-F10 and 4T1 to grow in non-metastatic sites when injected directly or provided mechanistic support to reach non-organotropic site. A 2011 paper by Li et al used hydrodynamic injections of B16-F1, 4T1 and Renca renal carcinoma cells to force colonization of organotropic and non-organotropic organs. This procedure was typically used to study the intravenous injection of DNA or RNAi into mice to illicit a genetic phenotype. Hydrodynamic injections use high volume injections of anywhere between 8-10% of body weight to force an increase in pressure in the inferior vena cava which in turn creates high internal hematological pressure. The increase in hemodynamic pressure induces systemic endothelial leakage leading to increased extravasation and colonization of the lungs, liver and the non-organotropic kidneys with B16-F1 and 4T1 cells. Contrary to the findings of the seed-and-soil hypothesis this indicates that given the ability to enter the perivascular parenchyma tumors can grow regardless of their etiology. Further evidence for this was published in 2013 when Antonio et al. showed that 4T1 mammary fat pad cells could be injected directly into the cortex of the kidney and grow and even metastasize from the kidney to the lung. They further showed that by damaging the kidney with renal ischemia reperfusion experiments they could provide a hypoxic environment that benefited tumor metastasis and thus showed increased spread to the lungs. Furthermore, the human cancer cell line MDA-MB-231 has also been shown to be capable of growth in the kidneys if



it is injected in the renal capsule. In this model they were additionally able to show that the MDA-MB-231 cells could invade from the renal capsule into the cortex of the kidney (Liu 2007).

The evidence for both Paget's seed-and-soil and Ewing's vasculature hypothesis are numerous from both sides. Research has shown that tumors do indeed have a propensity to spread to and grow in specific organs, while additional research shows that by by-passing the endothelial barrier by forcing vascular leakage or direct injection to parenchyma allows for non-organotropic growth. Rather than a one or the other argument, much like nature versus nurture, both hypothesis are likely correct. However, rather than an effect on the parenchymal space as argued by the existence of the pre-metastatic niche, it is the effect that a primary tumor has on the organ specific vasculature that may determine metastatic organotropism.

### **Vascular System**

From the microbiological standpoint research into vascular biology has yielded interesting developments since its description as the cardiovascular system by Hippocrates. The endothelium is the inner most layer of the vascular tubing that makes up the circulatory system. This one cell layer thick barrier separates the luminal side of the hematopoietic system from the parenchymal space of organs, the abluminal perivascular side. While the luminal side is always exposed to the rapid flow of the circulatory system the abluminal side has profound differences depending on whether it is found in an artery, arteriole, metartiole, capillary, venules, or vein. The layers of the vasculature consist of three layers, the tunica intima (the innermost endothelial layer), the tunica media and the tunica adventia, the outermost layer which connects the vessels to the surrounding tissue (Grey 2005, Junqueira 2010).

Arteries: Branching out from the heart these arteries are large elastic arteries. These have an tunica intima similar to other aspects of the circulation. The tunica media consists of thick layer called the internal elastic lamina that can stretch under the high pressures found in the large arteries. The media of the arteries is the most distinguishing feature due to its thickness and layers of smooth muscle fibers. The adventia is thinner than the media, but contains immune cells, nerves and the vaso vorum (the vessel capillaries). These branch into the muscular arteries which begin the distribution of blood to the organs (Grey 2005, Junqueira 2010).

Arterioloes: The muscular arteries repeatedly begin branching off into smaller and smaller arterioles. Arterioles have a much smaller tunica media with only two smooth muscle layers as compared to the 40-50 layers in the arteries. In this layer there is almost no visible adventia layer. The arterioles denote the beginning of organ vasculature (Grey 2005, Junqueira 2010).

Capillaries: It is at the stage of the capillaries that the majority of nutrient and gas exchange occurs with the surrounding organ in capillary beds. Capillaries have a single endothelial layer forming the vascular tube, and being only one cell thick they allow only single cell luminal transport at a time. They no longer have a smooth muscle layer. While they are the smallest of the vessels they are almost the most numerous, making up 90% of the vasculature (**Figure 3**) (Grey 2005, Junqueira 2010).

It is important to note that capillaries differ significantly in number and type based on which organ they are found. Three different types of capillaries exist:

- 1) Continuous: These have no junctional spaces between endothelial cells and are marked by well-defined tight junctions. They are the most numerous type of

capillary and are found in muscle, lungs and exocrine glands. Their tight-junctions allow for the highly regulated transport of molecules across the vascular barrier (Grey 2005, Junqueira 2010).

- 2) **Fenestrated:** The second type of capillary has what is described as a sieve-like structure. These have many small openings along the endothelium allowing for the transport of larger more extensive molecules. One would expect to find these in organs that require rapid transport of multiple macro-molecules across the vascular barrier such as the bodies filter, the kidney, food absorption in the intestine and endocrine glands (Grey 2005, Junqueira 2010).
- 3) **Discontinuous:** Sinusoidal capillaries have large openings between endothelial cells allowing for maximum exchange of molecules across the vascular barrier. This discontinuous layer also allows for cells to cross the vascular barrier with more ease than other capillaries and can thus be found in the liver and spleen predominantly (Grey 2005, Junqueira 2010).

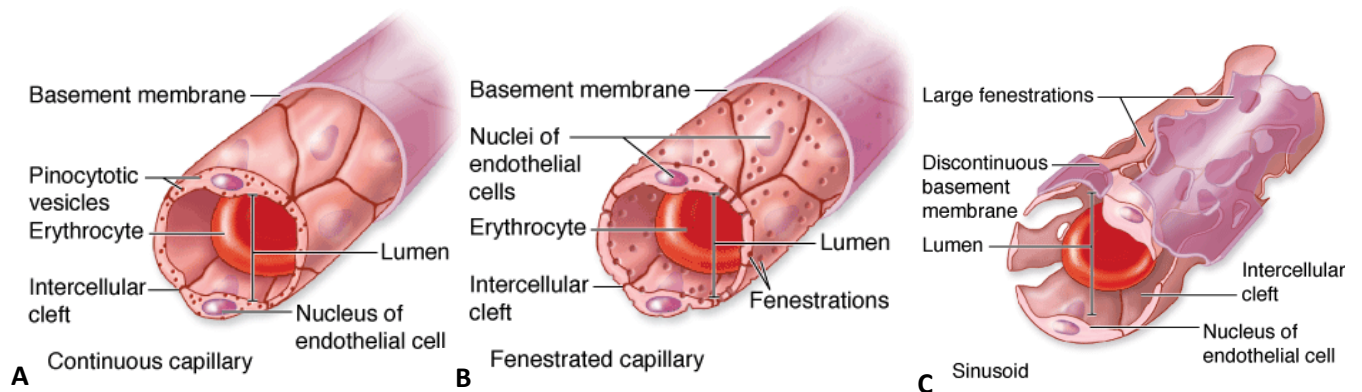


Figure 3: Schematic representation of A) continuous B) fenestrated and C) sinusoidal capillaries. (Junqueira, L. C. U. a., J. Carneiro and A. N. Contopoulos Basic histology. A Concise medical library for practitioner and student. Los Altos, Calif). Copyright Clearance 11611970.

Pericytes: In addition to differences in types of capillaries, there is also a marked variation in the coverage of pericytes in differing organ capillary vasculature.

Pericytes are a mesenchymal cell that wraps around the capillaries with foot processes (**Figure 4**). They have been implicated in vessel stability, involvement in contractile functions of the vasculature and have been shown to communicate directly with the endothelial cells to which they are attached (Armulik 2011).

Through electron microscopy, immunofluorescence and histology pericytes have been shown to wrap around endothelial cell capillaries at varying intervals depending on the organ observed. In the retina the ratio of pericyte to endothelial cell is close to 1:1, while in other tissues it may be closer to 10:1 and has yet to be characterized for all organs (Armulik 2011). Thus, to date there has been no extensive characterization of pericyte coverage comparison between each organ. By reviewing publications that have used healthy controls of either kidney or lungs stained with NG2, PDGFRb or Desmin it is evident that the kidney cortex pericyte coverage is less than that of the pericyte coverage in the lungs (Armulik 2011). Regardless, this is an insufficient methods of analysis and an in depth characterization of organ specific pericyte coverage is required.

Pericytes share a basement membrane with the endothelial cell on which they are found and connect to the endothelial cell via an adhesion plaque and peg-and-socket joints. The adhesion plaque consists primarily of fibronectin and structurally resembles adherence junctions. The peg-and-socket joint on the other hand has shown evidence of gap junctions (Armulik 2011). Particularly the Connexin 43 gap junction has been shown to allow for communication between endothelial cells and pericytes (Winkler 2011).

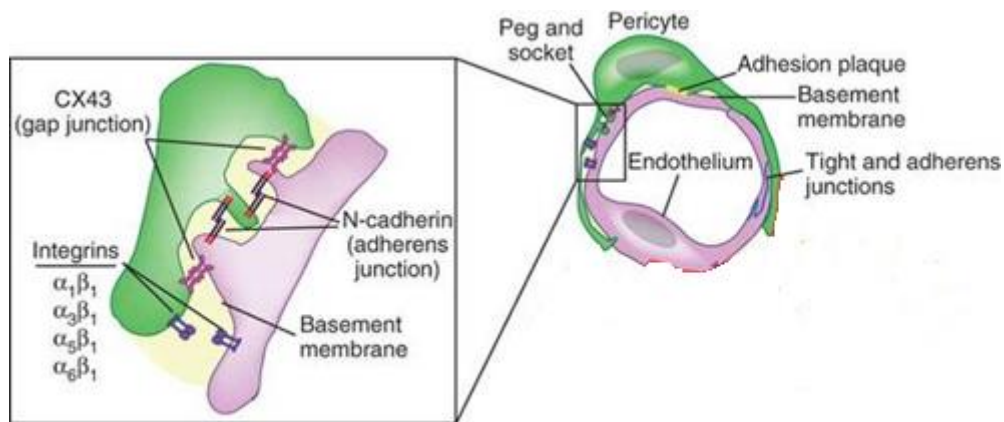


Figure 4: The Structural and Molecular Connections between Pericytes and Endothelial cells. (Winkler, E. A., R. D. Bell and B. V. Zlokovic (2011). "Central nervous system pericytes in health and disease." *Nat Neurosci* 14(11): 1398-1405). Pericytes connect to endothelial cells by Adhesion plaques and Peg-and-Socket joints. Right provided by Nature Publishing group.

While pericytes were first identified in 1873 by Dr. Charles-Marie Benjamin Rouget, research into their roles and function in normal physiology and pathology has been limited to a select few researchers (Armulik 2011). One key issue with pericyte research has revolved around a lack of unilateral agreement of identifying markers. Currently the markers that have been validated for pericytes are PDGFRb, NG2, CD13, aSMA, and desmin (**Figure 5**). PDGFRb and NG2 markers appear to be associated with pericyte recruitment to vasculature and thus would seem to represent a possibly more immature stage of pericyte (Armulik 2011). In contrast, Desmin, which is a contractile filament predominantly expressed in the heart and muscle is a marker for mature pericytes and lends to the generally accepted view that pericytes are involved in vascular constriction and relaxation. It is important to note that in addition to being positive for the following markers pericytes are also identified by their proximity to vessels. While this can be done using an electron microscope, co-immunofluorescent staining is necessary to show both pericyte markers and endothelial cells (Armulik 2011).

Pericyte Marker	Gene Symbol	Examples of Other Cell Types Expressing the Marker	Comments	References
<b>Validated Markers</b>				
PDGFR- $\beta$ (platelet-derived growth factor receptor-beta)	Pdgfrb	Interstitial mesenchymal cells during development; smooth muscle; in the CNS certain neurons and neuronal progenitors; myofibroblasts; mesenchymal stem cells	Receptor tyrosine kinase; functionally involved in pericyte recruitment during angiogenesis; useful marker for brain pericytes	Lindahl et al., 1997; Winkler et al., 2010
NG2 (chondroitin sulfate proteoglycan 4)	Cspg4	Developing cartilage, bone, muscle; early postnatal skin; adult skin stem cells; adipocytes; vSMCs; neuronal progenitors; oligodendrocyte progenitors	Integral membrane chondroitin sulfate proteoglycan; involved in pericyte recruitment to tumor vasculature	Ozerdem et al., 2001; Rüter et al., 1993; Huang et al., 2010
CD13 (alanyl (membrane) aminopeptidase)	Anpep	vSMCs, inflamed and tumor endothelium; myeloid cells; epithelial cells in the kidney, gut	Type II membrane zinc-dependent metalloprotease; useful marker for brain pericytes	Dermietzel and Krause, 1991; Kunz et al., 1994
$\alpha$ SMA (alpha-smooth muscle actin)	Acta2	Smooth muscle; myofibroblasts; myoepithelium	Structural protein; quiescent pericytes do not express $\alpha$ SMA (e.g., CNS); expression in pericytes is commonly upregulated in tumors and in inflammation	Nehls and Drenckhahn, 1993
Desmin	Des	Skeletal, cardiac, smooth muscle	Structural protein; useful pericyte marker outside skeletal muscle and heart	Nehls et al., 1992

Figure 5: Pericyte markers in murine research. PDGFRb, NG2, CD13,  $\alpha$ SMA, and Desmin have all been validated as murine markers of pericytes when associated with vasculature (Armulik, A., G. Genove and C. Betsholtz (2011). "Pericytes: developmental, physiological, and pathological perspectives, problems, and promises." *Dev Cell* 21(2): 193-215). Elsevier user license CC BY 4.0.

More recent research from Dr. Raghu Kalluri and Dr. Valerie LeBleu has highlighted the role of pericytes in pathological states. The 2015 paper by Keskin et al. showed the role of pericytes at different stages of tumor development by selectively ablating proliferating pericytes at either early or late stage of tumor development in a mouse model of breast cancer. In 2013 LeBleu et al. used genetically engineered mouse models to fate map the source of myofibroblasts in kidney fibrosis. She noted that the majority of myofibroblasts that contribute to excess collagen in fibrosis are derived from local fibroblasts that differentiate into myofibroblasts when exposed to certain cytokines. The remaining myofibroblasts were derived from the bone marrow, endothelial cells undergoing EndMT and epithelial cells undergoing EMT. However, they found that NG2 and PDGFb pericytes while increasing during kidney fibrosis did not contribute to the myofibroblast population within kidney fibrosis.

The role of pericytes in lung fibrosis has also been characterized using similar methodologies. In 2013 Hung et al. used Foxd1 tagged to Tomato red to show that this population overlapped with PDGFRb positive cells and was thus a pericyte population. Utilizing Bleomycin to induce lung fibrosis they showed that this population contributed significantly to the fibrotic environment. However, in 2013 Rock et al. used NG2 expressing GFP under the control of Tamoxifen inducible promoter to map the expression of pericytes during bleomycin induced lung fibrosis. While they noted an increase in NG2 and PDGFRb positive cells in lung fibrosis they did not see a costaining with aSMA, which would indicate the transition from pericyte to myofibroblast. These conflicting reports underline the issue of the need for agreement on pericyte identification.

Venules: After leaving the capillaries the circulation travels to the venules which also have pericyte coverage. In post-capillary venules it has been found that these are the primary sites that white blood cells diapedesis to parenchymal tissue during the inflammatory process. The observation that white blood cells diapedesis specifically at venules is of importance as it highlights the heterogeneity of endothelial cells. As the venules increase in size towards veins, they show an ever increasing tunica media with smooth muscle layers. A key characteristic of venules is they have a lumen that is far wider in diameter than the thickness of their wall (Grey 2005, Junqueira 2010).

Veins: Unlike arteries veins have a relatively low pressure and thus move blood flow back to the heart via the contraction of large smooth muscle around the vessel. This function leads to the structural characteristic that veins have a prominent intima, a small media and an adventia with large smooth muscle fibers for contraction (Grey 2005, Junqueira 2010).

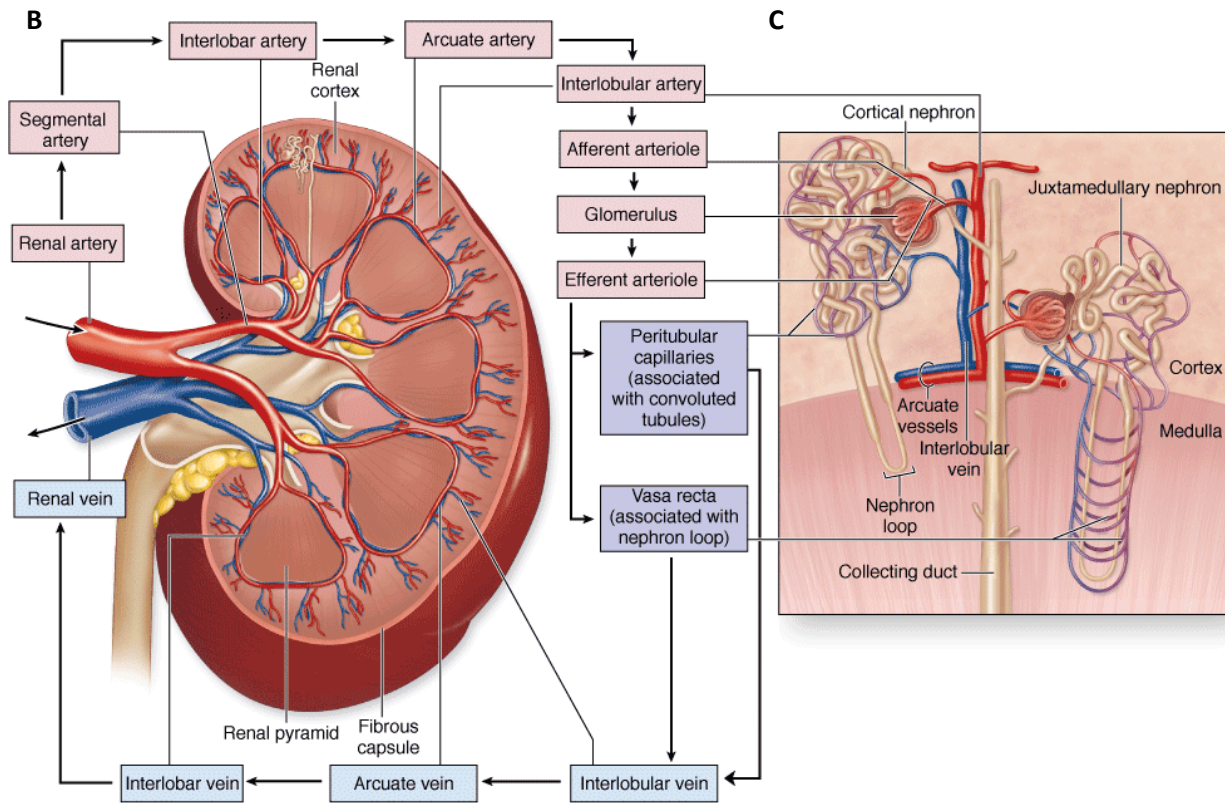
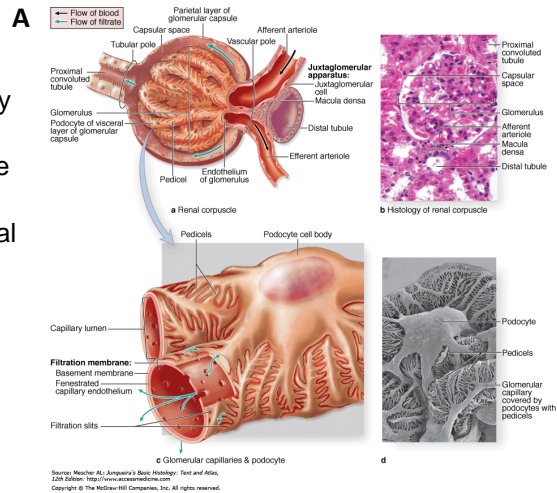
The description of the vascular system highlights that most circulating tumor cell extravasation occurs in capillaries responsible for organ oxygenation and nutrient supply. Of interesting note is that despite the different capillary types this does not seem to correlate with organotropism. For example, lungs have continuous endothelial capillaries whereas kidneys are known to have fenestrated capillary endothelium. Given the presence of the small holes and macromolecules crossing the endothelial border it would stand to reason that the kidney should be a site of metastatic spread. However, as is apparent from Figure 2, the kidney is not a common site of metastatic spread in any primary tumor.

In addition to the endothelium of the lungs being continuous and that of the kidneys being fenestrated both have unique vascular structure, but are highly vascularized. Blood flow to the kidney enters via the renal artery at the hilus, flows into the interlobar artery, the arcuate artery, the interlobular artery, then efferent arteriole of the glomerulus (**Figure 6A**) and into the capillary tuft that forms the glomerulus (**Figure 6B**). From here blood flows out of the glomerular tuft via the efferent arteriole and into either peritubular capillaries or the vasa recta capillaries depending on the cortical location of the glomerulus. The peritubular capillaries and vasa recta are the capillary structure of the kidney and ensure the cortex and medulla of the kidney are highly vascularized as this is where water,  $\text{Na}^{2+}$ ,  $\text{Cl}^-$  and other ions are reabsorbed (**Figure 6C**). Blood then leaves the kidneys via veins with the same names as the capillaries and arteries (Grey 2005, Junqueira 2010). The glomerular tuft is a unique structure in that the capillaries in this structure are covered by a specialized cell called a podocyte. Podocytes, similar to pericytes form foot processes around the capillaries. These foot processes interdigit and form a filtration slit diaphragm, therefore in addition to having to cross the endothelial layer, molecules and or cells also have to cross the filtration slit diaphragm in order to enter the parenchymal space of the kidney. Research



has shown that in some pathologies such as Alport syndrome red blood cells can cross the endothelial layer in the glomerular tuft and enter the filtrate. Of interest is recent research showing that under other pathological conditions the slit-diaphragm can in fact tighten with the increased expression of Claudin-1 between pedicel processes. This increased expression of Claudin-1 would generate tight junctions that are less permeable to molecules crossing the glomerular basement membrane barrier. However, upon leaving the efferent arteriole only a single layer of capillary endothelial cells separates the circulation from the parenchymal space in the peritubular arteries and the vasa recta. Finally, the hydrostatic and osmotic pressure within the kidney is highly unique due to its filtration function. As the glomerulus filters out ions but is not permeable to larger molecules such as Albumin there is an increase in protein concentration within the plasma circulating in the kidneys. This increases as water is absorbed by the proximal tubules and further ions are absorbed by the tubules further along the nephron. Thus typical pressures in the vasculature of the kidney are 20-30mmHg starting at the glomerulus and increasing as more ions are transported out and the protein to plasma concentration increases (Grey 2005, Junqueira 2010).

Figure 6: Vasculature and blood of the kidney. A) The Glomerular tuft consists of capillaries surrounded by podocytes that form the filtration slit diaphragm. B) Kidney blood flow route. C) The peritubular capillaries and vasa recta capillaries surround the kidney nephron for reuptake of solutes and water (Junqueira, L. C. U. a., J. Carneiro and A. N. Contopoulos Basic histology. A Concise medical library for practitioner and student. Los Altos, Calif). Copyright Clearance 11611970.



Source: Mescher AL: Junqueira's Basic Histology: Text and Atlas, 12th Edition: <http://www.accessmedicine.com> Copyright © The McGraw-Hill Companies, Inc. All rights reserved.

Relative to the kidney, the pressures in the lung are much lower ranging from 5-25mmHg (Grey 2005, Junqueira 2010). This allows the pulmonary vessels to be thin allotting to the function of the lungs of transport of Oxygen and Carbon Dioxide within the

alveolar ducts. The alveolar ducts are made up of alveoli that are capable of diffusing  $O_2$  and  $CO_2$  with blood in the surround capillary network (**Figure 7**). Blood leaves the left ventricle of the heart and enters the lungs through the pulmonary artery where it branches into capillaries that line the alveoli. Once reoxygenated the blood then returns to the heart via the pulmonary vein and is ultimately pumped to the systemic circulation by the aorta (Grey 2005, Junqueira 2010).

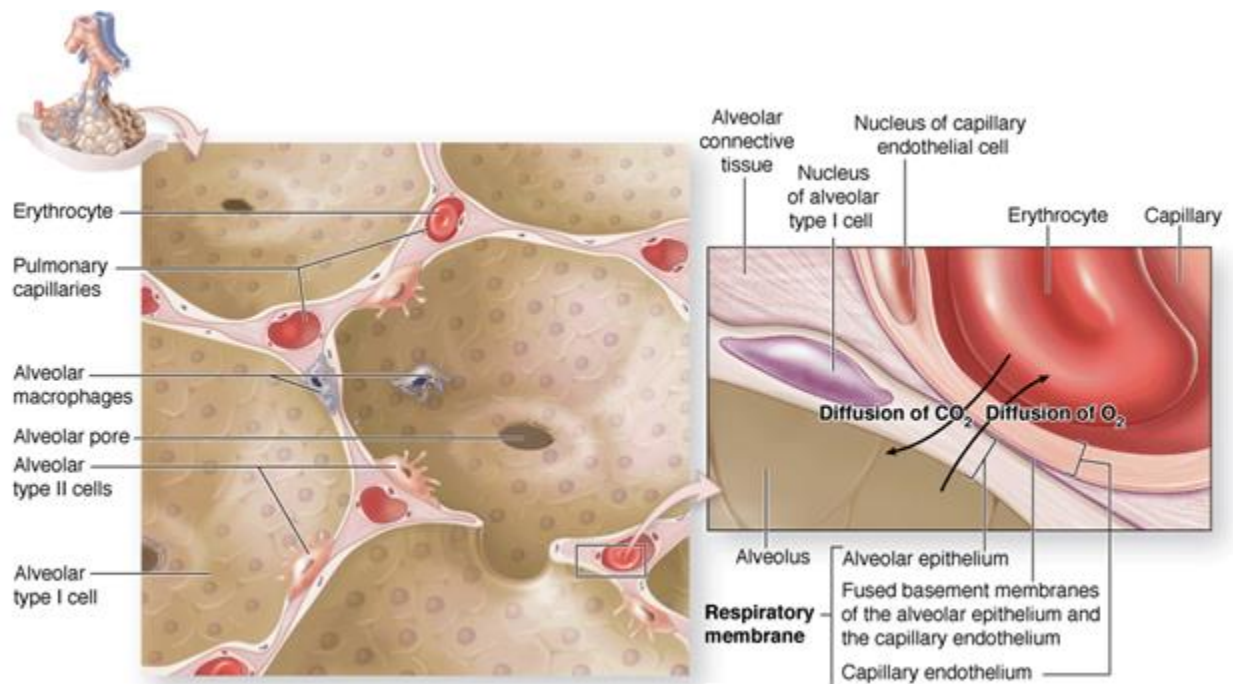


Figure 7: Vasculature of the Lung. Pulmonary capillaries allow for the diffusion of  $O_2$  and  $CO_2$ . Type I cells are primarily responsible for the gas diffusion. Type II cells are primarily responsible for the production of surfactant to lubricate the lungs and prevent larger macromolecules crossing into perivascular spaces. (Junqueira, L. C. U. a., J. Carneiro and A. N. Contopoulos Basic histology. A Concise medical library for practitioner and student. Los Altos, Calif). Copyright Clearance 11611970

## Angiogenesis and Angiopoietins

In 1779 surgeon Dr. John Hunter stated whenever “Nature has considerable operations going on, and those are rapid, then we find the vascular system in a proportionable degree enlarged (Eiseman 1984).” This observation was likely the first description of the changes that the vascular system undergoes in both normal healthy physiology beginning *in utero* and under many pathological conditions as well. The term angiogenesis was coined first during the description of the formation of the placenta (Hertig 1935). However, it was not until 1971 when Dr. Judah Folkman published his work describing the angiogenic process in tumor growth and cancer dependence on angiogenesis that the importance of the angiogenic process became evident in both normal and pathological conditions (Folkman 1971).

Vasculogenesis begins *in utero* and is the first aspect of embryo development beginning after gastrulation to ensure the formation of the cardiovascular system. This differs from angiogenesis in that it is the *de novo* formation of vessels from the mesoderm. It can also occur *post utero* with the development of new vessels from angioblasts. Angiogenesis on the other hand is the formation of blood vessels from existing vessels and can occur via two differing mechanisms (**Figure 8**) (Hunt 2002):

- 1) Sprouting Growth: Sprouting angiogenesis occurs with the formation of a tip cell from an existing capillary or vessel. This requires that surrounding basement membrane be proteolytically degraded, that endothelial cells migrate and proliferate, and ultimately that they are finally stabilized by mature pericytes. The tip cell begins the process by budding off from the parent vessel and moving towards the direction of a pro-angiogenic factor (such as VEGF). By utilizing filapodia tip cells are able to degrade surrounding basement membrane and

extracellular matrix to allow for the growth of vessels. Once the tip cell has reached another vessel they anastomize and become a connected capillary with a fully formed lumen. At this point pericytes will cover the endothelial cells and ensure stabilization.

- 2) Intussusceptive Growth: In contrast to Sprouting angiogenesis, this process involves the splitting of the vessels and lumen into two vessels. This was first observed in the lung and is believed to be a more rapid form of angiogenesis.

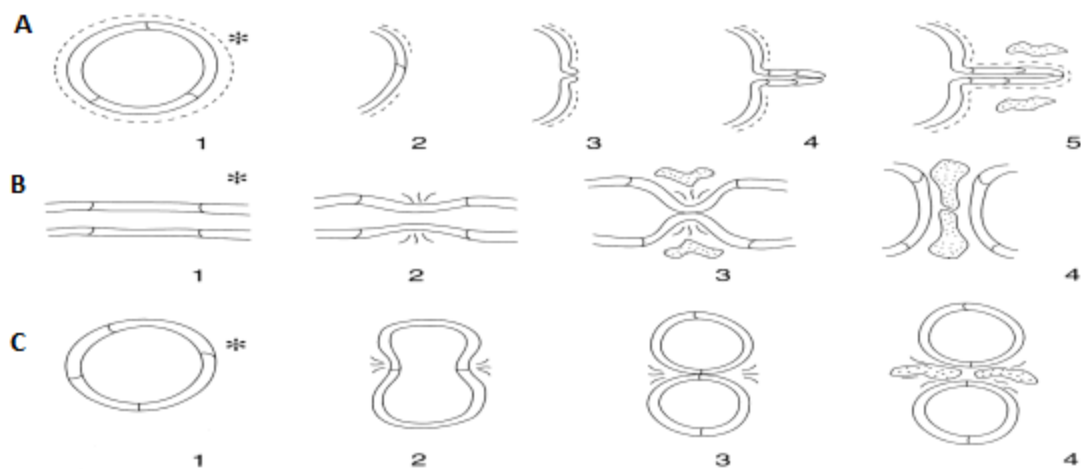


Figure 5.1 (a) Classical capillary growth. In response to an angiogenic stimulus (1), basement membrane disruption (2) occurs, allowing endothelial cell migration (3) followed by proliferation and tube formation (4) and finally reestablishment of the basement membrane and migration of pericytes (6). (b) Intussusceptive growth. The angiogenic stimulus (1) induces compression of two opposing endothelial cells towards each other, accompanied by interstitial cells and filaments (2), which meet (3) and ultimately separate as two separate daughter capillaries (4). (c) Longitudinal growth. As a capillary tube lengthens, a stimulus (1) induces bulging of the capillary wall into the lumen (2), which meet (3) and then cause division of the capillary in a longitudinal axis (4).

Figure 8: The three methods of angiogenic growth A) Classical capillary growth B) Intussusceptive growth C) Longitudinal growth (Hunter, J. (2007). "A treatise on the blood, inflammation, and gun-shot wounds. 1794." Clin Orthop Relat Res 458: 27-34).

Both forms of angiogenesis require either mechanical or growth factor stimulus to begin the process of vessel growth. Evidence suggests that angiogenesis is a balance process in that vessels are generally quiescent when there is a balance between pro-angiogenic factors and anti-angiogenic factors (Hunt 2002). Upon stimulation by either mechanical means or by growth factors the scales can be tipped in one direction to initiate



the angiogenic process. Mechanistically anything from cold, changes in blood flow pressure, and shear stress can initiate angiogenesis. The presence of hypoxia in tissues is a key initiator for angiogenesis (Hunt 2002). For example, exercise has been shown to initiate angiogenesis in the heart and muscles, while excess adipose tissue development has shown an increase in angiogenesis as well (Hunt 2002). While exercise is beneficial and excess adipose tissue growth is considered non-beneficial this highlights the role of angiogenesis in both normal and pathological processes. Angiogenesis is key in normal wound healing, but is implicated in tumor growth and many other pathologies.

In association with the mechanical stimulus there are also a number of growth factors that have been shown to be pro-angiogenic and anti-angiogenic (**Figure 9**). As previously mentioned hypoxia is well established to induce the angiogenic process, and this occurs when epithelial and stromal cells begin secreting pro-angiogenic factors in response to hypoxia so as to ensure vessel growth to increase vascularization of that hypoxic area (Hunt 2002).

Promoters of angiogenesis	Inhibitors of angiogenesis
Angiogenin	Angiostatin
EGF/TGF- $\alpha$	C-X-C chemokines:
FGFs-1, -2, -5	Platelet factor IV
G-CSF	IP-10, gro- $\beta$
HGF	Hyaluronan
Hyaluronan oligosaccharides	IL-12
Hypoxia	Interferons
IL-8	MMP and PA inhibitors
PDGF-BB	16 kDa prolactin fragment
PLGF	Proliferin-related protein
Proliferin	Steroids/metabolites:
Prostaglandins	Glucocorticoids
TGF- $\beta$	2-Methoxyestradiol
Tissue factor	Retinoids
TNF- $\alpha$	Ribonuclease inhibitor
VEGFs	TGF- $\beta$
	Thrombospondin
	TNF- $\alpha$

EGF, endothelial growth factor; TGF- $\alpha$ , transforming growth factor- $\alpha$ ; FGFs, fibroblast growth factors; G-CSF, granulocyte colony-stimulating factor; HGF, hepatocyte growth factor; IL-8, interleukin-8; MMP, matrix metalloproteinases; PA, plasminogen activator; PDGF-BB, platelet-derived growth factor BB; PLGF, placental growth factor; TNF- $\alpha$ , tumour necrosis factor- $\alpha$ ; VEGFs, vascular endothelial growth factors.

Figure 9: Factors affecting angiogenesis as determined from in vitro studies (Hunter, J. (2007). "A treatise on the blood, inflammation, and gunshot wounds. 1794." Clin Orthop Relat Res 458: 27-34).

VEGF is considered a key indispensable growth factor for angiogenesis, but nonetheless there are significant other factors that are involved in initiating and maintaining the angiogenic process (Hunt 2002). The angiopoietins are an interesting angiogenic growth factor as they come in multiple isoforms which work antagonistically to ensure a balance of pro and anti angiogenic factors.

The tyrosine kinase receptor Tie-2 has been shown to be expressed predominantly on endothelial cells and given that it has been shown through xray-crystallography studies that both Angiopoietin 1 and Angiopoietin 2 are highly specific ligands for Tie-2 extensive research has been focused on the effects of these angiopoietins on the vascular system (Barton 2006). Significant research has shown that these two ligands act antithetically on endothelial cells; Angiopoietin 1 stabilizes endothelial cell-cell interactions and limits vascular permeability, Angiopoietin 2 has the opposite effect and decreases the endothelial cell-cell interaction and leads to increased vascular leakage (Fagiani 2013). In combination with increased levels of VEGF, Angiopoietin 2 has been shown to promote the angiogenic process. While this may prove beneficial in normal healthy regulated physiology such as wounds, in the pathological circumstances when excess Angiopoietin 2 is created this can lead to systemic vascular leakage (Parikh 2006). In fact, excess expression of Angiopoietin 2 has been linked with poor prognosis for breast cancer patient metastatic disease (Keskin and Kalluri 2015).

The angiopoietins work by binding to Tie-2 on endothelial cells and causing intracellular downstream alterations that lead to either the stabilization or destabilization of tight and adherent junctions between cells (**Figure 10A, B**). Angiopoietin 2, on binding to Tie-2 increases the intracellular cytoplasmic levels of Rac to RhoA ratio, which in turn is

believed to destabilize both tight junction complexes and adherent junction complexes (Felcht 2012).

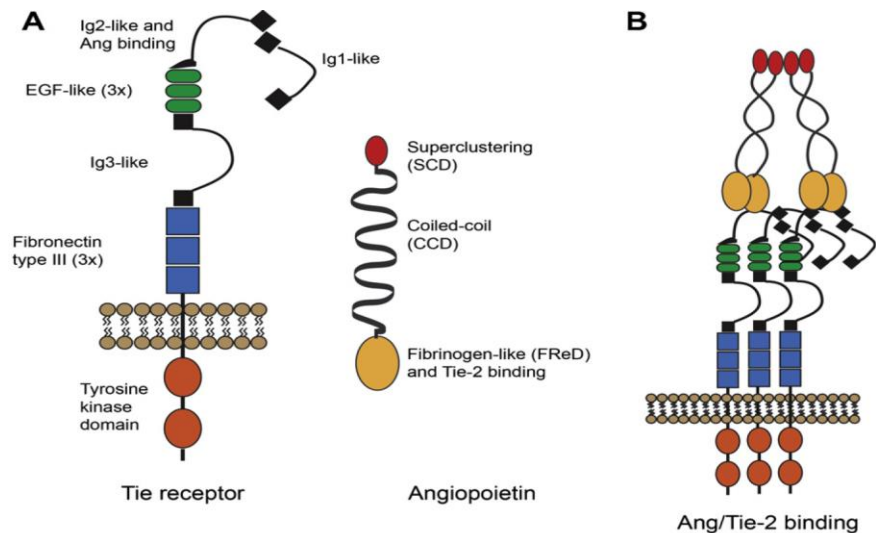


Figure 10: A) Representation of Tie 2 receptor and Angiopoietin structure. B) Representation of Angiopoietin binding to Tie 2 (Fagiani, E. and G. Christofori (2013). "Angiopoietins in angiogenesis." *Cancer Lett* 328(1): 18-26). Elsevier user license CC BY 4.0.

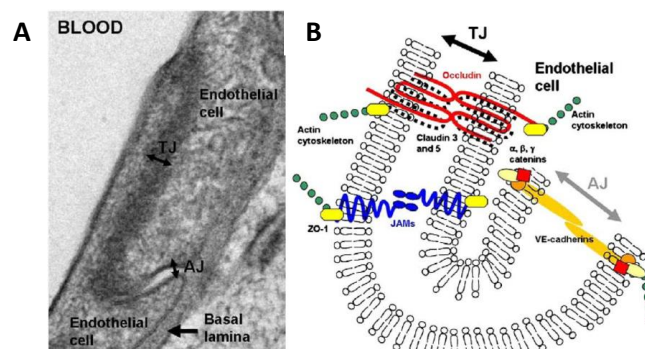
The antagonistic nature of the angiopoietins has led to research showing that under normal physiological conditions the ratio of Angiopoietin 1 to Angiopoietin 2 shows higher levels of the former. Conversely, when tissue damage occurs there is a rapid release of Angiopoietin 2. This occurs as Angiopoietin 2, with a half-life of 18 hours is stored in Weibell-Palade bodies, which are small organelles found in endothelial cells (Rondaij 2006). Weibell-Palade bodies were initially studied for their storage properties of Von Willibrand factor, a fundamental clotting factor responsible for platelet binding during tissue damage. Later research found that Angiopoietin 2 is also stored in Weibelle-Palade bodies and rapidly released to tip that balance towards the pro-angiogenic process so as to re-vascularize damaged tissue (Valentijn 2011). More recent research has shown that Weibelle-Palade bodies are in fact a heterogeneous population in that some have Angiopoietin 2 stored, while others seem to store P-selectin in an exclusive manner (Valentijn 2011). Lending further evidence to the argument that vasculature in different organs may in fact respond



differently to the same stimulus. In fact, on comparison of quiescent lung and kidney endothelium it has been found that significantly higher levels of Angiopoietin 2 are expressed in the kidneys (Gale and Yancopoulos 2002). This indicates that the kidneys store Angiopoietin 2 in Weibell -Palade bodies at higher levels than the lungs.

## Tight Junctions

Tight Junctions are the most apically located junctions that are responsible for cell-cell contact and can be found in epithelial and endothelial tissues (**Figure 12B**) (Steed 2010). Typically, fibroblasts have been shown to not express tight junction proteins. Due to the apical location of tight junctions in the endothelial cells they are key structures involved in the regulation of vascular permeability (Anderson 2009). This is predominantly true for large structures crossing the endothelial barrier such as immune cells or circulating tumor cells. Whereas smaller molecules may be transported through endothelial cells via a process known as transcellular transendothelial migration, larger structures such as cells have been shown to almost exclusively cross by paracellular transendothelial migration which is by passing between two endothelial cells (Erika 2009). In the presence of complete tight junction complexes between endothelial cells there is a limited capability for cells or larger macromolecules to cross the endothelial barrier (**Figure 11**). However, as mentioned above when there is increased expression of pro-angiogenic growth factors such as VEGF and Angiopoietin 2, the proteins of tight junction complexes become dissociated leading to increase vascular permeability.



1. Figure 11: A) Electron Microscope Image of endothelial cells tight junction. B) Schematic representation of transmembrane proteins responsible for tight junction formation. (Weiss, N., F. Miller, S. Cazaubon and P. O. Couraud (2009). "The blood-brain barrier in brain homeostasis and neurological diseases." *Biochim Biophys Acta* **1788**(4): 842-857). Elsevier user license CC BY 4.0.

Tight junction complexes consist of multiple proteins bound together to form the connection between two cells. The three transmembrane proteins directly responsible for cell-cell binding are the claudins, occludin and the junction adhesion molecules (Steed 2010). Knock out experiments have shown that occludin is not required to form the tight junction, but is involved in recruitment of the proteins to the tight junction complex (Yu 2005). There are three junction adhesion molecules (Jam1,2,3) that have also been shown to be involved in stabilization of tight junctions and their knockout has led to increased sensitivity to inflammation (Anderson 2009). The claudin family of proteins, of which there are 27 isoforms in *mus musculus* (Ouban 2012), are the primary proteins that form tight junctions. Research has shown that there are two types of claudins, tight junction forming and channel forming. The tight junction forming claudins are responsible for the binding of cells to adjacent cells and barrier function, while the channel forming claudins form communication pores between adjacent cells, similarly to the gap junction connexins (Krause 2008). Claudins have been shown to bind to claudins on adjacent cells, and although every combination and permutation has not been tested it does appear that claudins can bind to like claudins and some can also bind to different isoforms (Anderson 2009).

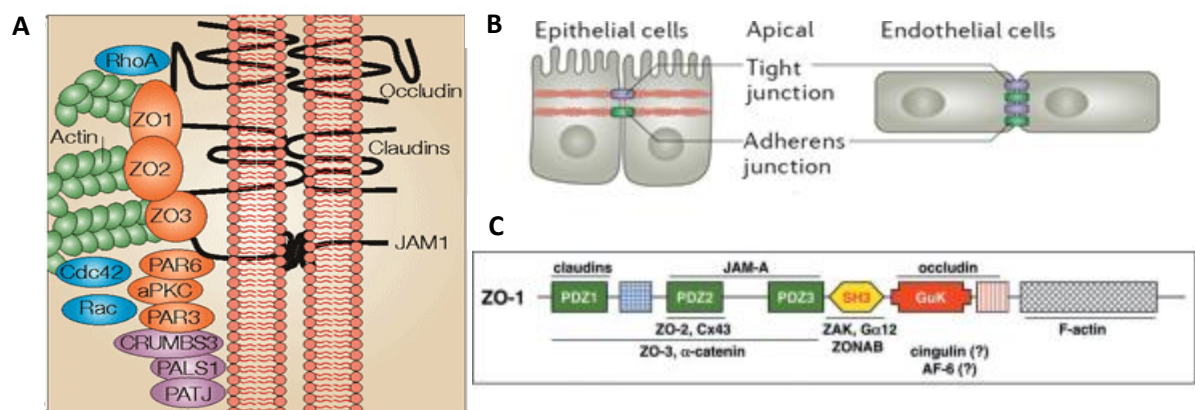
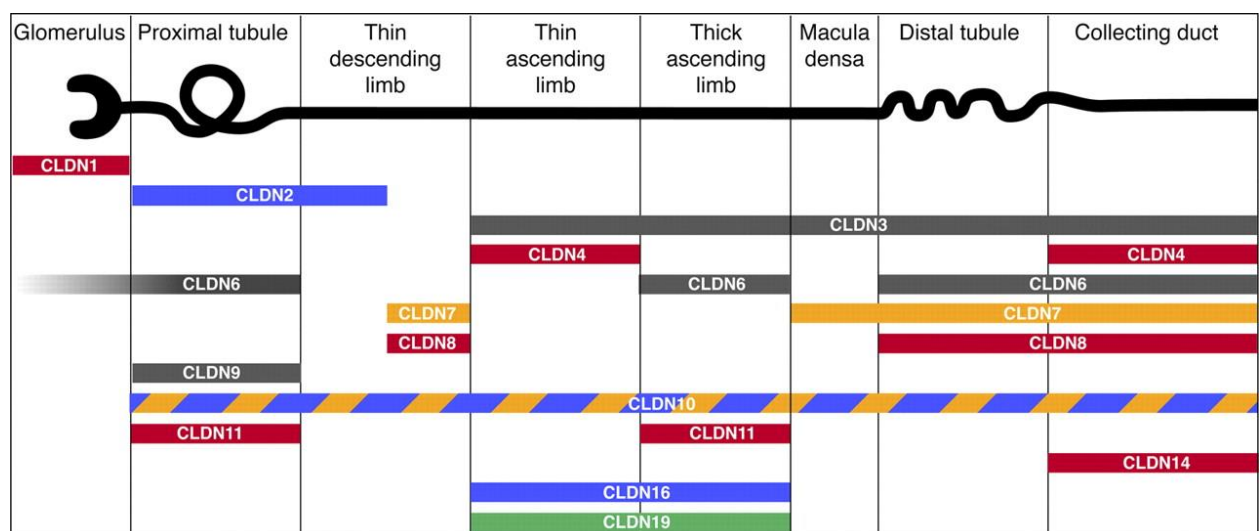


Figure 12: A) Representation of transmembrane proteins interactions and binding to proteins of the Tight Junction complex. B) Image depicting the apical localization of the tight junctions in both epithelial and endothelial cells. C) Schematic of ZO-1 binding sites. (Bazzoni, G. and E. Dejana (2004). "Endothelial cell-to-cell junctions: molecular organization and role in vascular homeostasis." *Physiol Rev* 84(3): 869-901). Permission is not required for this type of use.

To localize to and stabilize tight junctions as transmembrane proteins the claudins, occludin and the JAMs intracellular domains bind to the Zonula Occludin 1 (ZO-1) protein on specific domains (**Figure 12A**) (Bazzoni 2004). The claudins have been shown to bind to the PDZ1 domain, the JAMs to the PDZ2 and PDZ3 and occludin binds to the GuK domain (Bazzoni 2004). There is an additional SH3 domain that has been shown to be necessary for PDZ binding stabilization (Lye 2010). Upon dissociation of the transmembrane proteins from ZO-1, the ZO-1 protein delocalizes from the membrane and moves towards the nucleus, although it's function at and near the nucleus is not known (**Figure 12C**) (Bauer 2010). In fact, it has been shown that during the process of EMT there is a decrease in membrane ZO-1 as the tumorigenic cells gain the ability to survive without cell-cell contacts (Zeisberg 2009).

Unfortunately, there has been limited research on the tight junctions that exist between endothelial cells within different tissues and organs. The majority of tight junction research has focused on epithelial cells and is inferred to endothelial cells. For example, it has been shown that different claudins predominant at different stages along the epithelial



KEY	
Anion-selective:	Cation-selective:
Red: Cation barrier	Green: Anion barrier
Yellow: Anion pore	Blue: Cation pore
	Grey: Unknown

Figure 13: Representation of the location of the Claudin tight junction proteins along the kidney nephron. (4. Angelow, S., R. Ahlstrom and A. S. Yu (2008). "Biology of claudins." Am J Physiol Renal Physiol 295(4): F867-876). Permission is not required for this type of use.

cells of the kidney nephron (**Figure 13**) and that there is a kidney specific Claudin-10a that is also expressed between vasa recta of the kidney (Angelow 2008). Additionally, at least within the kidney it appears that there exist two isoforms of the ZO-1 protein, being either positive or negative for an 80 amino acid alpha motif (Anderson 1993). While the epithelial cells and parietal cells of the Bowman's capsule express the  $\alpha+$  isoform the slit-diaphragm and endothelial cells to express the  $\alpha$  isoform.

A search of the literature found two papers in which they also show that the  $\alpha$  isoform is expressed in the endothelium of the lung as well. However, research into the specific endothelial tight junction complex appears to be limited. The research that has been done into the endothelial tight junctions has identified Claudin-5 as a key component of vascular tight junctions (Escudero-Esparza 2011). Claudin-5 has been shown to be dysregulated in gliomas (Karnati 2014), in the blood-brain barrier in brain metastasis (Avraham 2014), and in lung pathologies such as acute lung injury leading to pulmonary edema (Chen 2013). It has also been shown to be found in the endothelial cells of the kidneys (Morita 1999). A 2014 study by Camire et al showed that when brain endothelial cells are treated with 3-chloropropanediol there is a loss of tight junctions (Camire 2014). Using a time course post-treatment, they showed that Claudin-5 expression goes down 90 minutes after exposure, but returns to normal levels after 120 minutes. By using PI3K and AKT inhibitors they determined that the PI3K pathway is predominantly responsible for Claudin-5 expression in brain endothelial cells. These findings implicate Claudin-5 as a key regulator of vascular permeability in multiple organs.

While significantly more characterization of the differences in endothelial tight junctions is required between each organ, there does appear to be organ specific endothelial tight junction complexes regulating organ vasculature.

## Wound Healing, Cancer and Fibrosis

In 1986, the researcher credited with the discovery of VEGF, Dr. Harold Fisher Dvorak wrote that “tumors are wounds that do not heal” (Dvorak 2015). The histopathological similarities between tumors and the wound healing process led him to this statement that has been used ever since. Since this declaration significant biochemical, biophysical and histological research has indeed shown that wound healing, pathological wound healing (fibrosis), and tumorigenesis have significant similarities (Arwert 2012).

The wound healing process is a well-characterized process that can be broken down into four overlapping phases that begin at differing times post tissue insult. The process begins with hemostasis and inflammation in which the body ensures the prevention of blood loss through the secretion of clotting factors such as Von Willibrand factor, and the recruitment of immune cells to the location of damage which are the first two steps. The third phase is marked by proliferation with increased angiogenesis to revascularize the wounded area and an increase in myofibroblasts to close the wound. The final stage is called granulation in which the deposition and cross-linking of collagen to replace the functional epithelial tissue that was damaged by the insult occurs (Gurtner 2008). The deposited collagen tissue cannot perform the function of the epithelial tissue that it replaces and acts like a scaffold as opposed to performing a parenchymal role. This would be akin to an elevator being replaced by building rebar, the elevator no longer works but the building stays standing. It is for this reason that skin scars do not grow hair, sweat or tan and is thus the prime cause of thermodyregulation in patients with significant skin burns as their epithelial tissue that was responsible for thermoregulation has been destroyed and replaced with non-functional scar tissue (Church 2006). In the normal wound healing process this process is self-regulating and once revascularization and granulation have occurred the

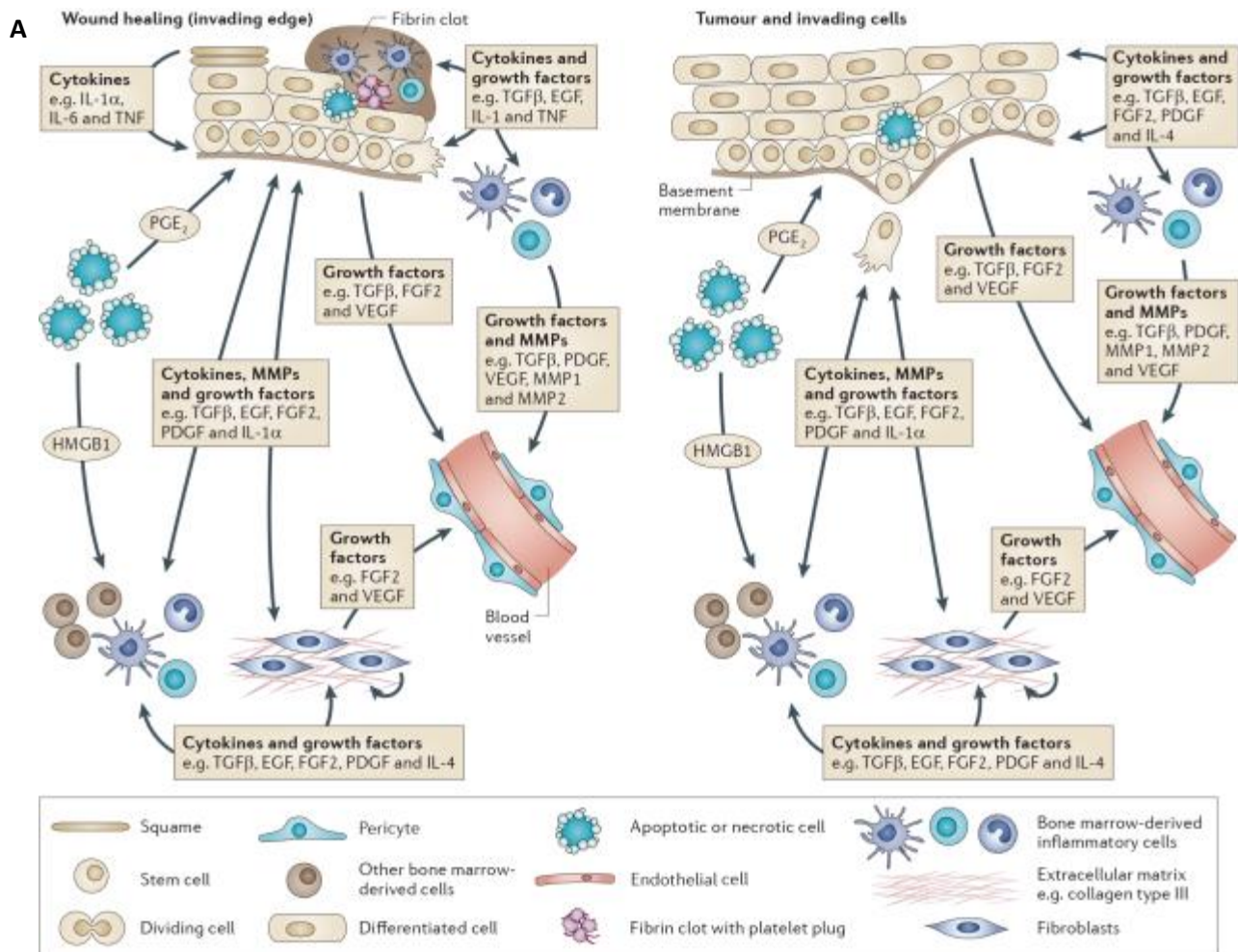
pro-wound healing factors are downregulated and the process resolves (Gurtner 2008). In the case of fibrosis and tumorigenesis these factors are constitutively upregulated and overexpressed leading to a self-perpetuating wound healing process and thus the excess deposition of collagen tissue, continued angiogenesis, and the destruction of surrounding functional parenchymal tissue. When this occurs in a vital organ, if left unchecked can lead to organ failure and death.

Given that the varying stages of wound healing involve angiogenesis and the proliferation of myofibroblasts, the similarities between fibrosis and tumorigenesis become evident (**Figure 14A**) (Arwert 2012). It is the kinetics that makes the key difference between healthy wound healing and pathological fibrosis and tumorigenesis. A 2001 paper by Kampfer et al characterized the mRNA expression levels of skin Angiopoietin 1 and Angiopoietin 2 in mice with cutaneous wounds and found that after initial injury the levels increased, but rapidly declined to basal levels after day 7. Conversely in mouse models of diabetes the skin mRNA levels of Angiopoietin 2 did not resolve after day 7 (Kämpfer 2001). Fibrosis research has shown that due to the presence of fibrotic tissue in patients with liver cirrhosis, chronic gastritis, and other fibrotic disorders predisposes them to the development of cancer in the afflicted organ. For example, liver cirrhosis is a significant risk factor for hepatocellular carcinoma (Bugianesi 2002). Thus the presence of excess wound healing factors promotes the development of tumor growth (**Figure 14B, Figure 15**).

Numerous studies focusing on individual factors increased in the fibrotic environment have shown their pro-tumorigenic properties. A prime example of this is Lysyl Oxidase (LOX) and its significant increase during fibrosis. Increase LOX during fibrosis occurs as it is involved in and necessary for proper cross-linking of newly developed collagen fibers. Dr. Janine Erlner published works showing in Bleomycin induced fibrotic lungs and Carbon



Tetrachloride induced fibrotic livers there was increased metastatic spread from 4T1 cells to those fibrotic organs as compared to their non-fibrotic controls (Cox 2013).



**Comparison between the hallmarks of cancer and wound healing**

B

Cancer	Wound healing
Sustained proliferative signalling	Transient proliferative signalling
Evasion of growth suppressors	Transient evasion of growth suppression
Invasion and metastasis	Activation of cell migration without invasion or metastasis; basement membrane repair*
Enabling replicative immortality	No
Inducing angiogenesis <sup>†</sup>	Yes
Resisting cell death	Transient decrease in terminal differentiation; transient increase in cell death

Figure 14: A) Diagrammatic comparison between the wound healing process and the process of tumor growth and invasion. B) A Comparison between wound healing and cancer. (Arwert, E. N., E. Hoste and F. M. Watt (2012). "Epithelial stem cells, wound healing and cancer." Nat Rev Cancer 12(3): 170-180). Right provided by Nature Publishing group.

Furthermore, they showed that high levels of secreted LOX from primary tumors alters the environment of organotropic organs such as the bone to develop a pre-metastatic niche (Cox 2016). They also found that secreted LOX binds to fibronectin in the lungs as similar to their bone findings prepares the lungs soil for seeding from the primary tumor. LOX is one of many pro-tumorigenic factors that have been published showing similarities between the fibrotic environment and the tumor microenvironment (Cox 2016).

Cytokines, chemokines and growth factors that influence wound healing and tumour progression*				
Cytokines, chemokines and growth factors	Receptors	Functions in wounds	Functions in cancer	Refs
<b>Growth factors</b>				
EGF family (EGF, TGF $\alpha$ , HB-EGF, amphiregulin and heregulin)	EGFR, ERBB2 and ERBB4	Epidermal and mesenchymal regeneration; accelerates wound healing	Cancer cell invasion, macrophage signalling and autocrine growth of tumour cells	113–115
FGF family (FGF2)	FGFR1 and FGFR2	Early angiogenesis, fibroblast proliferation and re-epithelialization via keratinocyte migration	Angiogenesis and fibroblast proliferation	116–119
TGF $\beta$ family	TGF $\beta$ R1 and TGF $\beta$ R2	Attracts neutrophils and macrophages, mediates ECM deposition, angiogenesis, epithelial cell migration and wound healing	Tumour development, tumour cell invasion and metastasis	120–125
PDGF	PDGFR	Attracts neutrophils and macrophages, and mediates ECM deposition and angiogenesis. Stimulates wound healing when applied topically	Recruits inflammatory infiltrate and mediates angiogenesis and lymphangiogenesis	126–129
VEGF	VEGFR1–3	Angiogenesis	Tumour cell invasion and angiogenesis	118,130, 131
<b>Cytokines and chemokines</b>				
IL-1 $\alpha$ and IL-1 $\beta$	IL-1R	Fibroblast and keratinocyte proliferation and neutrophil recruitment	Tumour cell proliferation, angiogenesis and inflammation	82,132
IL-6	IL-6R	Fibroblast proliferation and neutrophil recruitment	Tumour development, tumour cell invasion and metastasis	133,134
TNF	TNFR1 and TNFR2	Leukocyte infiltration	Tumour promotion or suppression	73,113, 135,136
CSF1	CSF1R	Recruitment of macrophages and re-epithelialization	Tumour cell invasion and migration	138–140
CCL2 (also known as MCP1)	CCR2, CCR4, UL12, D6 and duffy	Macrophage recruitment, re-epithelialization, angiogenesis and ECM production	Monocyte recruitment, tumour cell invasion and metastasis	140,141
CXCL1 (also known as GRO $\alpha$ and KC)	ECRF3, KSHV, duffy and CXCR2	Neutrophil infiltration, epithelial migration and neovascularization	Angiogenesis, invasion and migration	141,142
CXCL2 (also known as MIP2 $\alpha$ and GRO $\beta$ )	CXCR2	Epithelial proliferation	Recruits inflammatory infiltrate and migration	143,144
CXCL8 (also known as IL-8)	CXCR1, duffy and KSHV	Inflammation, wound contraction and epithelial proliferation	Angiogenesis, migration and invasion	145,146
CXCL12 (also known as SDF1 $\alpha$ )	CXCR4 and KSHV	Angiogenesis	Migration, invasion and angiogenesis	147–149

CSF1, colony stimulating factor 1; CSF1R, CSF1 receptor; ECM, extracellular matrix; EGF, epidermal growth factor; EGFR, EGF receptor; FGF, fibroblast growth factor; FGFR, FGF receptor; HB-EGF, heparin-binding EGF-like growth factor; IL, interleukin; MCP1, monocyte chemoattractant protein 1; MIP2 $\alpha$ , macrophage inflammatory protein 2 $\alpha$ ; PDGF, platelet-derived growth factor; PDGFR, PDGF receptor; SDF1 $\alpha$ , stromal cell-derived factor 1 $\alpha$ ; TGF, transforming growth factor; TGF $\beta$ R, TGF $\beta$  receptor; TNF, tumour necrosis factor; TNFR, TNF receptor; VEGF, vascular endothelial growth factor; VEGFR, VEGF receptor. \*The cytokines, chemokines and growth factors were included on the basis that they have been shown to influence both wound healing and tumour invasion or progression *in vivo*.

Figure 15: Table showing the cytokines implicated in both wound healing and in the cancer growth and development. (Arwert, E. N., E. Hoste and F. M. Watt (2012). "Epithelial stem cells, wound healing and cancer." *Nat Rev Cancer* 12(3): 170-180). Right provided by Nature Publishing group.



Despite the fact that metastasis is the primary cause of mortality in patients with a cancer diagnosis, there are limited therapies to treat metastatic disease. Even armed with the knowledge of where specific tumors are likely to spread to we still have limited knowledge about the etiology of organotropism and why certain organs are more susceptible to metastatic spread over others, for example why are the lungs a common site of metastasis while the kidney is rarely ever found to have metastatic disease. Both are major sites of blood flow, have significant capillary coverage, high perfusion rates and require the diffusion of macromolecules across the endothelial barrier for function. Furthermore, direct injection to bypass the endothelial barrier or mechanical manipulation of systemic vasculature has shown that cancer cells can grow in non-organotropic parenchyma if able to reach that environment. This clearly indicates that if cancer cells are able to cross the endothelial barrier that they will likely be able to grow in the parenchymal space of whatever organ they disseminated to. This appears to be a contradiction to Paget's generally accepted seed-and-soil hypothesis.

Rather than seemingly contradicting Paget or Ewing's hypothesis, an amalgamation of the two theories might help to explain metastatic organotropism. The vascular system is not a homogenous system, and it is clear that the vasculature of different organs is not only physically different but may also respond differently to the same secreting cytokines. This would indicate that metastatic organotropism is likely due at least in part to the heterogeneous nature of organ specific vasculature and its response to circulating pro-tumorigenic factors.

Such pro-tumorigenic factors can be found in the wound healing process, but are found both in excess and for chronically longer durations post insult during fibrosis, tumorigenesis and other pathological states. During these pathological states these factors

are secreted into the circulation and will thus have systemic effects. Cytokines once in circulation will make direct contact with the luminal side of the endothelium prior to any other cell type. Given that these cytokines are pro-angiogenic and are by all essential reasoning bombarding the endothelium, one would expect there to be wide ranging systemic organ damage in any disease which leads to excess circulating fibrotic or tumorigenic factors. However, that is not the case. For example, in patients with Sepsis, who have increased levels of circulating Angiopoietin 2, TNF $\alpha$  and TGF $\beta$ , all factors associated with pro-fibrosis and pro-tumor growth, the lungs are predominantly effected leading to an increase in pulmonary edema due to vascular leakage. While some other organs are also affected, not every organ appears to have vascular alterations in these circumstances leading to further evidence that the endothelial responses to cytokines are organ specific.

Here we hypothesize that organ specific vasculature responds differently to the same cytokines in circulation. Thus in the presence of tumor or fibrosis secreted cytokines only certain organs would show altered vasculature that increases their vascular permeability and increases the likelihood of paracellular transendothelial migration of circulating tumor cells. By inducing fibrosis in both organotropic lungs and non-organotropic kidneys in mouse models of breast cancer we can determine whether the pro-tumorigenic fibrotic environment is capable of redirecting metastasis to a non-tropic organ. Furthermore, this allows us to determine the differential organ specific vascular response of excess secreted cytokines from fibrosis or tumors.

## Chapter 2 Material and Methods

Anesthesia: Mice will be anesthetized with Ketamine/Xylazine (Ketamine (100mg/kg body weight); Xylazine (10g/kg body weight)). The duration of the anesthesia is 30-60minutes.

Analgesia: Bupreorphine will be given subcutaneously (0.1mg/kgBW in 100ul PBS) prior to skin incision, then at 12 and 24 hours after operation.

Wound Induction: The wound induction is a unilateral 8mm dorsal wound that resolves in 10-17 days. The right dorsal aspect of the mice will be shaved and the skin prepped with betadine and alcohol. Approximately 1cm right from the dorsal central axis of the mouse a Miltex 8mm Sterile Disposable Biopsy Punch will be used to remove the dermal layer down to the peritoneum, without interrupting the peritoneum. The wound will be carefully cleaned with iodine post surgery and the mouse monitored for signs of infection.

Bleomycin: Intratracheal Bleomycin injections will be used to induce lung fibrosis. Place the mouse supine on a surgical board. Elevate the surgical board to at least a 45-degree angle so that the mouse's head is elevated above its thorax. A 1 cm incision will be made vertically along the trachea ensuring clear visualization of the muscle layer. The Sternohyoid muscles will be gently displaced to reveal the trachea. Using fine tip tweezers, the tracheal peritoneal layer will be removed so as to visualize the tracheal cartilage rings. Using a 28-gauge needle 100ul of Bleomycin (15 units) will be injected between two cartilage rings. Confirmation of a successful injection will be visualized by a momentary pulmonary distress. Pulmonary distress should resolve within 5-10 seconds. The Sternohyoid muscles will be replaced and the epidermal layer will be sutured with continuous non-absorbable sutures. The wound will be cleaned and the mice monitored.

UUO: UUO or unilateral ureteral obstruction (mild to severe fibrosis that does not resolve, the mice are euthanized at 10 days' post UUO). One 1.5 cm long longitudinal incision will be made on the abdomen, approximately at 0.5cm left of the nipples on the left flank of the animal (starting at the level of the 4<sup>th</sup> set of nipples and continuing 1.5cm toward the head of the animal and will not exceed 1.5cm). The skin will be gently separated from the peritoneum to expose the peritoneum. A second incision will be made in the peritoneum, longitudinally starting at the level of the 4<sup>th</sup> nipple and continuing 1cm toward the head of the animal, not to exceed 1cm in total length. The abdominal cavity is now open and the organs gently moved to expose the ureter. The ureter is then ligated with non-absorbable nylon string at 0.5 cm below the kidney. The peritoneum is then sutured with simple interrupted absorbable sutures while the skin is sutured with simple interrupted non-absorbable sutures or surgical staples. Control mice include sham operation, which consists of exposing the ureter and closing peritoneum and skin.

Breast Pad/ Mammary Gland Injection: Bilateral incisions will be made on the abdomen of the mice without interrupting the peritoneum. Each incision will begin towards the hind leg of the animal between the 4<sup>th</sup> and 5<sup>th</sup> sets of nipples and extend towards the head of the animal no more than 1.5 cm. The skin will then be gently separated from the body cavity in order to expose the breast pad/mammary fat glands that are situated on the underside of the skin. Tumor cells (500,000 cells/20ul PBS per breast pad) will be injected into each breast pad using a Hamilton syringe fitted with a 25G needle. The abdominal incision will be closed using either simple interrupted vicryl sutures with non-absorbable nylon string or surgical staples.

Retroorbital Injection: Cell injections will be in 100ul volume and 500,000 cells in PBS retroorbitally.

Breast Pad/Mammary Gland Injection+No Surgery/Wound/Sham/UUO: Mice will be implanted with 4T1 breast cancer cells into the mammary fat pads. When the tumors reach 500mm<sup>3</sup>, cohorts will receive 1) no treatment, 2) Wound Induction, 3) Sham surgery, 4) UUO surgery, 5) Sham+IgG, 6) UUO+IgG 7) Sham+anti- Angiopoietin 2, or 8) UUO+anti-Angiopoietin-2. All Mice will be sacrificed 10 days following surgery including control mice.

Retroorbital Injection+No Surgery/Wound/Sham/UUO: Mice will be retroorbitally injected with 4T1 breast cancer cells. On the same day the mice will be also receive 1) no treatment, 2) Wound Induction, 3) Sham surgery, 4) or UUO surgery. All Mice will be sacrificed 10 days following surgery including control mice.

Retroorbital Injection+Recombinant Angiopoietin 2 Treatment: A cohort of mice will receive 2 intraperitoneal injections of 100ug recombinant mouse Angiopoietin 2 (7186-AN-025). The first injection will be given at day -1; the second injection will be given at day 3. The control group will receive PBS only. The mice will be euthanized at day 10. An additional cohort will be retroorbitally injected with 500,000 cancer cells at Day 0. The mice will be euthanized at day 10.

Mouse Monitoring: The mice will be euthanized 10 days post wound induction. The dermal wound will be monitored daily for infection and 10% weight loss together with significant decreased activity/reactivity will be used to determine whether mice require euthanasia before the 10-day sacrifice time point. Tumor bearing mice will be monitored daily, tumors measured, and tumors necrosis, 10% weight loss together with significant decreased

activity/reactivity will be used to determine whether mice require euthanasia before the 10-day sacrifice time point. All mice be euthanized upon tumor size reaching 1500mm<sup>3</sup>.

Tissue collection during euthanasia: 1 hour prior to euthanization mice will be injected with FITC-Dextran 70,000kD at 100 mg/ml (46945). Mice will be anesthetized with Ketamine/Xylazine and cervically dislocated after collection of whole blood.

Retroorbital Whole Blood Collection: Utilizing a glass pipet, 10ul of heparin will be collected into the pipet. The tip of the glass pipet will be inserted into the medial canthus of the eye under the nictitating membrane. Light pressure will puncture the sinus membrane and blood will begin to flow into the glass pipet.

Tissue Collection: Post cervical dislocation, the mouse will be secured to a dissection board so its abdomen is exposed, and sprayed lightly with 75% ethanol to wet the fur and skin to prevent contamination. Perform an incision 1cm above the central axis of the genitalia, then continuing towards the mouse's head will expose the abdominal cavity and the rib cage. The femoral artery will be perforated to allow blood to flow. Using surgical scissors, the rib cage will be removed exposing the lungs and heart. A 10ml syringe with PBS and a 20-gauge needle will be inserted into the left ventricle of the heart and gentle pressure will be placed on the syringe. Successful perfusion will be evident by clear PBS flowing from the femoral perforation, and paling of the liver, kidneys, and lungs.

Formalin Fixed Paraffin Embed: All tissues for FFPE will be collected into tissue cassettes and placed in formalin jars. They will be processed overnight and embed in paraffin no more than 2 days later.

Snap Frozen Tissue: All snap frozen tissue will be immediately placed in a 1.5ml Eppendorf Tube and put into liquid nitrogen. All snap frozen samples will be stored at -80C.

Lungs: The left lung lobe will be collected for FFPE. The right superior and inferior lobes will be collected for OCT. The middle and post-caval lobe will be snap frozen.

Liver: The median lobe will be collected for FFPE.

Kidney: The fibrotic and contralateral kidney will be removed and separated into anterior and posterior sections using a surgical blade. The anterior of each kidney will be collected for FFPE. The posterior kidney will be separated into apical and basilar sections. The apical section will be processed for OCT and the basilar will be snap frozen.

Tumor: Tumors will be weighed upon resection. Tumors will be separated into anterior and posterior sections using a surgical blade. The anterior tumor will be collected for FFPE. The posterior tumor will be separated into proximal and distal sections. The proximal tumor will be processed for OCT. The distal tumor will be snap frozen. Sections of all remaining tissue will be collected for FFPE and snap frozen tissue.

Angiopietin 2 ELISA: Whole blood will be spun down at 1500rpm for 5 minutes at 4C. Serum will be transferred to another 1.5ml Eppendorf tube. Angiopietin-2 ELISA will be performed on serum using Abcam Angiopietin-2 Mouse ELISA kit (ab171335).

Metastasis Analysis: At least 2 5um thick representative sections of the lungs from each mouse will be stained with H&E. These slides will be scanned using Panoramic 250 Flash II. Each slide will be analyzed for metastasis on Panoramic Viewer. Metastatic burden will be calculated by dividing the area of metastasis by the total area of the lung. Differential



analysis will be performed using Prism. Statistical analysis will be a unpaired 1-Way Anova comparing the mean of each group to the mean of each other group at 95% confidence to determine statistical significance.

Immunofluorescence: 4 images will be taken per slide. Using Zeiss Zen Blue software, a 10 by 10 grid will be overlaid on the image. This grid will allow us to determine the percent of fluorescence positivity in each image taken based on the analysis we are performing. For analysis requiring visualization of structural components a brightfield image will also be used to determine specific histological structures. Statistical analysis will be a unpaired 1-Way Anova comparing the mean of each group to the mean of each other group at 95% confidence to determine statistical significance.

Quantitative (Real-Time) Polymerase Chain Reaction (qPCR): RNA will be isolated from snap frozen tissue using traditional Trizol extraction methods. RNA will be measured using Nanodrop for purity. cDNA will be synthesized using High-Capacity cDNA Reverse Transcription Kit (4368814). qPCR will be performed using SYBR Green Real-Time PCR Master Mixes (4367659) on QuantStudio™ 7 Flex Real-Time PCR System from ThermoFisher.

Fibronectin F	GCTCAGCAAATCGTGCAGC
Fibronectin R	CTAGGTAGGTCCGTTCCCACT
Col1α1 F	GCTCCTCTTAGGGGCACT
Col1α1R	CCACGTCTCACCATTGGGG
LOX F	TTCTTCTGCTGCGTGACAACC
LOX R	AATAGGGGTTGTGTCGTCGGAGT
TNFα F	CCAGTGTGGGAAGCTGTCTT
TNFα R	AAGCAAAAGAGGAGGCAACA
FGF F	GCGACCCACACGTCAAACATA
FGF R	TCCCTTGATAGACACAACCTCCTC
VEGF F	AAAGCCAGCACATAGGAGAGATGAG
VEGF R	CTCGAAGAGTCTCCTCTTCCTTCATG
Ang2 F	CAGCCACGGTCAACAACCTC
Ang2 R	CTTCTTTACGGATAGCAACCGAG
CD31 F	TGCACAGTGATGCTGAACAA
CD31 R	CCATGAGCACAAAGTTCTCG
GAPDH F	GCAAGGTGTATGAATCTGTGCT
GAPDH R	TCAAGGTAACAAAGAGTGCCA
TGFβ1 F	CACTGGAGTTGTACGGCAGTG
TGFβ1 R	AGAGCAGTGAGCGCTGAATC
Tie 2 F 1	GAGTCAGCTTGCTCCTTTATGG
Tie 2 R 1	AGACACAAGAGGTAGGGAATTGA
Tie 2 F 2	CGGCAGGTACATAGGAGGAA
Tie 2 R 2	TCACATCTCCGAACAATCAGC

**Statistical Analysis:** Data are represented as the mean  $\pm$ SEM. \*p < 0.05, \*\*p < 0.01, \*\*\*\*p < 0.0001. ns, not significant. Analysis of two samples or indicated by comparison bars was performed by Unpaired Student's T-test. Multiple group analysis was performed using One-way Anova.

**Cell Culture:** Renal and lung endothelial cells were obtained from the laboratory of Dr. Isaiah Fidler and cultured as previously described ((Langley and Fidler 2003). For

Angiopoietin 2 stimulation, 1ug of murine recombinant Angiopoietin 2 (7186-AN-025) was added to the culture media for the indicated times. 4T1 cancer cells were tagged with GFP and grown to 80-85% confluence. Cells were trypsinized and washed in PBS prior to intravenous or orthotopic injection.

Quantification of metastatic burden and tumor necrosis: Hematoxylin and eosin staining of the lung and kidney sections from paraffin-embedded tissue was generated. Image of an entire lobe was obtained using the Panoramic 250 Flash III slide scanner. Metastasis were identified using via histopathological analysis based on H&E staining and metastatic area was quantified using Panoramic Viewer software as a percentage of total lung area. High magnification images of the metastatic area are provided for each lung photomicrographs.

ELISA: Blood was collected at the time of euthanasia and 200ul was spun down at 1500rpm for 5 minutes. Serum was separated and stored in -80C. Samples were thawed and 20ug was diluted in the sample diluent buffer provided in the Angiopoietin 2 Mouse ELISA kit (Abcam ab171335) and the ELISA was then carried out following the manufacturer's directions.

Western Blot: Cells were grown on 6cm dishes and treated as indicated. Cells were washed with PBS and removed from the dish using a cell scraper and transferred to a 1.5ml Eppendorf tube. Cells were spun down at 1500rpm for 5 minutes and supernatant removed. Cell pellet was resuspended in 200-300ul of RIPA buffer and sonicated every 10 minutes for 30 minutes at 4C. Lysate was spun at 12,000rpm for 10 minutes and supernatant was transferred to a new 1.5ml Eppendorf tube. Protein concentration was measured using BCA assay reagents (Pierce). Western blot was run using standard BioRad protocol. Membranes were blocked in 5% milk in PBS for 1 hour and incubated in Actin

(1:1000 Cell Signaling 4970), pTie2 Tyr1108 (1:100 Thermo Fischer PA5-38339) and pERK (1:500 Cell Signaling 9101) overnight in 4C. Membranes were washed and incubated in secondary HRP conjugated antibody and exposed.

Immunofluorescence/ Immunostaining: Harvested tissues, tumor, lungs, and kidneys, and skin were fixed in 10% neutral buffered formalin, dehydrated and embedded in paraffin. For Sirius Red the deparaffinized tissues were stained in hematoxylin for 8 minutes, washed for 10 minutes and then stained in Sirius Red solution for 1 hour. Slides were then scanned using Panoramic 250 Flash III slide scanner and quantified on Photoshop software using a 10 by 10 grid to count positive areas for  $\geq 3$  fields/tissue per x20 image. Alternatively, deparaffinized tissues were incubated in 10mM citrate buffer (ph 6.0) for 15 minutes at 95C prior to blocking with 4% Cold Water Fish Gel in PBS. Tissues were incubated overnight in following blocking in  $\alpha$ SMA(1:500 Sigma C6198), Claudin 5 (1:100 Thermo Fischer 35-2500), Ki67 (1:500 Abcam ab15580), and Isolectin B4 (1:500 Thermo Fischer I21411) followed by secondary fluorescent antibodies. Slides were mounted with DAPI to label nuclei. Positive staining was quantified in  $\geq 3$  visual fields/tissue at x63 or x100 using Photoshop software by placing a 10 by 10 grid to count positive areas or costaining. Statistical analysis was done using the average staining per tissue. Stainings were visualized on a Zeiss microscope. For the cell culture staining cells were grown on 8 well chamber slides and treated as indicated with either PBS or murine recombinant Angiopoietin 2. Cells were washed in PBS and fixed for 10 minutes in 4% paraformaldehyde then blocked for 1 hour in 4% Cold Water Fish Gel in PBS. Cells were incubated overnight in ZO-1 (1:100 Thermo Fischer 61-7300) and Phalloidin (1:1000 Thermo Fischer T7471).

Microarray analysis and quantitative real time PCR analysis: Total RNA was isolated from healthy and wounded skin, healthy and fibrotic lungs and healthy and fibrotic kidneys Trizol (Invitrogen) and RNA was extracted according to manufacture's instructions.. An equal amount of RNA was submitted from each cohort (n=3) to the Microarray core facility at MD Anderson. Microarray analysis was performed using Mouse Ref8 Gene Expression Beadchip (Illumina) software. Ingenuity Pathway Analysis (IPA) was performed on the microarray data set, with a threshold of 1.2 and 1.5 fold. For RT PCR analyses, tissues were homogenized in Trizol (Invitrogen) and RNA was extracted according to manufacture's instructions. cDNA was generated using High Capacity cDNA Reverse Transcriptase Kit (Applied Biosystems). Gene expression was determined using Applied Biosystems 7300 Sequence Detector System and SYBR green as the fluorescence reporter. Measurements were standardized to the housekeeping gene (CD31 or GAPDH).



## Results

### Chapter 3: Kidney and Lung Fibrosis express similar pro-tumorigenic factors

Fibrosis and the tumor microenvironment have been shown to share a number of biochemical and biophysical similarities including secreted cytokines. Previous research has shown that fibrotic environments are pro-tumorigenic for primary tumor growth and can also enhance metastatic growth to organotropic organs. Furthermore, the fibrotic environment and the pre-metastatic niche have been also been shown to be similar and the pre-metastatic niche has been implicated as a potential driving factor towards organotropism. The majority of metastasis and organotropic research has been focused on the tropic organs while limited research has focused on the organs that rarely develop metastasis. Here we choose to focus not only on the tropic organs within breast cancer, but to also determine if we created a fibrotic, and thus pro-tumorigenic, pre-metastatic niche environment in a non-organotropic organ could we re-route metastasis to that organ. Given previous publications implicating the increased levels of TGF $\beta$ , LOX, TNF $\alpha$ , Collagen,  $\alpha$ SMA among other factors in the fibrotic environment, tumor microenvironment and pre-metastatic niche, we aimed to determine whether this was sufficient to re-route metastasis to a non-organotropic organ.

For the purposes of this study we choose to utilize two well-established mouse models of metastatic breast cancer. The mouse derived 4T1 mammary fat pad cancer cell line and the MMTV-PyMt models have both been shown to metastasize to multiple organs including the lung, liver and brain with similar tropism to human breast cancer. The advantage of these models is that they both have consistent temporal tumor growth rates. This allows for the induction of specific treatments at known tumor sizes providing for a consistency across the two models. Furthermore, both of the models are in the BALB/c background allowing for the comparison of the two different breast cancer models. Currently



there are no studies utilizing these models to determine whether they can be rerouted to metastasize to a non-tropic organ. It has been shown that direct injection of 4T1 cells into the kidney can form a tumor within the cortex indicating that if capable of entering the parenchymal space of the kidney these cells would be capable of forming a metastatic nodule.

To elucidate the contribution and control of the fibrotic environment on metastasis we evaluated three models of tissue damage in 4T1 and MMTV-PyMt tumor bearing mice. By inducing a cutaneous wound, lung fibrosis and kidney fibrosis we can observe a normal resolving wound, an organotropic fibrosis and a non-organotropic fibrosis effect on metastatic spread in breast cancer. Given that clinically surgery, a wound, has not been shown to enhance metastasis and other research has indicated that pro-fibrotic factors go down by day 7 in normal resolving wounds in mice the wound will act as the control for normal kinetics. Comparison of the wound to the lung fibrosis and kidney fibrosis allows us to compare acute normal wound versus chronic fibrotic damage. Utilizing Bleomycin to induce lung fibrosis we aim to develop a pro-tumorigenic environment in an organotropic organ, while surgically induced kidney fibrosis will act as the non-organotropic organ.

Based on the pro-tumorigenic and pro-metastatic nature of the fibrotic environment and its secreted cytokines, we hypothesized that both lung fibrosis and kidney fibrosis would have the necessary factors to enhance metastasis in a systemic manner. In accordance with previous studies we expect to see an increase in metastasis to the fibrotic lung, and given the induction of a similar pro-tumorigenic environment in the fibrotic kidney we would hypothesize that this would induce metastatic growth in the damaged non-organotropic organ.

*Histopathological characterization of cutaneous wound, lung fibrosis and kidney fibrosis shows increased collagen deposition and aSMA+*

To understand the role of the fibrotic environment in breast cancer metastasis we began by evaluating and comparing the pro-tumorigenic factors expressed in a resolving wound, lung fibrosis and kidney fibrosis. Cutaneous wound skin at day 6 post injury (an open wound), Bleomycin induced fibrotic lungs, and surgically induced fibrotic kidneys were harvested at day 10 post insult. The insulted organs were each stained with H&E, Sirius Red and immunofluorescently stained with aSMA. Morphometric analysis for Sirius Red and aSMA was performed comparing each fibrotic organ with its healthy control. Sirius Red is a cationic dye that binds by reacting to the basic groups in collagen. The dye binds to the collagen molecules in a parallel orientation, which results in an increased birefringency and is counterstained with picric acid and hematoxylin for nuclear stain. An increase in positive red area indicates an increase in collagen. There is a significant increase in Sirius Red positive areas in the skin wound at day 6 and both lung and kidney fibrosis (**Figure 16B,D,F,H**). Additionally, aSMA, a marker for the collagen depositing myofibroblasts is also significantly increased in the day 6 wound, and lung and kidney fibrosis. (**Figure 16C, E,G,I**). Taken together these results indicate that an open wound, lung and kidney fibrosis all show increases in the production of fibrotic tissue.

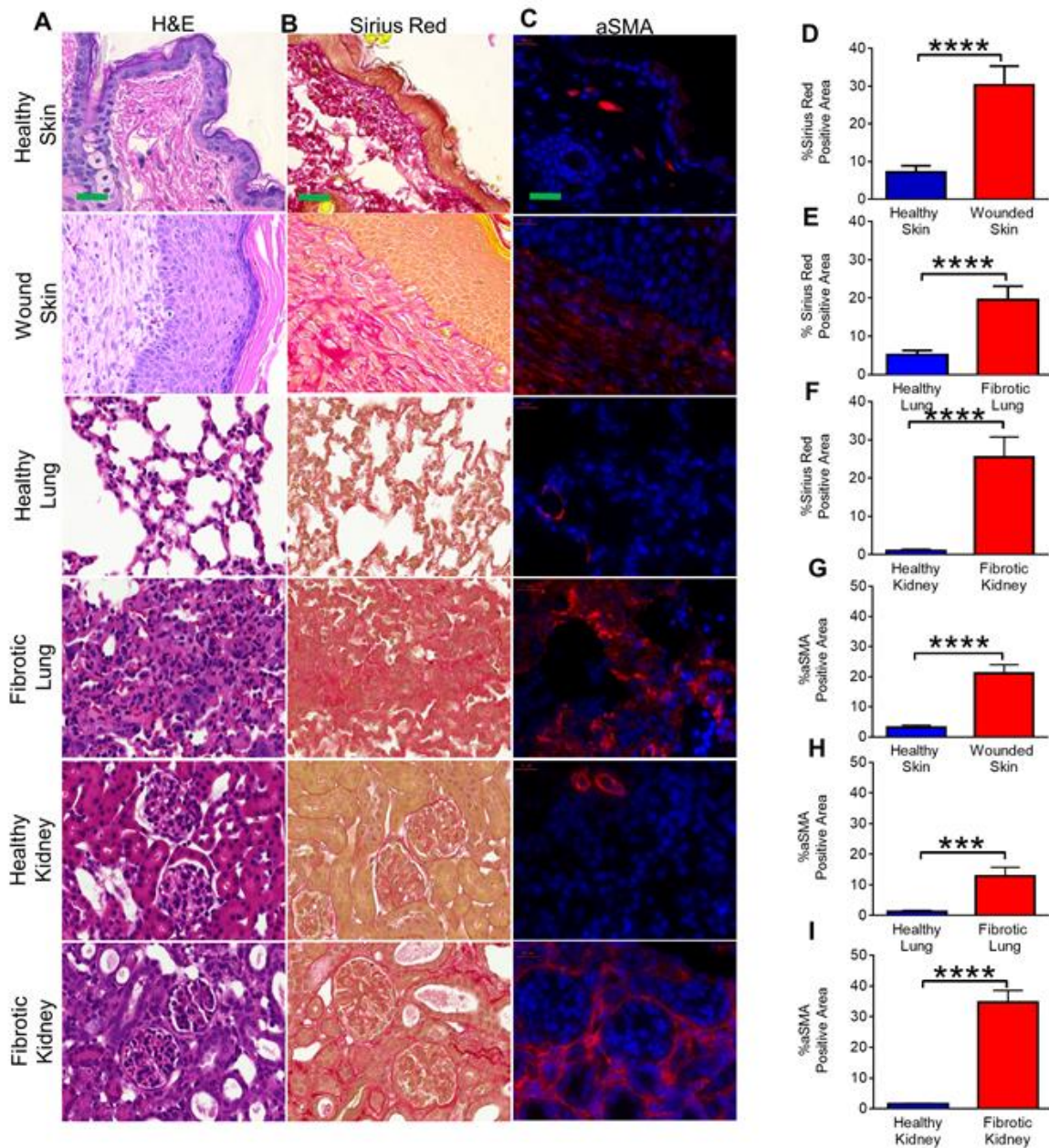


Figure 16: Histology of fibrosis in skin, lung and kidney. A) H&E of healthy skin, wounded skin, healthy lung, fibrotic lung, healthy kidney, and fibrotic kidney. B) Sirius Red of healthy skin, wounded skin, healthy lung, fibrotic lung, healthy kidney, and fibrotic kidney. C) aSMA immunofluorescence of healthy skin, wounded skin, healthy lung, fibrotic lung, healthy kidney, and fibrotic kidney. D) Quantification of skin Sirius Red. E) Quantification of skin aSMA. F) Quantification of lung Sirius Red. G) Quantification of lung aSMA. H) Quantification of kidney Sirius Red. I) Quantification of kidney aSMA. Scale bar=25um. Data are represented as the mean  $\pm$  SEM using Student's T-test for \* $p < 0.05$ , \*\* $p < 0.01$ , \*\*\*\* $p < 0.0001$ . ns, not significant.

*Fibrotic environments show sustained increased chronic expression of pro-tumorigenic factors*

Given that healthy wounds begin resolving and are typically fully closed in healthy mice by day 10-17, versus fibrosis which persists beyond day 10 post insult we performed Illumina gene expression arrays on skin at day 6 and day 17 post injury, and on fibrotic and healthy lungs and kidneys. Using previous publications, we compiled a list of genes shown to be present in the pre-metastatic niche and to be pro-tumorigenic. The open wound and closed wound were normalized to healthy unwounded skin, while the fibrotic lung and fibrotic kidney were normalized to a healthy respective organ. By comparing the differential gene expression levels in a healthy open wound versus a healthy closed wound it is evident that the pro-tumorigenic genes do not significantly increase their expression and/or return to basal levels once the wound is closed. Conversely, when both the fibrotic lung and fibrotic kidney are compared to their respective healthy control organ at day 10 post insult a number of genes associated with pro-tumorigenic growth are still upregulated (**Figure 17**). To confirm the chronic upregulation we performed qPCR on select genes to confirm their upregulation at day 10 in the kidney fibrosis models (**Figure 18**).

The sustained increase in similar pro-tumorigenic factors in the fibrotic lung and kidney versus the resolved factors in the wound will enable us to test the effects of forming a pro-tumorigenic environment in the tropic and non-organotropic organ.

	Healthy Skin	Open Wound	Closed Wound	Healthy Lung	Fibrotic Lung	Healthy Kidney	Fibrotic Kidney
Lox	3.07516	2.99499	3.51942	3.19066	3.96621	3.67244	4.07286
S100a9	2.52799	2.95912	2.47023	2.96241	3.57985	3.51871	3.91676
Col2a1	0.82962	1.28102	1.07378	1.01479	2.87156	2.2508	3.89936
Egfr	1.48372	1.31751	1.54426	1.14661	2.82625	2.25604	3.85253
Tnfsf11	1.11608	1.32976	1.31108	1.98621	2.57638	3.19077	3.80382
Col4a5	2.42596	2.17558	2.09437	1.92902	2.5956	2.78117	3.65615
Fn1	1.74539	1.64242	2.16098	2.45451	3.01414	3.56865	3.64291
Tnc	1.12137	1.63376	1.3383	1.17239	2.46639	2.56055	3.62416
Fgf5	1.70817	1.62636	2.21022	2.03669	2.83057	3.22394	3.57394
Col4a4	1.18115	0.79161	1.24613	3.24429	3.1767	3.71251	3.54702
Col2a1	1.26176	1.32693	1.07301	1.54373	2.37888	3.14634	3.48971
Fgf1	1.40207	1.1788	1.22497	1.36244	2.52038	1.86251	3.44674
Tnc	2.11921	2.68497	2.61349	3.31644	3.0477	3.57746	3.4245
Pgf	1.09858	1.19162	1.28294	1.41341	2.43486	1.8195	3.36082
Bmp1	3.32336	3.40661	3.41699	1.42514	2.32591	2.37397	3.23717
S100a8	3.06729	3.46458	3.00079	2.18961	2.87175	2.93829	3.12252
Tnc	0.5744	0	0	2.75454	2.61335	3.16644	3.05962
Mmp9	2.09755	2.48452	2.03868	2.82927	3.04739	2.73911	3.00835
Vcam1	0	0.95053	0.84107	2.16958	3.06282	2.91328	2.95902
Egfr	2.38	2.33424	2.42526	3.03257	2.7595	3.19395	2.95499
Bmp1	2.67688	2.83847	3.04746	3.05755	2.84022	2.65884	2.85478
Col3a1	3.15878	2.90131	3.4211	2.84716	2.50255	2.55714	2.76221
Vegfa	2.75737	2.83327	2.53691	2.58851	2.68738	2.9303	2.70316
Mmp2	3.87634	3.93833	4.10482	1.50605	2.39911	2.48027	2.69469
Col1a1	3.87219	3.82965	3.90811	1.58152	2.33967	2.41593	2.68331
Fn1	3.0167	3.20661	3.48508	1.33133	2.10299	2.08419	2.67964
Col1a2	2.52293	2.66912	2.907	2.61653	2.08288	1.94897	2.62145
Icam1	2.59898	2.66762	2.77833	2.56603	1.93394	2.62557	2.56651
Hif1a	2.19976	1.81598	2.11418	2.27009	2.05307	1.85555	2.47642
Csf1	1.9531	2.19934	2.18274	1.19512	1.58642	1.72339	2.46989
Hgf	1.05806	1.32256	1.35914	1.63885	2.28366	2.48026	2.4544
Tnf	1.62469	1.39708	1.43867	1.43708	1.40927	1.76283	2.37243
Timp1	2.25759	2.78318	2.84318	2.24454	2.11981	2.29104	2.30543
Bmp1	2.72837	2.89092	3.08015	2.46205	2.272	2.18203	2.30318
Csf3	1.29238	1.42205	1.40061	1.46876	1.86449	2.26442	2.30228
Egfr	3.30709	3.09667	3.12687	1.08085	1.37059	1.68059	2.26762
Col4a4	1.57483	1.11538	1.53388	1.24054	1.27396	1.50652	2.25393
Col3a1	2.85899	2.38077	2.10783	2.43231	2.15422	2.11218	2.16594
Tgfb1	1.96307	2.30993	2.25692	2.11976	1.8621	2.49792	2.13853
Tnc	1.17956	1.4138	0.7979	1.00206	1.2666	1.60306	2.09738
Cxcl12	2.7264	2.76148	2.80516	1.27767	1.92381	2.04381	2.08667
Vegfa	2.21878	2.40585	2.09912	2.33723	2.08814	1.9554	1.97809
Col4a1	3.41646	3.31531	3.65304	1.45265	1.49612	1.76201	1.91993
S100a4	2.13106	2.05779	2.27296	1.15885	2.05593	2.18249	1.91554
Tnf	1.27524	1.26078	1.06739	1.45757	1.44886	1.59642	1.88886
Col4a5	2.01362	1.92238	1.993	1.12722	1.39618	1.65973	1.79192
Col4a6	1.03995	1.05944	1.03041	1.14556	1.3985	1.48253	1.71283
Hgf	1.03937	0.98032	1.06239	1.1566	1.38243	1.60542	1.65289
Cxcl12	2.55536	2.7018	2.51801	1.29762	1.42976	1.67404	1.64661
Col4a3	1.38324	1.24115	1.35518	1.05609	1.14629	1.5022	1.60297
Fn1	0.64991	1.08793	1.21446	0.72173	1.11748	1.49549	1.60108
Cxcl12	3.19471	3.22633	3.1383	1.25097	1.28119	1.59152	1.59509
Tnc	2.02675	2.63619	2.49761	1.34475	1.30371	1.56971	1.5896
Col4a2	3.14479	3.28968	3.41125	1.30921	1.29608	1.51072	1.58268
Egfr	2.27099	2.27177	2.26764	1.18884	1.24272	1.5265	1.58082
Fgf1	2.00836	1.8891	1.98608	0.29011	1.10437	1.55939	1.56979
Timp1	2.15812	2.78285	2.79905	1.22848	1.20551	1.54661	1.54392
Hif1a	0	0.97212	0	1.11172	1.30132	1.57073	1.50972
Vcam1	1.90279	2.29729	2.55015	1.18701	1.05701	1.61636	1.48801

Figure 17: Increase in expression of genes associated with pre-metastatic niche in the fibrosis environment. Probes fluorescent units are shown in log scale. N=3 for each group.



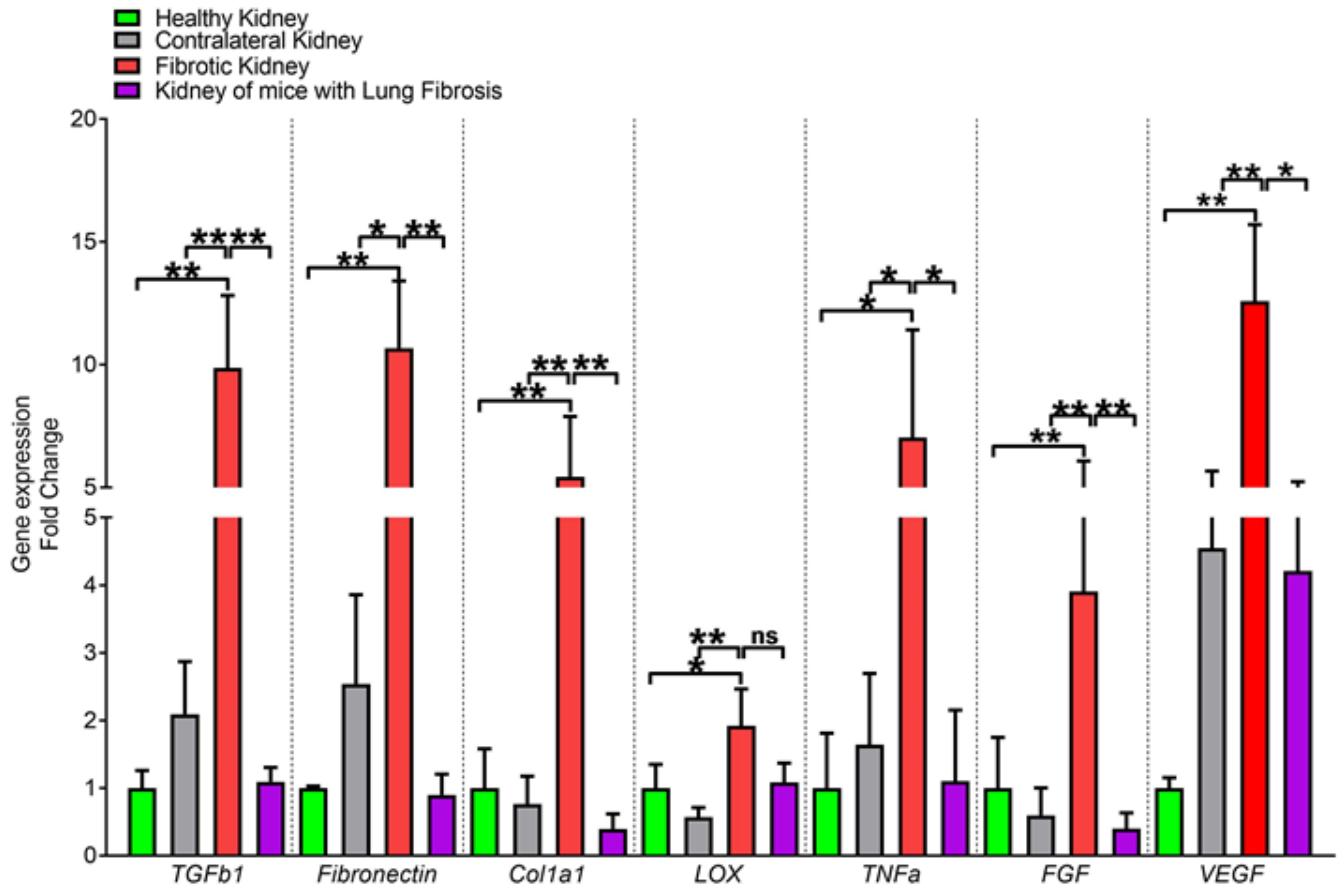


Figure 18: Fold Change expression for genes associated with the pre-metastatic niche and tumor microenvironment in kidneys of indicated groups. The fold change in TGFB1, Fibronectin, Col1a1, LOX, TNFa, FGF and VEGF in healthy kidneys, contralateral kidneys, fibrotic kidneys and the kidneys of mice treated with bleomycin. Normalized to GAPDH. Data are represented as the mean  $\pm$ SEM using One-Way Anova for \* $p < 0.05$ , \*\* $p < 0.01$ , \*\*\* $p < 0.0001$ . ns, not significant.

#### **Chapter 4: The effect of organotropic and non-organotropic fibrosis on breast cancer metastasis**

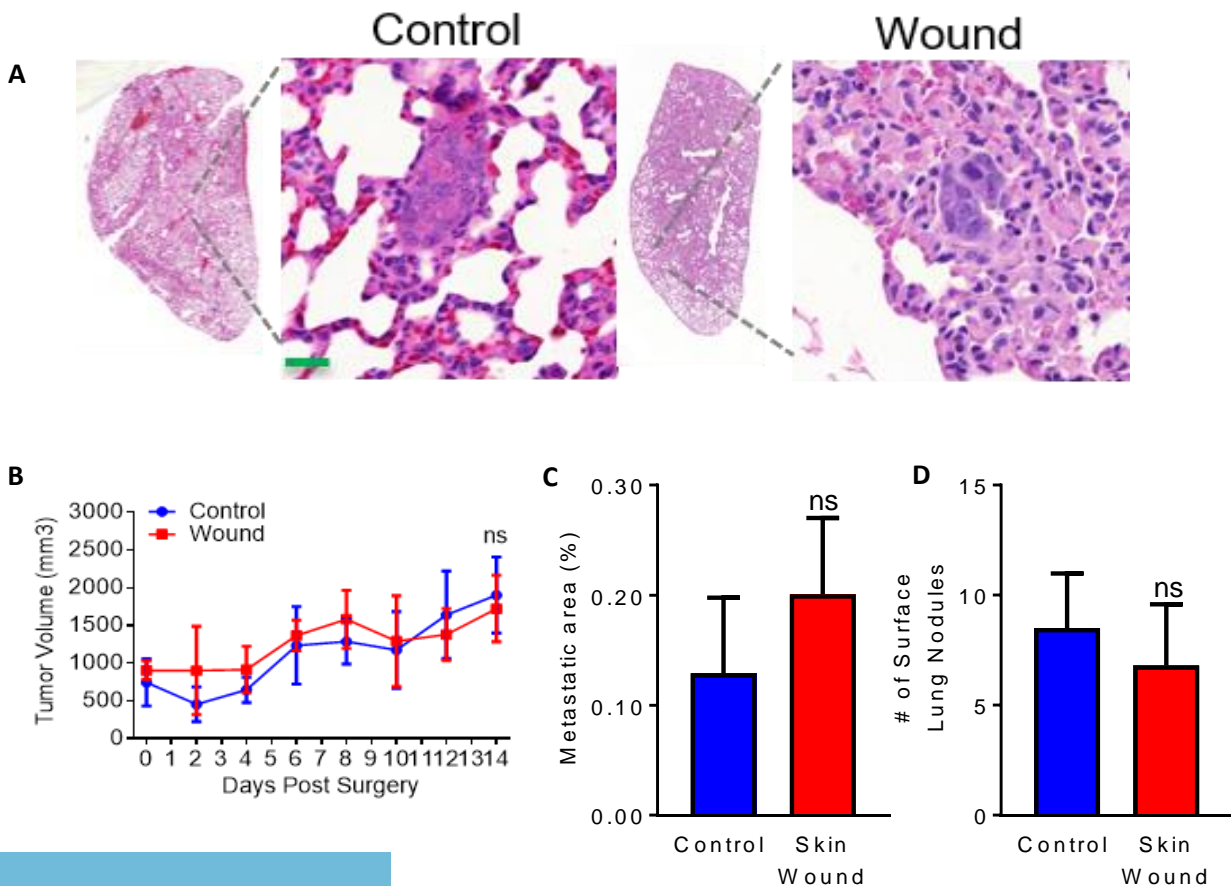
To test the capacity of pro-tumorigenic fibrosis to enhance and/or reroute metastatic disease we induced cutaneous skin wound, lung fibrosis, or kidney fibrosis in mice that received 1) orthotropic 4T1 injections 2) intravenous 4T1 injections 3) or MMTV-PyMt tumor bearing mice. By injecting 4T1 cancer cells orthotopically and utilizing the MMTV-PyMt model we are able to model the spread of metastatic disease from the primary tumor following the metastatic cascade. The use of the intravenous model allows us to remove any influence from the primary tumor and to test the effects of fibrosis on both vasculature and extravasation and on other host organs.

##### *The effect of cutaneous skin wound on breast cancer metastasis*

A long-standing concern within the surgical community has been the effect of surgery on the spread of metastatic disease. Although there is limited evidence to show that surgical wounds promote metastatic disease, and given that pro-tumorigenic factors from wounds resolve after a few days we opted to determine whether induction of a cutaneous wound could have any effects on the spread of metastatic disease. Mice were initially injected bilaterally with 4T1 cancer cells into their mammary fat pads and monitored for tumor growth. Once the 4T1 tumors had reached a combined growth of 500mm<sup>3</sup> the mice were anesthetized and an 8mm dorsal non-peritoneal penetrating wound was surgically induced. The same progression was used for the MMTV-PyMt with mice receiving a wound once the combination of their tumors had reached a combined 500mm<sup>3</sup>. Once the tumors reached a combined 1500mm<sup>3</sup> the mice were euthanized and tissues collected for analysis. Additionally, we injected 4T1 cancer cells intravenously and induced wound on the same day. Given the propensity for both these models to metastasize to the lungs we primarily

focused our metastatic analysis on the pulmonary system. We also collected the kidneys from all mice to analyze for potential metastatic spread and to compare to the other cohorts with fibrotic lung and kidney.

To compare metastatic spread in mice with and without cutaneous wound we performed H&E staining on the lungs and kidneys and counted metastasis microscopically. As hypothesized, there was no significant difference between metastatic spread to the lungs in the mice with and without cutaneous wound in either the 4T1 (**Figure 19E, F, G**) model or the MMTV-PyMt model (**Figure 19A, C, D**). Similarly, we noted no difference in colonization of the lungs in the intravenous 4T1 with or without cutaneous wound (**Figure 19I, K, L**). There was no metastatic growth or colonization of the kidneys in any these mice (**Figure 22A, B**). There was no change in the growth rates of the tumors (**Figure 19B, I**).





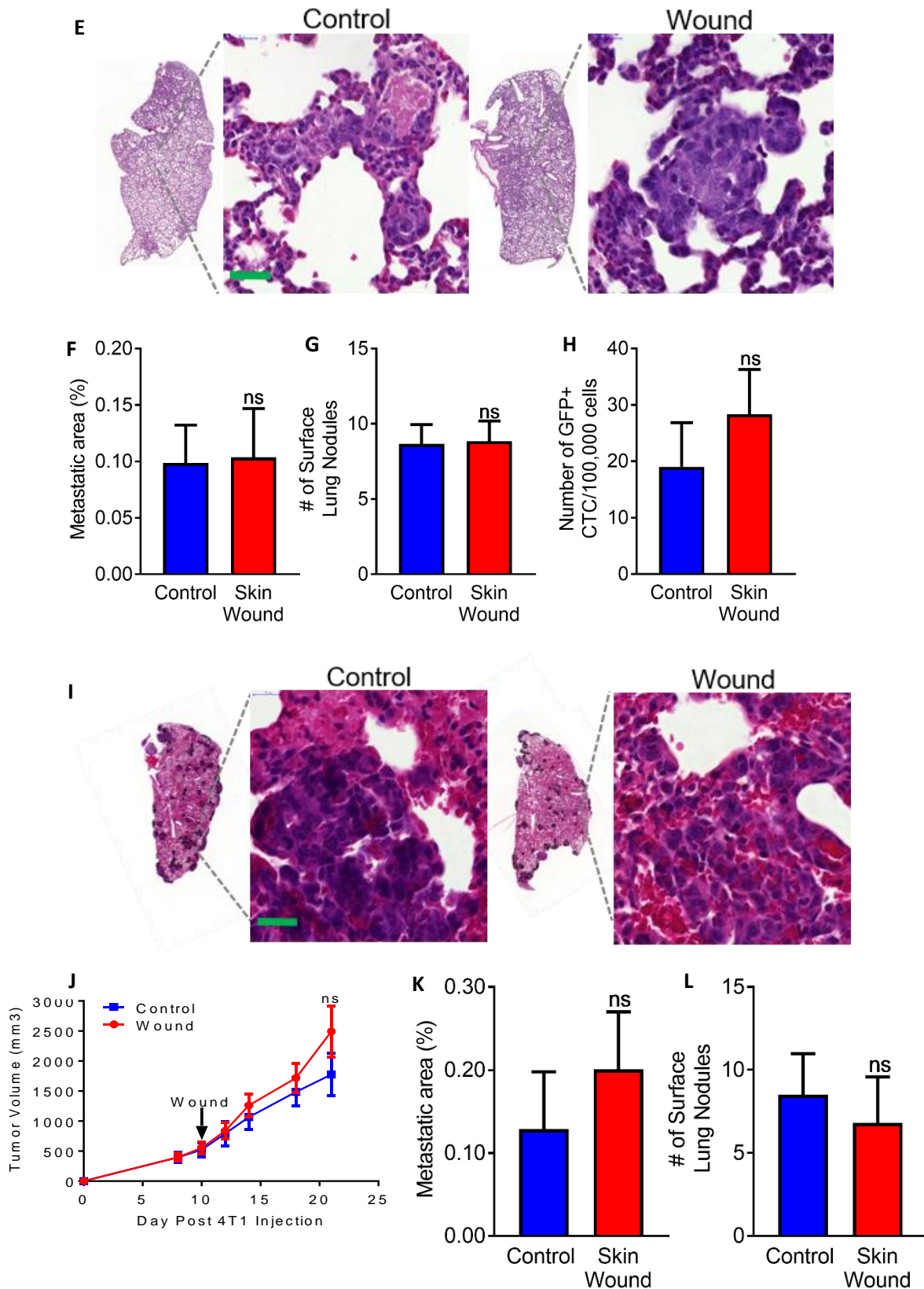
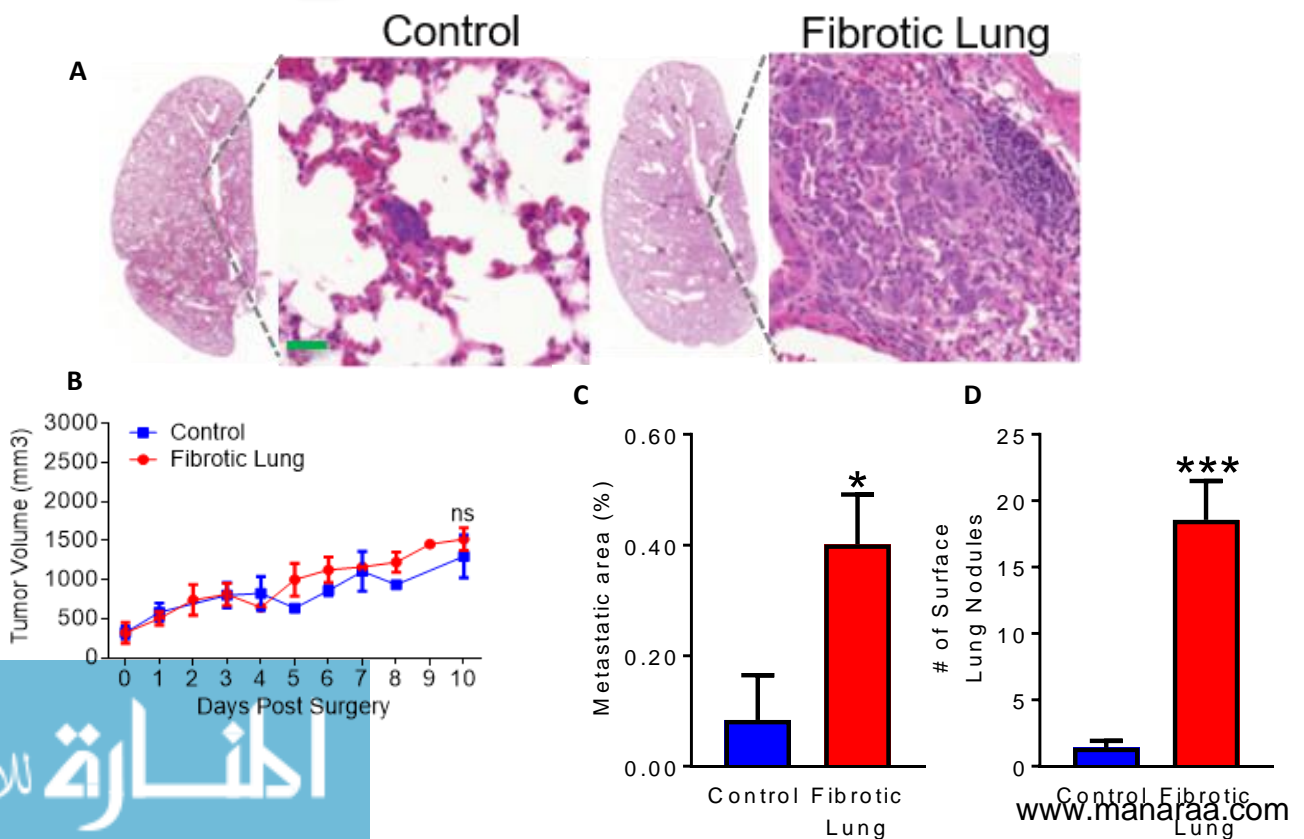


Figure 19: Metastatic Analysis in Cutaneous Wound A) Histological representation of MMTV-PyMt metastasis with and without cutaneous wound. B) PyMt Tumor growth curve C) Metastatic and D) surface lung nodule quantification of MMTV-PyMt mice with and without cutaneous wound. E) Histological representation of 4T1 orthotopic metastasis with and without cutaneous wound. F) Metastatic, G) surface lung nodule quantification and H) CTC analysis of 4T1 orthotopic mice with and without cutaneous wound. I) Histological representation of 4T1 IV metastasis with and without cutaneous wound. J) 4T1 Orthotopic growth curve K) Metastatic and L) surface lung nodule quantification of 4T1 IV mice with and without cutaneous wound. N=6 for each group. Scale bar=25um. Data are represented as the mean  $\pm$ SEM using Student's T-test for \* $p < 0.05$ , \*\* $p < 0.01$ , \*\*\*\* $p < 0.0001$ . ns, not significant.

### *The effects of lung fibrosis on breast cancer metastasis*

Using the same methodology as in with the cutaneous wound we induced lung fibrosis in 4T1 orthotopic, 4T1 intravenous, and MMTV-PyMt mouse models of breast cancer either once the tumors had reached 500mm<sup>3</sup> or on the same day as 4T1 intravenous injection. These mice were euthanized 10 days post intratracheal Bleomycin lung fibrosis inducing surgery. The 10 days euthanization was both for humane reasons and also due to the rapid progression of metastatic disease in these mice. Analysis of these mice revealed significant spread of 4T1 (**Figure 20 E, F, G**) and PyMt (**Figure 20 A, C, D**) metastasis and colonization (**Figure 20I, K, L**) of the lungs in mice with lung fibrosis as compared to mice that received only intratracheal PBS injections. None of these had metastasis to their kidneys (**Figure 22**) or changes to their tumor growth (**Figure 20B, J**). The increased metastasis and colonization of the fibrotic lungs in these mice indicates that the pro-tumorigenic fibrotic environment is able to enhance metastatic spread to organotropic organs. These results reflect previous publications and support the role of the aforementioned pro-tumorigenic factors in promotion of metastasis.



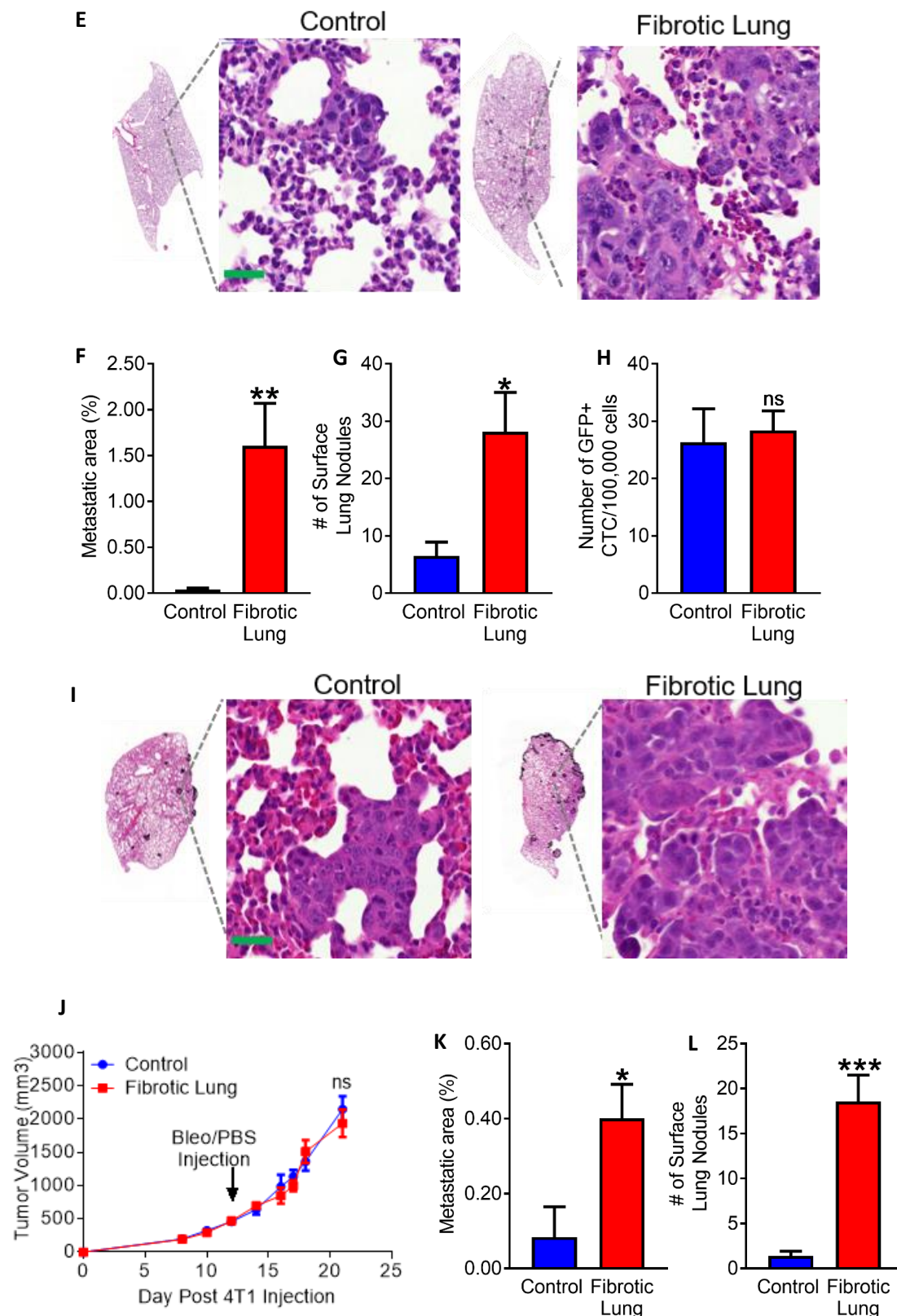


Figure 20: Metastatic Analysis in Lung Fibrosis A) Histological representation of MMTV-PyMT metastasis with and without lung fibrosis. B) PyMT Tumor growth curve C) Metastatic and D) surface lung nodule quantification of MMTV-PyMT mice with and without lung fibrosis. E) Histological representation of 4T1 orthotopic metastasis with and without lung fibrosis. F) Metastatic, G) surface lung nodule quantification and H) CTC analysis of 4T1 orthotopic mice with and without lung fibrosis. I) Histological representation of 4T1 IV metastasis with and without lung fibrosis. J) 4T1 Orthotopic growth curve K) Metastatic and L) surface lung nodule quantification of 4T1 IV mice with and without lung fibrosis. N=6 for each group. Scale bar=25um. Data are represented as the mean  $\pm$ SEM using Student's T-test for \* $p < 0.05$ , \*\* $p < 0.01$ , \*\*\* $p < 0.0001$ . ns, not significant.

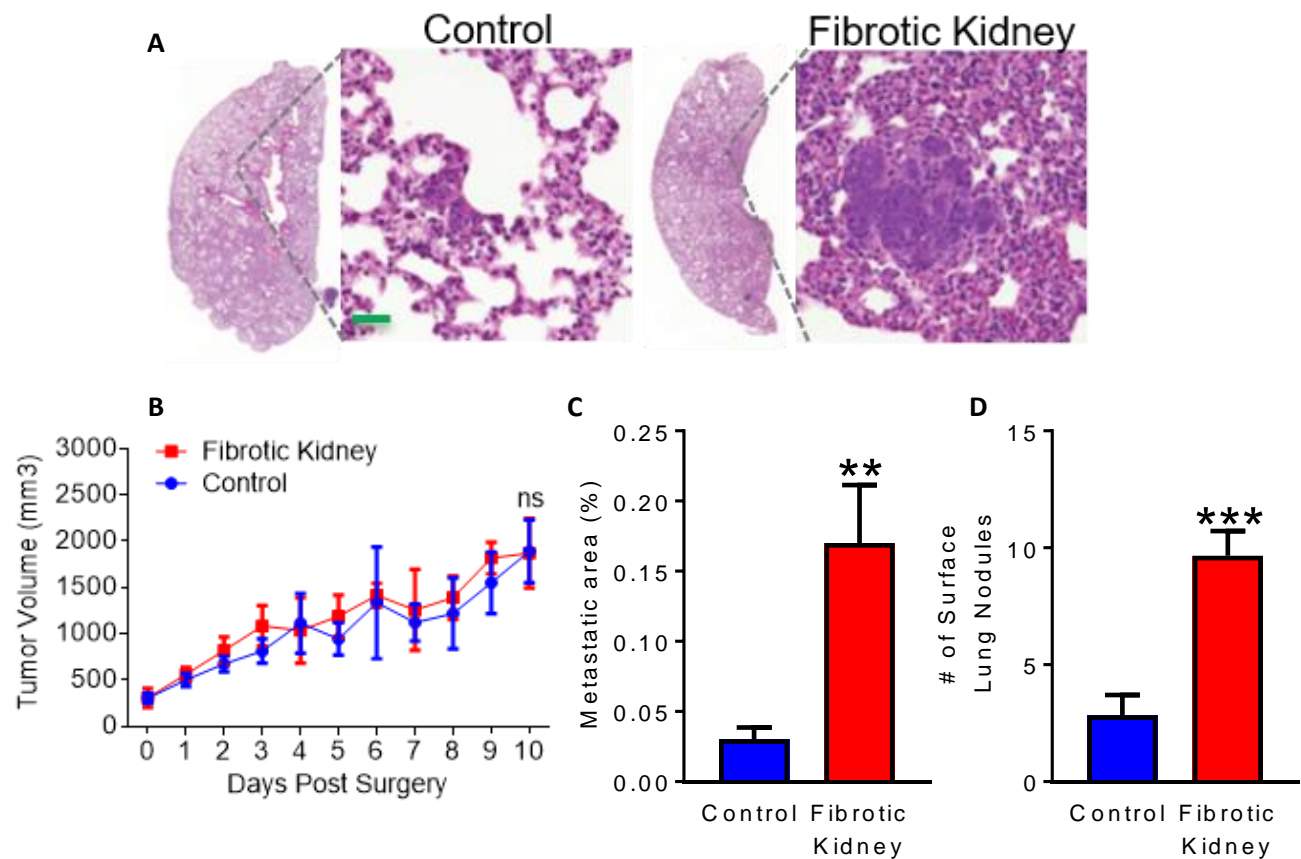
*The effects of kidney fibrosis on breast cancer metastasis*

To elucidate the ability of the pro-tumorigenic fibrotic environment to potentially reroute metastasis to a non-organotropic organ we surgically induced kidney fibrosis utilizing the same 4T1 and MMTV-PyMt methods and models and time course as the lung fibrosis cohort. Given the presence of chronically and significantly upregulated expression of pro-tumorigenic factors in the fibrotic kidney and publications reporting the chemotactic properties of upregulating these factors on cancer cells we surmised that this environment should reroute metastatic spread to the damaged kidney. Surprisingly, upon euthanization of the mice with kidney fibrosis there was no macroscopically apparent metastatic nodules in the 4T1 orthotopic, MMTV-PyMt of the 4T1 intravenous model (**Figure 22A, B**). Further histological analysis of the kidneys confirmed the induction of fibrosis, and that despite the development of this pro-tumorigenic environment, fibrosis was not able reroute metastatic spread to a non-organotropic organ. This result indicates that while the previously reported pro-tumorigenic factors found in the pre-metastatic niche are sufficient to enhance metastasis to an already tropic organ, they are not sufficient to redirect metastatic spread. The inability of the fibrotic environment to redirect metastatic disease indicates that there are additional factors that affect metastatic tropism in addition to the previously reported pre-metastatic niche alterations that occur in the tropic organs.

In addition to noting that fibrosis could not redirect metastatic disease to the non-tropic kidney we also analyzed metastasis in the lungs of mice with kidney fibrosis. Histopathological analysis revealed there was an increase in metastasis to the lungs of mice that had kidney fibrosis. Increased lung metastasis was observed in the 4T1 orthotopic model (**Figure 21A, C, D**) Similarly, metastasis to the lung was enhanced in the MMTV-PyMt model (**Figure 21E, F, G**) and also in the 4T1 intravenous model (**Figure 21 I, K, L**)



with kidney fibrosis. There was no effect of kidney fibrosis on primary tumor growth (**Figure 21B, J**). These results indicate that kidney fibrosis is able to systemically affect distant organs to enhance metastasis and colonization. However, given the similarities between the fibrotic environment, the tumor microenvironment, and the pre-metastatic niche this effect appears to be unrelated to the molecules that have previously been associated with determination of metastatic organotropism.



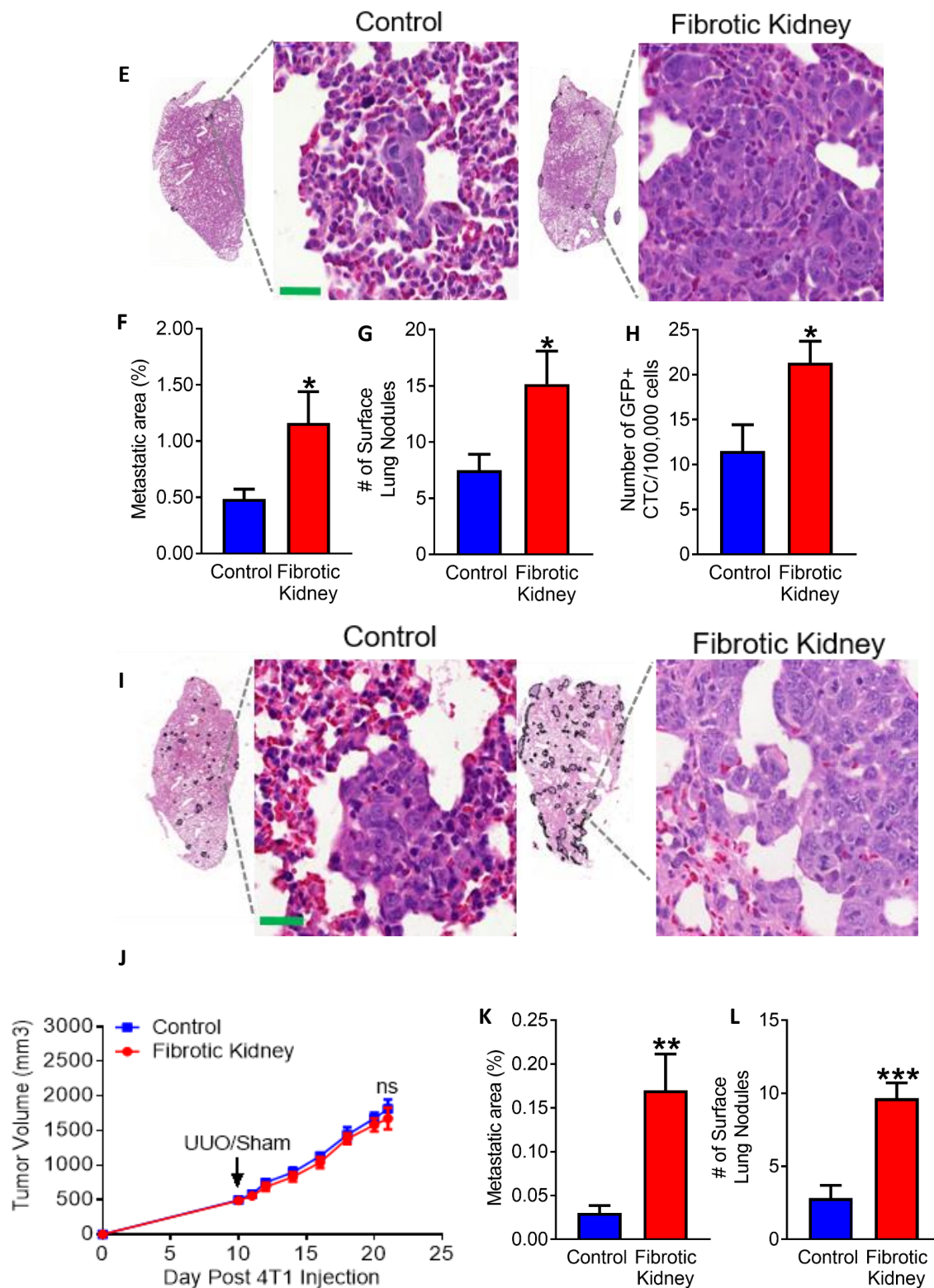


Figure 21: Metastatic Analysis in Kidney Fibrosis A) Histological representation of MMTV-PyMt metastasis with and without kidney fibrosis. B) PyMt Tumor growth curve C) Metastatic and D) surface lung nodule quantification of MMTV-PyMt mice with and without kidney fibrosis. E) Histological representation of 4T1 orthotopic metastasis with and without kidney fibrosis. F) Metastatic, G) surface lung nodule quantification and H) CTC analysis of 4T1 orthotopic mice with and without kidney fibrosis. I) Histological representation of 4T1 IV metastasis with and without kidney fibrosis. J) 4T1 Orthotopic growth curve K) Metastatic and L) surface lung nodule quantification of 4T1 IV mice with and without kidney fibrosis. N=6 for each group. Scale bar=25um. Data are represented as the mean  $\pm$ SEM using Student's T-test for \* $p < 0.05$ , \*\* $p < 0.01$ , \*\*\* $p < 0.0001$ . ns, not significant.

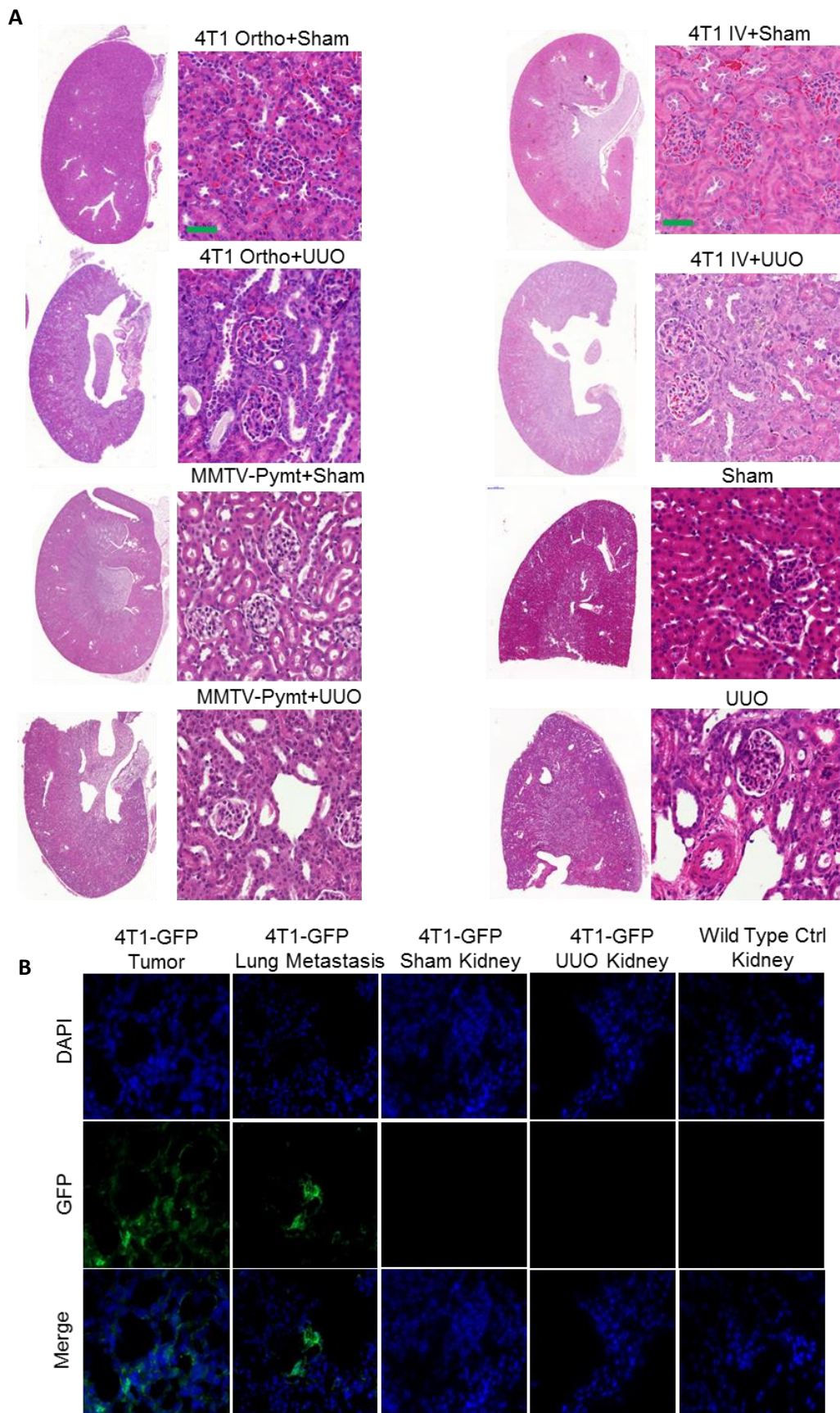


Figure 22: Metastasis did not spread to the kidneys despite the fibrotic environment. A) Representative images of kidneys from each cohort showing no metastatic growth. B) 4T1 GFP labelled cells were visualized in the tumor and lung metastasis, but could not be located in the kidneys of mice from any cohort. Scale bar=25um.



## Chapter 5: Kidney fibrosis increases the circulating levels of cytokines known to affect vasculature

The finding that fibrosis cannot reroute metastatic disease, but can systemically enhance the spread to tropic organs indicates that the fibrotic environment, similar in nature to the primary tumor microenvironment releases factors that travel systemically and effect various aspects of the host in an organ-specific manner. Given that in both the fibrotic lung and fibrotic kidney there were significant increases in the presence of pro-tumorigenic molecules in the stromal microenvironment we hypothesized that this organ-specific reaction to circulating fibrotic cytokines might occur within a non-stromal aspect of the organ.

### *Chronically elevated circulating cytokines during kidney fibrosis*

To determine the cytokines elevated during fibrosis we initially performed an analysis using Illumina array data of fibrotic kidneys as compared to their healthy kidneys. Utilizing genes that were increased in the fibrotic kidneys we performed pathway and gene ontology analysis using the online software DAVID. Analysis of this data revealed significant changes associated with both tight junctions and with vascular remodeling (**Figure 23,24, 25**). Categorical analysis revealed a number of vascular related genes upregulated in the fibrotic kidneys when compared to healthy kidneys. While these factors are associated with alterations in tight junction structure and vasculature further experimentation was required to determine which of the factors was also secreted into the circulation.



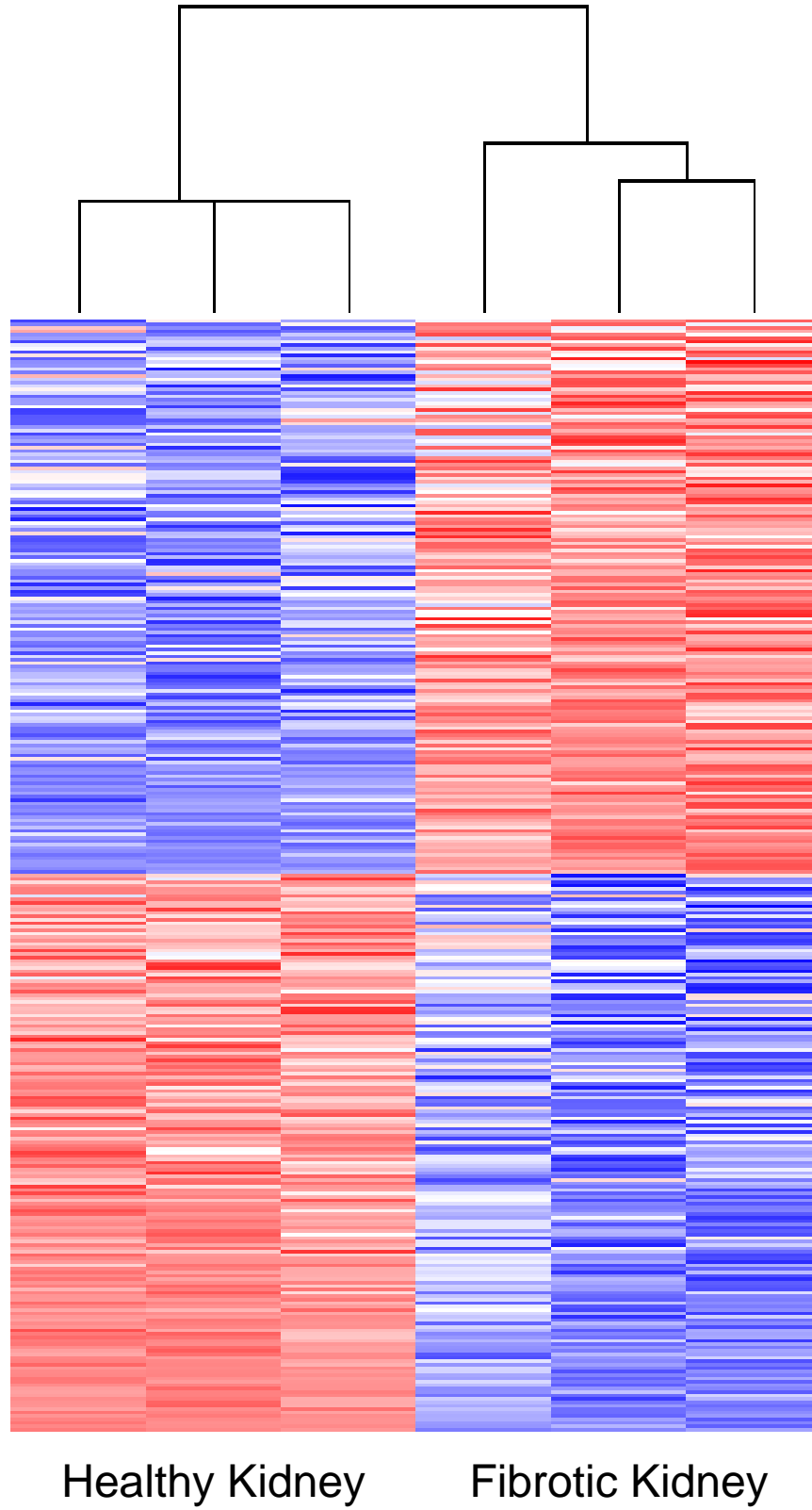


Figure 23: Heat Map of genes differentially expressed in healthy kidneys versus fibrotic kidneys. N=3 for each cohort.

A

Category	Term	Count	%	P-Value	Benjamini
GOTERM_BP_FAT	regulation of transcription	517	12.8	3.60E-05	3.40E-03
GOTERM_BP_FAT	transcription	432	10.7	1.20E-06	2.40E-04
GOTERM_BP_FAT	intracellular signaling cascade	247	6.1	1.30E-07	6.40E-05
GOTERM_BP_FAT	phosphate metabolic process	229	5.7	2.20E-06	3.60E-04
GOTERM_BP_FAT	phosphorus metabolic process	229	5.7	2.20E-06	3.60E-04
GOTERM_BP_FAT	cell cycle	195	4.8	1.70E-12	7.30E-09
GOTERM_BP_FAT	phosphorylation	195	4.8	2.20E-06	3.70E-04
GOTERM_BP_FAT	protein amino acid phosphorylation	188	4.7	8.50E-09	7.20E-06
GOTERM_BP_FAT	cell adhesion	177	4.4	5.80E-11	1.20E-07
GOTERM_BP_FAT	biological adhesion	177	4.4	6.90E-11	9.70E-08

B

Category	Term	Count	%	P-Value	Benjamini
KEGG_PATHWAY	Pathways in cancer	91	2.3	2.80E-04	4.00E-03
KEGG_PATHWAY	MAPK signaling pathway	85	2.1	2.60E-06	1.20E-04
KEGG_PATHWAY	Focal adhesion	71	1.8	2.10E-07	1.30E-05
KEGG_PATHWAY	Regulation of actin cytoskeleton	65	1.6	4.20E-04	5.20E-03
KEGG_PATHWAY	Chemokine signaling pathway	56	1.4	5.50E-04	6.00E-03
KEGG_PATHWAY	Cell adhesion molecules (CAMs)	53	1.3	3.40E-05	8.90E-04
KEGG_PATHWAY	Cell cycle	52	1.3	1.40E-07	1.30E-05
KEGG_PATHWAY	Endocytosis	52	1.3	3.80E-02	1.50E-01
KEGG_PATHWAY	Tight junction	46	1.1	1.60E-04	2.40E-03
KEGG_PATHWAY	Neurotrophin signaling pathway	45	1.1	1.30E-04	2.10E-03

Figure 24: Gene Ontology and KEGG analysis from DAVID. A) The top 10 gene ontology terms of upregulated genes in fibrotic kidneys as compared to healthy kidneys. B) The top 10 pathway terms upregulated in fibrotic kidneys as compared to healthy kidneys.

Based on the results of our gene array we selected a cytokine array from R&D systems and ran multiple samples from healthy, cutaneous wound, fibrotic lung, and fibrotic kidney serum. While a number of cytokines were increased in the serum of mice with fibrosis as compared to the healthy and wounded serum, we noted that Angiotensin 2 was elevated both in our gene array data (**Figure 25A**) and in the serum of mice with kidney fibrosis (**Figure 25B, 26**). To confirm our observations from the cytokine array we performed an Angiotensin 2 specific ELISA on the serum of all the cohorts and their respective controls. In accordance with previously published data our basal levels of Angiotensin 2 were around 2000pg/ml. Most notably the serum Angiotensin 2 levels of mice with kidney fibrosis were significantly elevated (**Figure 27**). Interestingly, Angiotensin 2 was not as elevated in the serum of mice with lung fibrosis as compared to the serum of mice with healthy lungs (Figure 27). Furthermore, we also confirmed that in the fibrotic kidney the gene expression of Angiotensin 2 was increased (Figure 27).

These results suggest that fibrotic kidney damage releases continuous Angiotensin2 into circulation at significantly elevated levels. Given that Angiotensin 2 has been shown to be an antagonist of Angiotensin 1 and a destabilizer of endothelium cell-cell interactions and tight junctions, we surmised that this could cause systemic alterations in vascular permeability leading to increased likelihood of extravasation of circulating cancer cells.

**A**

	Healthy Kidney	Fibrotic Kidney
72		
Angpt2	2.686827066	2.944020161
Angptl4	0.440827707	1.220089674
Arsi	1.151590481	1.31937287
Bmper	1.213160756	1.630819299
C1qtnf1	1.480110129	2.072651677
Car11	1.930841761	2.20601871
Cbln4	0.906188688	1.179973631
Ccdc80	1.788511187	2.411386852
Ccl27	1.825537314	2.094441672
Ccl4	1.559123474	2.250242769
Ccl6	1.301543707	1.909055509
Ccl7	0.953635732	2.130140806
Ccl9	1.532162764	2.769567054
Cd200	1.235598141	1.630507323
Chi3l1	1.448993189	2.008385578
Chi3l3	0.866542544	1.426706553
Col5a2	1.011755999	1.49785646
Cort	0.968446991	1.227021643
Crim2	0.780308201	1.150787709
Crif1	1.203350984	2.298479233
Csnk	0.666864813	1.37453911
Cst3	3.728588169	3.97733859
Cxcl1	1.985125312	3.100307702
Cxcl14	1.444282125	2.175404193
Cxcl16	1.666921676	2.113569709
Cxcl4	1.474289059	2.120267093
Cyr61	1.214319614	1.728536391
Defb1	0.508914138	0.887503202
Defb12	0.859861173	1.135325017
Defb13	1.083088772	1.355366568
Defb14	1.135813339	1.327082405
Defb25	1.19918823	1.55391393
Defcr6	1.14912075	1.370985645
Dkk3	2.561431809	3.002888414
Dmkn	1.178484511	1.46265147
Dpt	1.348692376	1.718518532
Emb	2.848215967	3.157201867
Emid2	1.863537392	2.41603864
Emilin1	1.914819011	2.317480076
Emilin2	1.439800124	2.078150069
Enam	0.66116617	1.067965168
Fam132b	0.928016812	1.375539206
Fgfbp1	1.359104123	1.715048026
Fgl2	0.775854487	1.333961836
Folr4	0.809812895	1.310729142
Gdf15	2.177485949	2.956504554
Gfod2	1.990271917	2.336560821
Gm414	0.990688003	1.296727894
Gm885	1.416115045	1.648327847
Gpx7	1.388463733	2.072632227
Havcr1	2.800393438	3.399482044
Ifna14	0.684274471	1.108147458
Igfbp1	1.017225321	1.342670058
Igfbp2	1.073919534	1.57076488
Igfbp6	1.137756888	1.453251027
Il17re	2.213389314	2.577406393
Il1f6	1.001721353	1.382612984
Il33	1.847048398	2.744233806
Ins1	1.02997853	1.316344332
InsI3	1.840328794	2.363545168
Kazald1	1.015736236	1.304760542
Kng1	2.661470364	2.997066779
Lcn2	1.673118004	3.511398968
Lcn4	1.114687036	1.430200166
Leap2	0.954293095	1.354988814
Lefty2	0.480528707	1.23418946
Lgals3bp	2.68997375	3.264611777
Liph	1.268710829	1.620070149
Ly86	1.601905932	2.348240152
Ly96	1.76402301	2.095665463
Lyz	3.105823828	3.846208793
Lyzs	1.855726435	2.655825017
Matn2	0.915509488	1.261216419
Metrn1	1.410531653	1.621258078
Mfap3	2.445204259	2.729570223
Mfap5	0.957038325	1.670752653
Muc2	0.929690555	1.218831046
Mxra8	2.278854884	2.678994299
Myoc	0.854172622	1.369251352
Nbl1	2.250096554	2.771443332
Nmu	0.832322176	1.130778531
Npff	1.376690753	1.593261903
Oit1	1.135063746	1.513477203
Olfm1	2.30018405	2.676212549
Olfm12b	1.630940008	2.06579486
Olfm13	2.483315186	2.965838441
ORF9	1.146817664	1.541802298
Pcolce2	1.244285569	1.728113857
Pdgfrl	1.070289172	1.370074261
Pglyrp	1.156006414	1.347330874
Pla1a	2.537746331	2.876818776
Prss23	1.47141378	1.943230841

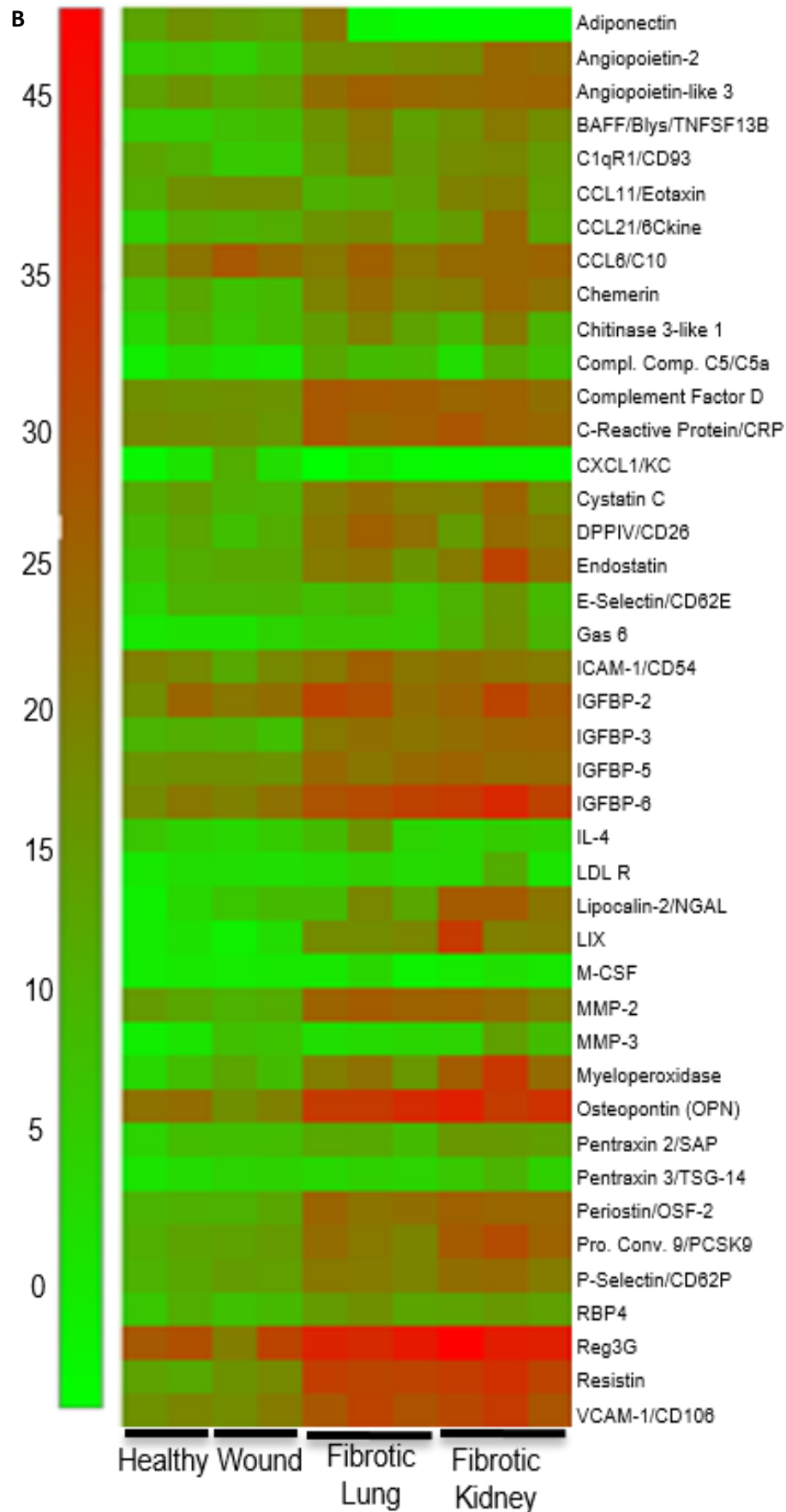
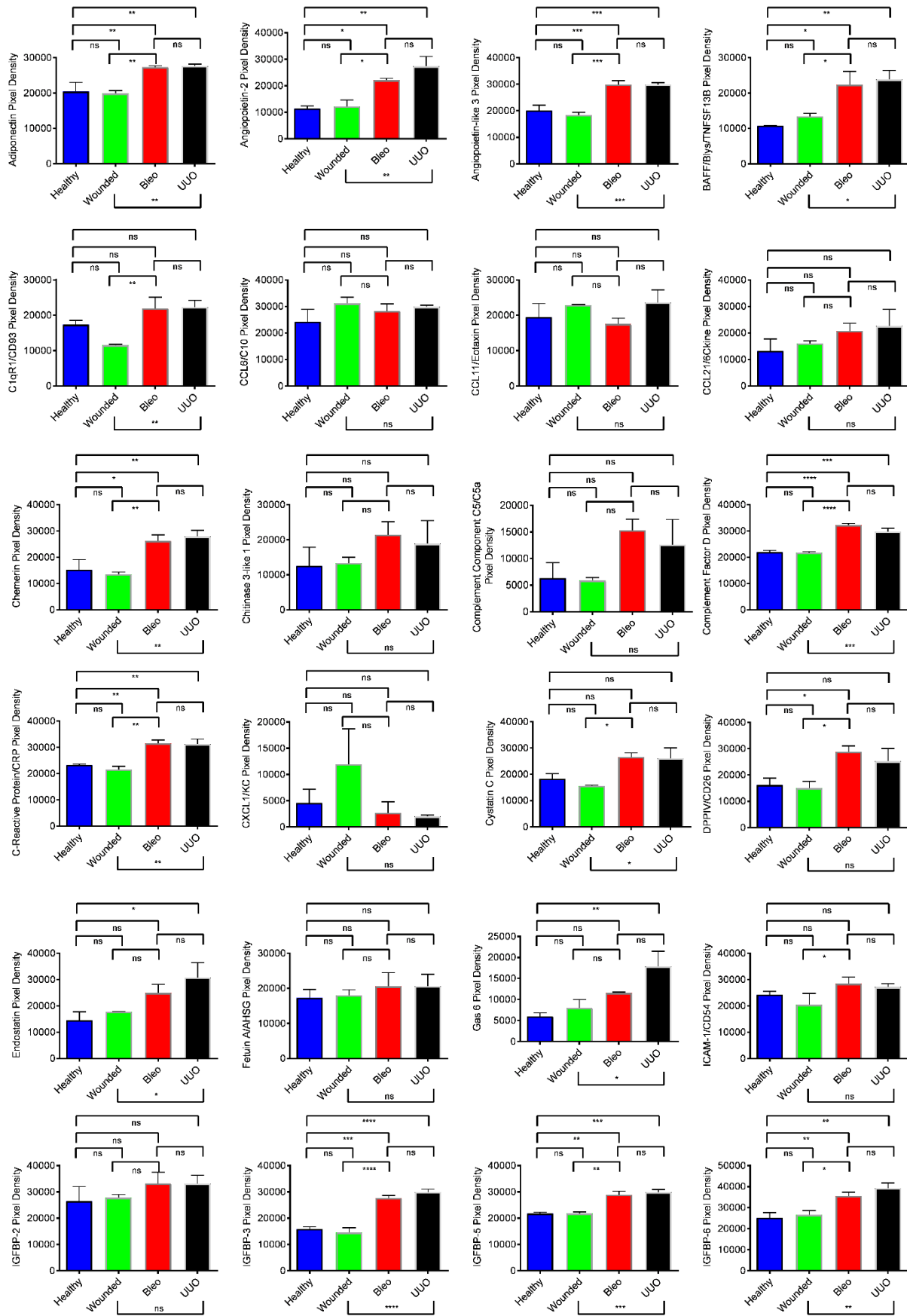


Figure 25: Vascular Adhesion Related Genes and Cytokine array in multiple models of fibrosis. A) Genes associated adhesion and tight junctions compared in healthy kidneys versus fibrotic kidneys. Probes fluorescent units are shown in log scale. B) Heatmap of cytokines from serum of healthy mice, mice with a cutaneous wound at day 10, mice with lung fibrosis at day 10, and mice with kidney fibrosis at day 10. N=4 for healthy and wounded, and n=6 for fibrotic lung and fibrotic kidney.



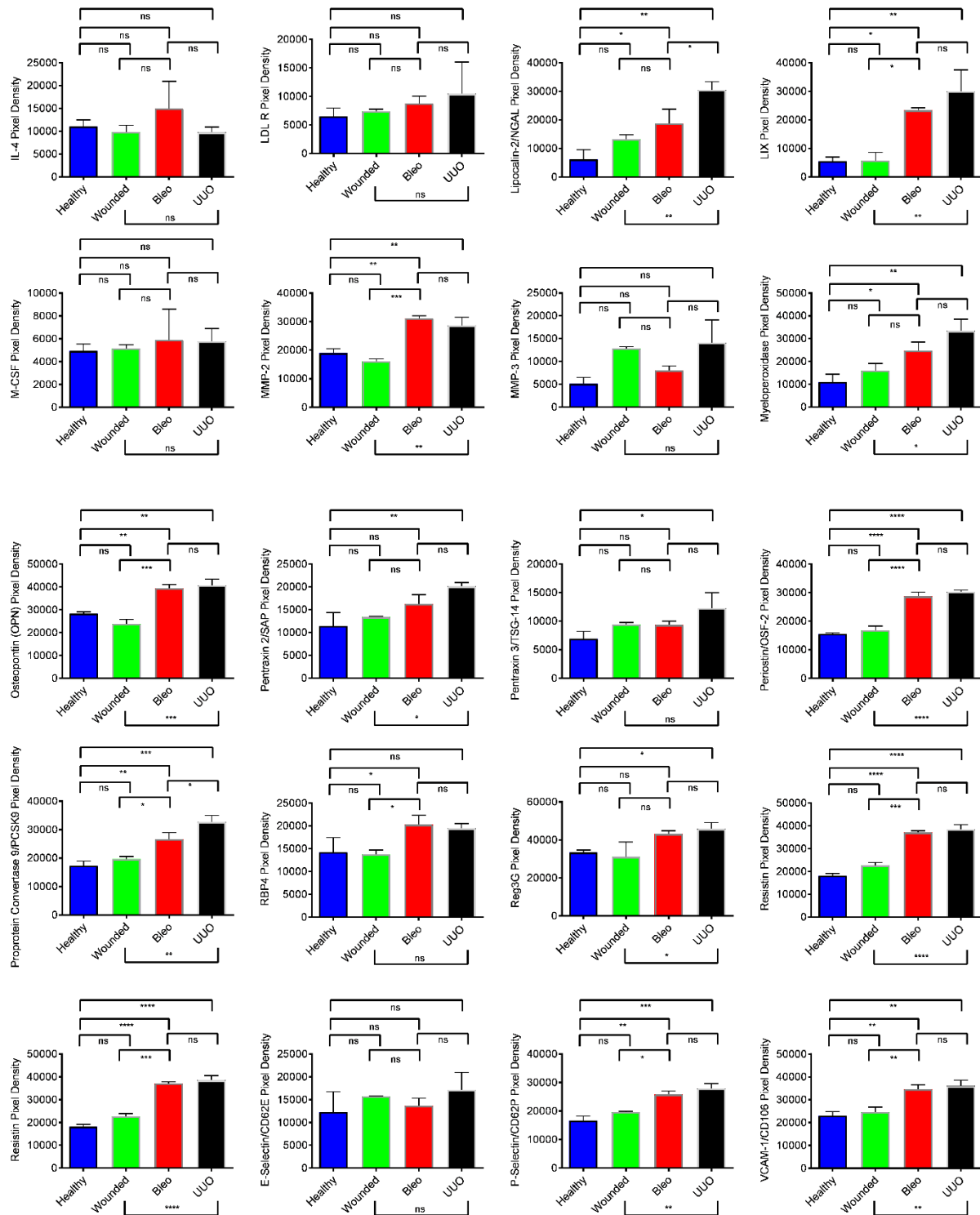


Figure 26: Quantitative Analysis of Serum Cytokine Array. The quantification of each cytokine in the cytokine array. Data are represented as the mean  $\pm$ SEM using One-Way Anova T-test for \* $p < 0.05$ , \*\* $p < 0.01$ , \*\*\*\* $p < 0.0001$ . ns, not significant.

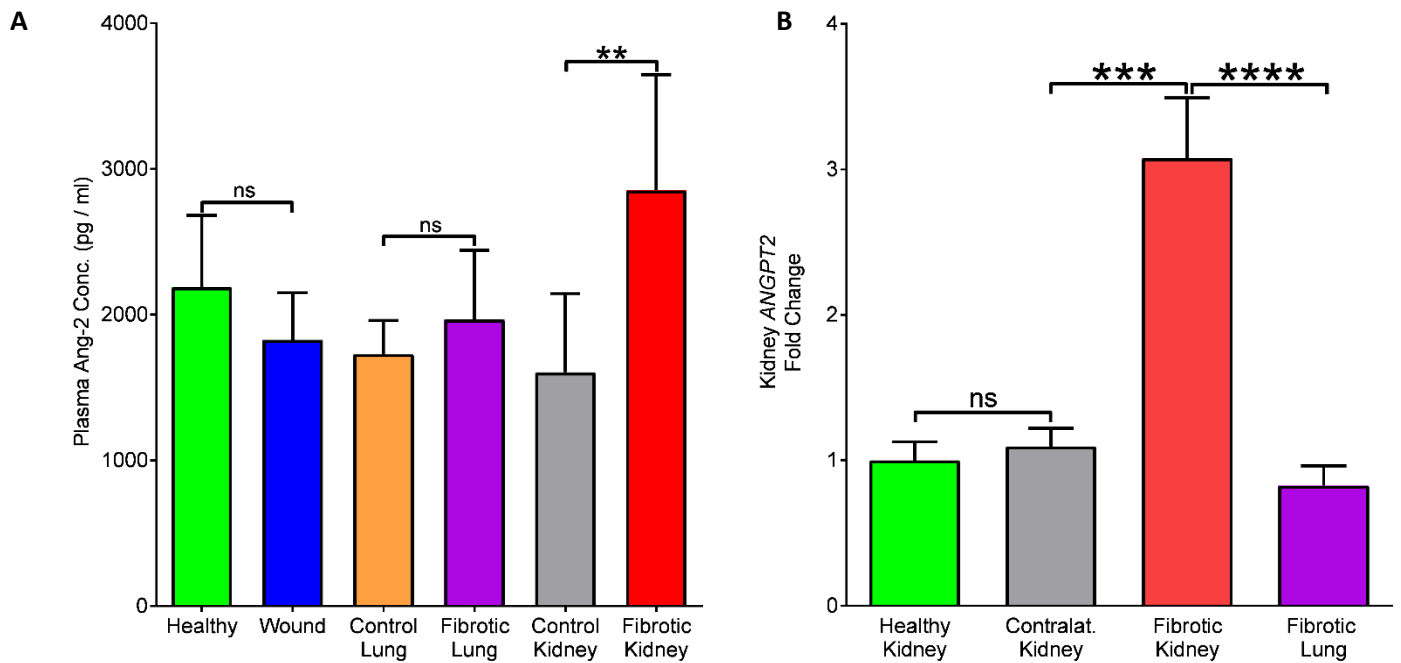


Figure 27: Increased serum and fibrotic kidney expression of Angiopoietin 2. A) Angiopoietin 2 ELISA comparing healthy, wounded, PBS treated lung, Bleomycin fibrotic lung, contralateral kidney and UUO induced fibrotic kidney serum for Angiopoietin 2. N=4 B) qPCR for Angiopoietin 2 expression in healthy kidney, contralateral kidney, UUO induced fibrotic kidney, and kidney of mice with lung fibrosis. N=3 per cohort. Data are represented as the mean  $\pm$ SEM using Student's T-test for \*p < 0.05, \*\*p < 0.01, \*\*\*\*p < 0.0001. ns, not significant.

## Chapter 6: Circulating Angiopoietin -2 alters vasculature in organ specific manner

The finding that fibrotic kidney increases circulating levels of Angiopoietin 2 led us to look into how Angiopoietin 2 might influence organ vasculature in different manners and whether this could have an effect on organotropism. This is of particular importance as elevated levels of circulating Angiopoietin 2 have been linked with multiple pathologies including diabetic retinopathy, pulmonary edema during sepsis, and a decrease in disease free survival in breast cancer patients and thus a worse prognosis.

Given that the fibrotic kidney was found to have an upregulated expression of Angiopoietin 2, but yet did not develop metastasis we hypothesized that the vascular response to Angiopoietin 2 may be different in varying organs. Given the various forms and functions of the mammalian organs it is reasonable that in addition to having physically

different endothelium (continuous, fenestrated, and sinusoidal) each different organ may respond to similar cytokines in different manners.

*Differential Vascular permeability responses in the lungs and kidneys of mice treated with Angiopoietin 2*

In order to assess the vascular permeability *in vivo* we utilized FITC labelled dextran (70,000kDa) injected into mice after two rounds of treatment with 100ug of Angiopoietin 2 intravenously. Control mice received PBS on the same day as the Angiopoietin 2 injections. The lungs and kidneys were harvested from these mice and histological analysis was performed on formalin fixed sections after antigen retrieval. By utilizing formalin fixed sections, as opposed to frozen OCT we are able to get a significantly better visualization of histological structure and thus a more precise analysis of location of FITC positivity. By counterstaining with Isolectin B4 we can visualize vasculature and differentiate between vascular spaces and parenchymal tissue. Analysis of the lungs of the mice treated with Angiopoietin 2 clearly showed an increase in FITC positivity in parenchymal spaces (**Figure 28A, B**). In comparison the lungs of the mice treated with PBS showed specific localization of FITC to within vessels in the lungs. These finding clearly indicate that elevated circulating Angiopoietin 2 induced pulmonary vascular leakage.



A

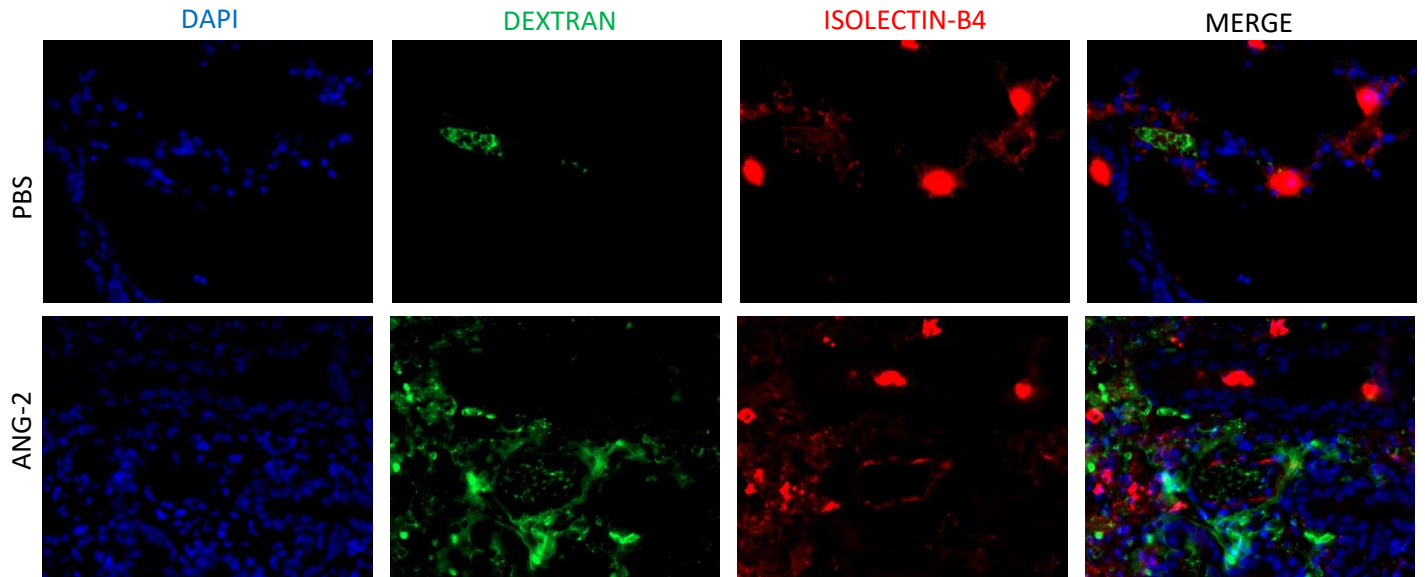
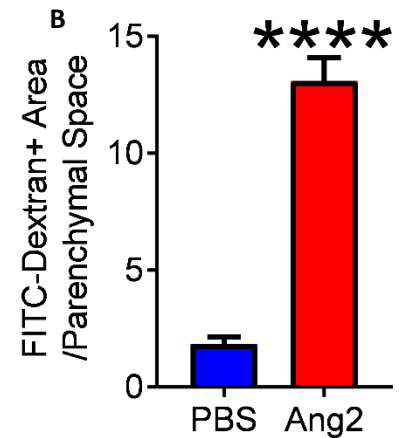


Figure 28: Increased dextran leakage in lungs of mice treated with Angiotensin 2. A) Representative immunofluorescent images of the lungs of mice treated with PBS versus Angiotensin 2 and stained for Isolectin-B4. N=5 for each cohort. B) Quantification of FITC positivity in perivascular parenchymal spaces in PBS versus Angiotensin 2 treated mice lungs. Scale bar=25um. Data are represented as the mean  $\pm$ SEM using Student's T-test for \* $p < 0.05$ , \*\* $p < 0.01$ , \*\*\*\* $p < 0.0001$ . ns, not significant.



Utilizing the same methodology, we also analyzed the effect of Angiotensin 2 on the vasculature of the kidney. In stark contrast to the increased vascular leakage found in the lungs of mice treated with Angiotensin 2, there was no difference in FITC analyzed vascular leakage of the kidney between the mice treated with Angiotensin 2 compared to the PBS treated mice. Given that the kidney consists of the cortex, outer medulla, and inner medulla, all of which have different vascular physiology we analyzed all three areas for potential vascular leakage. Yet, despite the highly vascular nature of the kidney we noted no permeability difference between PBS and Angiotensin 2 in the peritubular capillaries or the vasa recta capillaries (**Figure 29A, B**). Given that the lungs and kidneys were harvested

from the same mice we concluded that vascular endothelial response to circulating cytokines such as Angiopoietin 2 is organ specific.

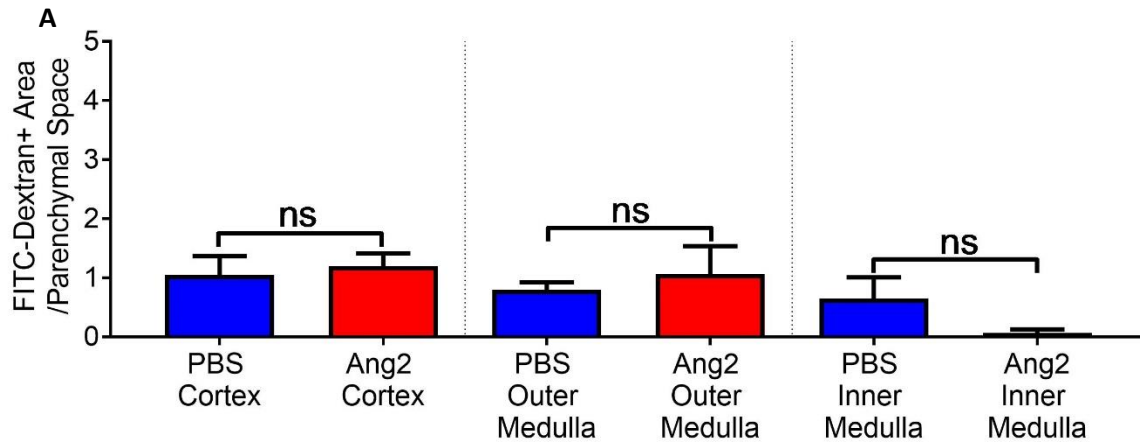
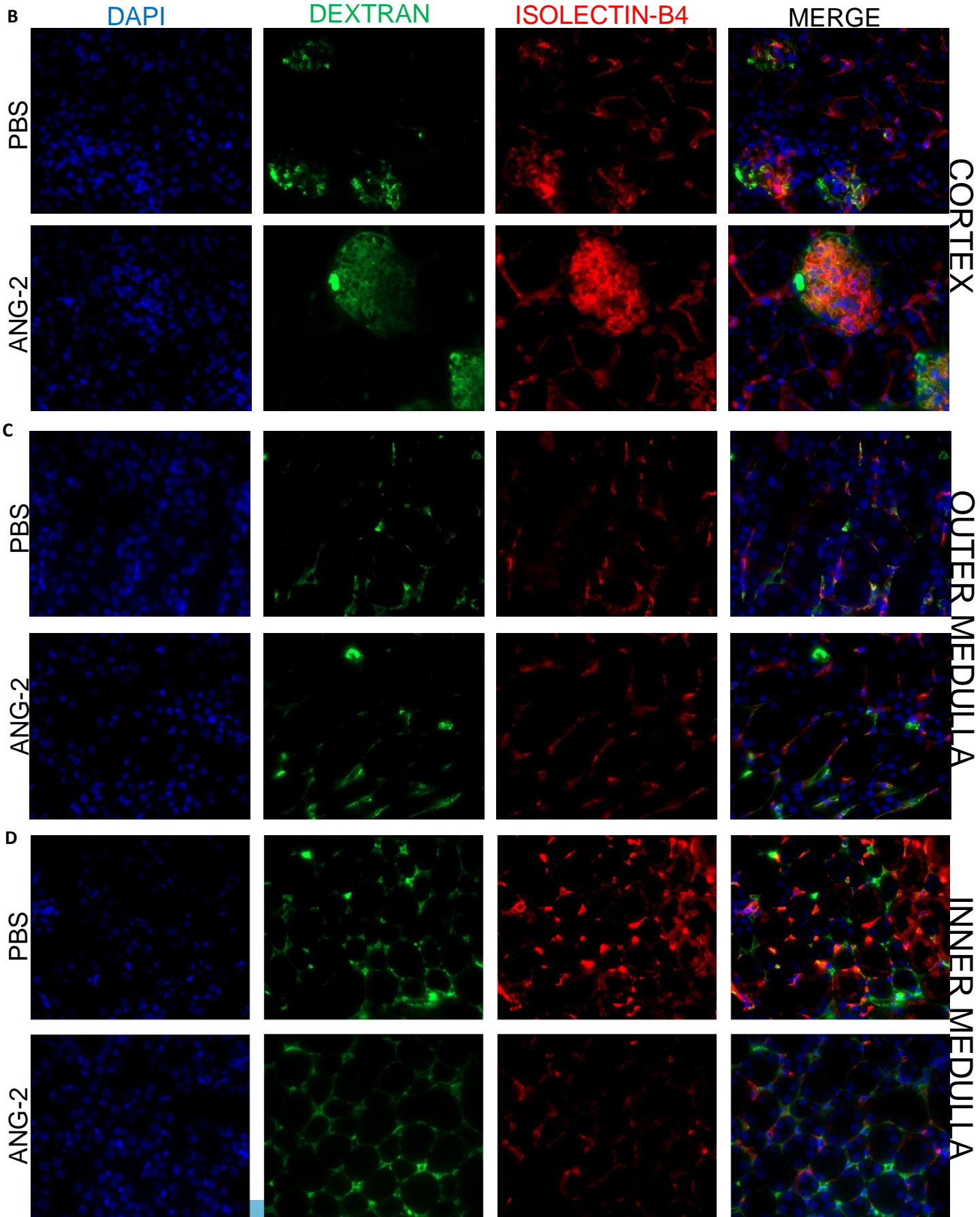


Figure 29: No dextran leakage in kidneys of mice treated with Angiopoietin 2. A) Quantification of FITC positivity in perivascular parenchymal spaces in PBS versus Angiopoietin 2 treated mice kidneys in the cortex, outer medulla and inner medulla. B) Representative immunofluorescent images of kidneys of mice treated with PBS versus Angiopoietin 2 and stained for Isolectin-B4 in the kidney cortex. C) Representative immunofluorescent images of kidneys of mice treated with PBS versus Angiopoietin 2 and stained for Isolectin-B4 in the kidney outer medulla. D) Representative immunofluorescent images of kidneys of mice treated with PBS versus Angiopoietin 2 and stained for Isolectin-B4 in the kidney inner medulla. N=5 per cohort. Scale bar=25um. Data are represented as the mean  $\pm$ SEM using Student's T-test for \* $p < 0.05$ , \*\* $p < 0.01$ , \*\*\*\* $p < 0.0001$ . ns, not significant.





To analyze the pathological vascular effects of wounds, lung fibrosis and kidney fibrosis on the lungs we performed histological analysis of the lungs from the mice with wounds, fibrotic lung or fibrotic kidneys. Edema was measured by finding the area of positive edema in both alveolar and pleural spaces. Pleural thickness was measured by measuring the thickness of the lung pleura at 8 areas in each different lung. Our analysis showed the lungs of mice with kidney fibrosis has significantly increased pulmonary edema (Figure 30B, D) and pleural thickness (Figure 30A, C).

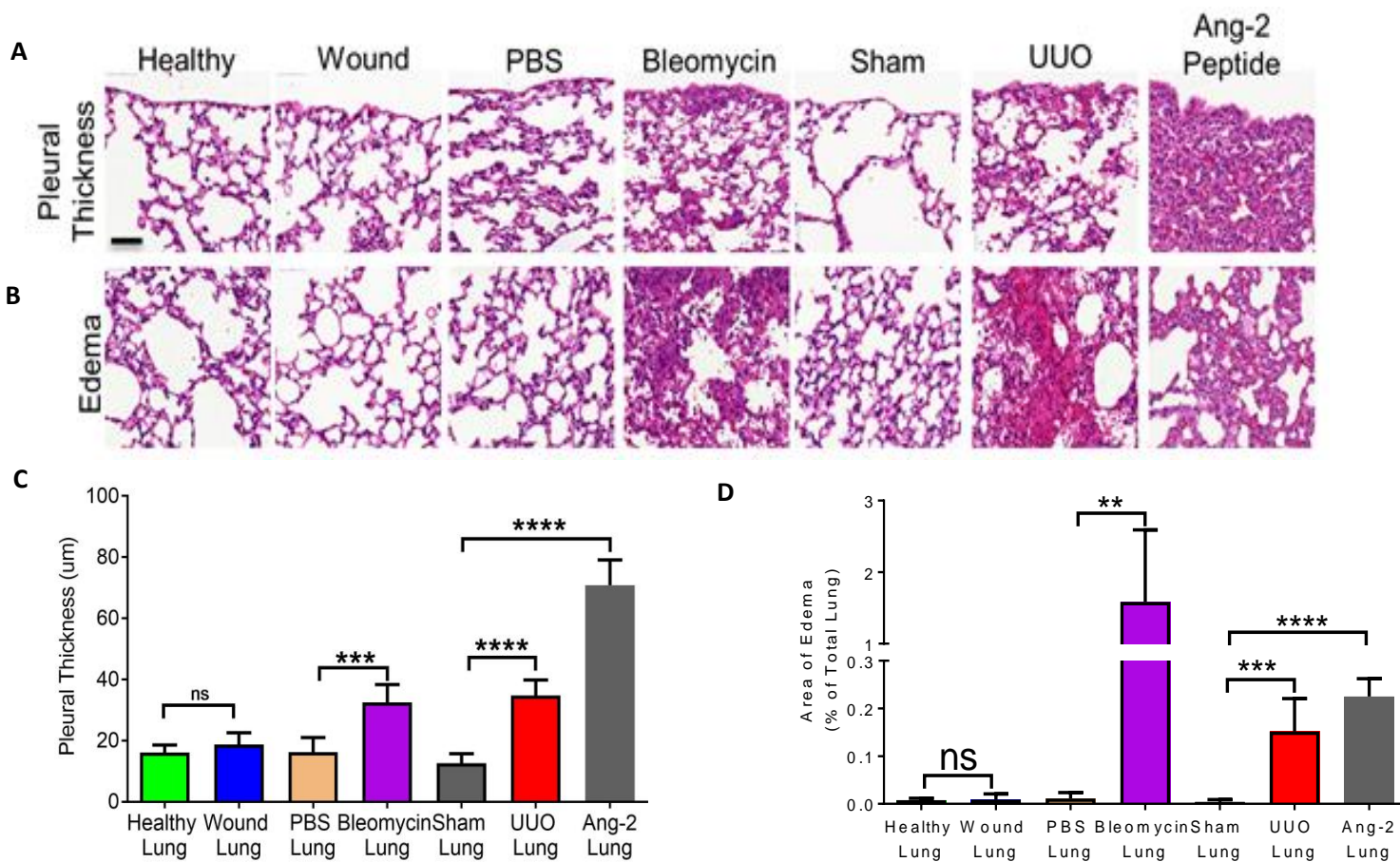


Figure 30: Increased edema and lung damage in lung fibrosis and lungs of mice with kidney fibrosis. A) Representative images of pleural thickness in the lungs of mice from each cohort. B) Representative images of alveolar and pleural edema from the lungs of mice from each cohort. C) Quantification of pleural thickness from the lungs of mice from each cohort. D) Quantification of alveolar and pleural edema from the lungs of mice from each cohort. N=6 for Healthy, wound, PBS, Bleomycin, sham, and UUO. N=3 for Angiotensin-2 cohort. Images taken at 63X. Data are represented as the mean  $\pm$  SEM using Student's T-test for \* $p < 0.05$ , \*\* $p < 0.01$ , \*\*\* $p < 0.0001$ . ns, not significant.

*Lung and kidney endothelial response to Angiopoietin 2 treatment in vitro*

Using two *in vitro* endothelial cells lines isolated from the lungs and kidneys of an SV-40 T-antigen mouse we tested the response to Angiopoietin 2 to determine if they had a differential effect. While the predominance of previous studies used HUVECs to study endothelial response *in vitro*, here we used endothelial cells isolated directly from the organs of interest. HUVECs were isolated from umbilical cord cells which are not shown to form metastatic disease, as compared to the lungs. This allowed us to compare the response of lung and kidney endothelial cells when exposed to Angiopoietin 2. By treating both cell lines with 1ug of Angiopoietin 2 we then immunofluorescently stained the cells for Phalloidin and ZO-1. Although previous publications have shown response in HUVECs as low as 400ng of Angiopoietin 2, we opted to use 1ug to ensure sufficient response of the treated cell lines. The non-treated cell lines received PBS vehicle. ZO-1 costained with Phalloidin permitted visualization of cellular borders and was additionally confirmed with bright field imaging. The visualization of the cellular borders is necessary for ZO-1 analysis as the tight junction complex is located between cells, with ZO-1 localizing to the cell membrane to bind the transmembrane proteins that form the tight junction.

Analysis of ZO-1 localization in non-treated and treated lung endothelial cells clearly indicated that after 30 minutes of Angiopoietin 2 treatment ZO-1 delocalized from the endothelial cell membrane (**Figure 31A, B**). As ZO-1 is a critical protein in the formation of the tight junction complex this indicates that lung endothelium become destabilized when exposed to Angiopoietin 2.

Furthermore, by performing western blot analysis for phosphorylated Tie-2 Tyr1108 on cells treated with Angiopoietin 2 we clearly show that while the lung endothelial cells react rapidly to the treatment, within 45 minutes to an hour they have returned to basal

levels (**Figure 31C**). This fast reaction and return response indicates that once Angiotensin 2 returns to basal levels in circulation the vasculature will rapidly stabilize. Conversely, with chronically elevated circulating Angiotensin 2 levels the vasculature will be unable to stabilize and the lung endothelium will lose functioning tight junctions. The result of which will be increased vascular permeability and increased potential for circulating tumor cells to extravasate. Furthermore, there was a direct activation and increase in pERK which coincided with the pTie2 in the lung endothelial cells treated with Angiotensin 2 (**Figure 31C**).

Upon testing kidney endothelial cells, we found that their ZO-1 did not delocalize from the membrane upon Angiotensin 2 treatment (**Figure 31D, E**), although their levels of pTie-2 responded rapidly within the first 5 minutes but decreased after that (**Figure 31F**). Furthermore, the changes in pERK observed in the lung endothelial cells did not occur in the kidney endothelial cells (**Figure 31F**). These results indicate that renal and lung endothelial cells appear to react in a dissimilar manner when exposed to Angiotensin 2. Given that we reported that *in vivo* we observed no vascular leakage in the kidneys of mice treated with Angiotensin 2, this indicates that the vasculature responds in an organ-specific manner.

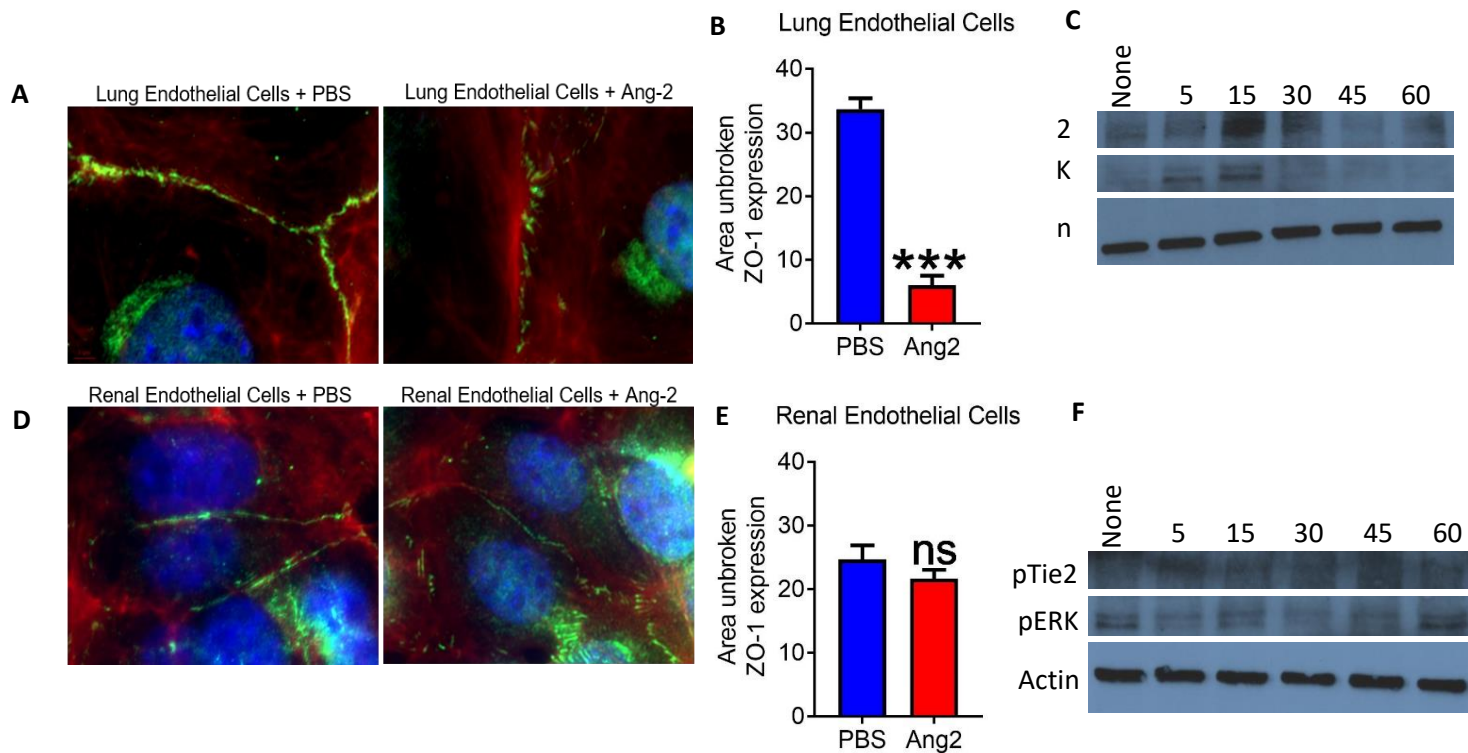


Figure 31: ZO-1 delocalized in lung endothelial cells, but not renal endothelial cells when treated with Angiotensin 2 in vitro. A) Representative images of ZO-1 expression and membrane localization in lung endothelial cells treated with PBS or Angiotensin 2. B) Quantification of ZO-1 membrane localization in lung endothelial cells treated with Angiotensin 2. N=3 C) Western blot showing phosphoTie-2 Ty 1108, and p-ERK in lung and renal endothelial cells treated with Angiotensin 2 at 5, 15, 30, 45 and 60 minutes. Actin is the control. D) Representative images of ZO-1 expression and membrane localization in renal endothelial cells treated with PBS or Angiotensin-2 E) Quantification of ZO-1 membrane localization in renal endothelial cells treated with Angiotensin 2. N=3 F) Western blot showing phosphoTie-2 Ty 1108, and p-ERK in renal endothelial cells treated with Angiotensin 2 at 5, 15, 30, 45 and 60 minutes. Scale bar=5um. Data are represented as the mean  $\pm$ SEM using Student's T-test for \* $p < 0.05$ , \*\* $p < 0.01$ , \*\*\*\* $p < 0.0001$ . ns, not significant.

### *Organ specific tight junction response to Angiopoietin 2 treatment*

As our *in vitro* results indicated that lung and kidney endothelial cells responded with a dissimilar delocalization of ZO-1 upon Angiopoietin 2 treatment, we surmised that an aspect of the vasculature must be responsible for organ-specific response to Angiopoietin 2 and the fibrotic environment. Given that capillaries are the predominant vascular structure we hypothesized that pericytes and tight junctions may respond in differential manners when endothelial cells are exposed to varying circulating cytokines. As capillaries do not possess smooth muscle and have been shown to be regulated by pericyte activity we choose to focus on the tight junction and pericyte response to fibrosis.

As fibrotic lungs enhanced metastasis, and fibrotic kidneys did not reroute metastasis, but did enhance it to the lungs we compared gene expression by Illumina array of healthy lungs versus healthy kidneys, healthy and fibrotic lungs, and healthy and fibrotic kidneys. The purpose of these comparisons was to determine how tight junction and pericyte gene expression response was differentially expressed in the healthy organs, and how the response was different in the fibrotic lung versus the fibrotic kidney. We hypothesized that gene signature differences in the fibrotic lung compared to the kidney fibrosis may be responsible for the organ specific vascular response. We also analyzed the gene expression level differences between healthy lungs and healthy kidneys to determine if either organ was more dependent on a specific tight junction. As vascular permeability is directly related the expression of tight junction proteins we analyzed the differential levels of claudins, occludin, the junction adhesion genes, the zonula occludin genes, and genes known to be associated with pericytes.

The gene expression analysis revealed significantly different organ specific responses to fibrotic insult within the fibrotic lung and kidneys. Analysis revealed that



Claudin-5 expression decreased in the fibrotic lung, while it was increased in the fibrotic kidney (**Figure 32A, B, C**). The importance of the differential changes in Claudin-5 expression were of particular interest given its role in the formation of tight junctions and that is considered a key protein in endothelial tight junction barrier formation and modulation of vessel permeability. Furthermore, we found that the expression of the Angiopoietin 2 receptor Tie 2 *TEK* gene expression in the healthy kidneys was significantly lower than in the healthy lungs (**Figure 32D**), indicating that Angiopoietin 2 would affect endothelium at different levels in the lung as compared to the kidneys. It is also possible that given the chemotactic relationship between Tie 2 and Angiopoietin 2 that the circulating cytokine moves more towards the lungs.

An analysis of the genes associated with pericytes noted no significant change in desmin in the fibrotic lungs, but a significant increase in desmin in the fibrotic kidneys (**Figure 32A**). Similarly, there was no significant change in PDGFRb in the fibrotic lungs, but an increase in the fibrotic kidneys (**Figure 32A**). Finally, there was no significant change in NG2 expression in either the fibrotic lung or the fibrotic kidneys (**Figure 32A**). Furthermore, there was a significant decrease in the expression of Endothelin-1 in the fibrotic lungs while the fibrotic kidneys showed a significant increase (**Figure 32A**). This is of interest given that Endothelin-1 is synthesized and secreted by the endothelial cells and its known receptor is expressed by pericytes. These differential responses indicate that the vasculature responds differently in each organ and there is thus a differential pericyte response.

These results indicate that pro-tumorigenic factors will illicit different responses in the lung versus the kidney vasculature. The differential response functionally results in either increased vascular permeability in the lung, or decreased vascular permeability in the kidney. In the context of breast cancer, the increase in pulmonary vascular permeability

enhances metastatic extravasation. Conversely a decrease in kidney vascular permeabilization in the presence of pro-fibrotic factors prevents the extravasation of circulating tumor cells and thus makes the kidney a rare organotropic organ in breast cancer metastasis.

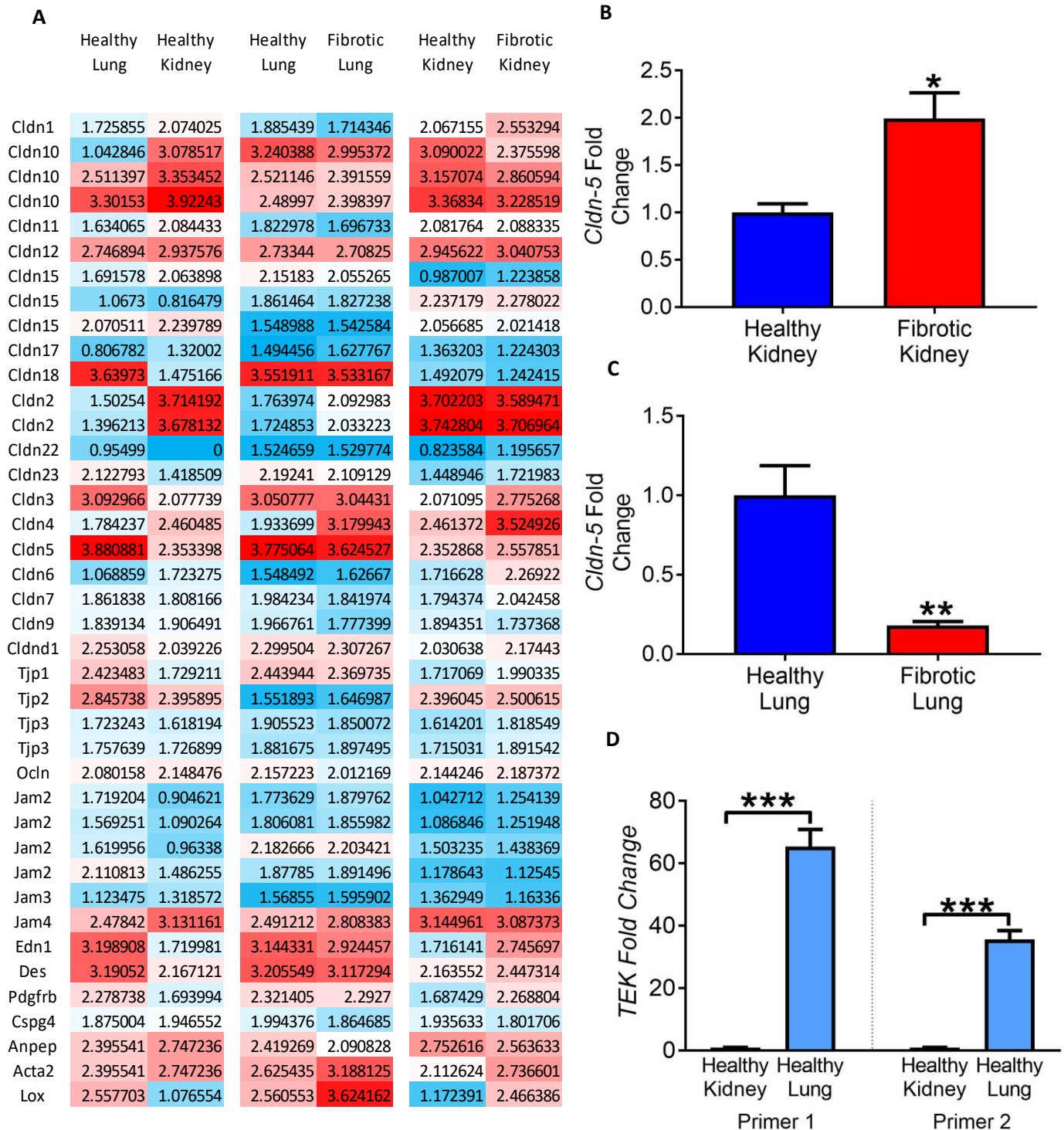


Figure 32: Lung and kidney fibrosis show different expression of tight junction proteins. A) Heatmap of probes for genes associated with tight junctions. Probes fluorescent units are shown in log scale. B) qPCR for *Cldn-5* in a healthy versus a fibrotic kidney. N=3 C) qPCR for *Cldn-5* in a healthy versus fibrotic lung. N=3. D) qPCR for *TEK* with 2 different primers sequences N=3. Data are represented as the mean  $\pm$  SEM using Student's T-test for \* $p < 0.05$ , \*\* $p < 0.01$ , \*\*\*\* $p < 0.0001$ . ns, not significant.

## Chapter 7: Anti-Angiopoietin-2 rescues the metastatic enhancement effects of kidney fibrosis

As we have identified Angiopoietin 2 as a factor secreted by the fibrotic kidney, and as it has also been implicated in other vascular related pathologies we next wanted to determine whether treatment of mice 1) with recombinant murine Angiopoietin 2 and injected intravenously with 4T1 cancer cells or 2) with Angiopoietin 2 antibody peptide that had both kidney fibrosis and breast cancer could rescue the enhanced metastatic phenotype. Mice injected with recombinant murine Angiopoietin 2 one day prior and one-day post intravenous injection with 4T1 cancer cells (**Figure 33A**) showed significant increase in colonization of the lungs (**Figure 33B, C, D**). We then utilized the orthotopic model either given control IgG or treated with the Angiopoietin 2 peptide. Mice treated with IgG had either no kidney fibrosis or kidney fibrosis, and similarly mice treated with the Angiopoietin 2 peptide had either kidney fibrosis or no kidney fibrosis. In the mice the control group treated with IgG we saw an increase in metastasis to the lungs similar to the previous phenotype in Figure 21 (**Figure 33F, G, H**). When the mice were treated with the Angiopoietin 2 peptide we saw the metastatic burden in the lungs of mice kidney fibrosis return similar levels of mice without kidney fibrosis (**Figure 33F, I, H**). These results indicate that Angiopoietin 2 was a key factor in the enhancement of metastatic spread and colonization of lungs in mice with kidney fibrosis.

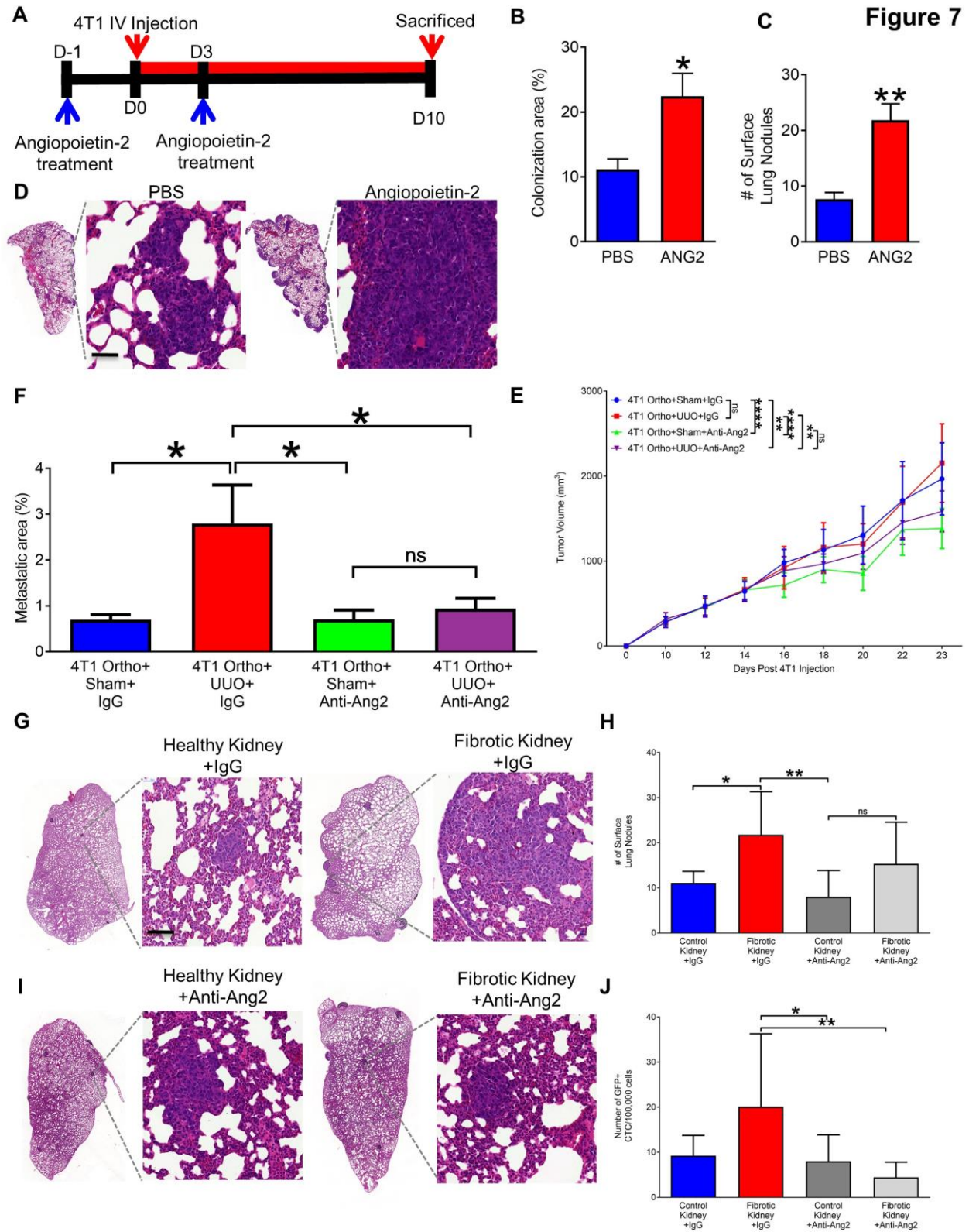


Figure 33: Anti-Angiopoietin 2 Antibody in Tumor Bearing mice with Kidney Fibrosis Reduces Lung Metastasis to Levels of Mice without Kidney Fibrosis. A) Schematic of time course treatment with recombinant murine Angiopoietin 2 and injected intravenously with 4T1 cancer cells. B) Quantification of colonization of the lungs of mice treated with PBS or recombinant murine Angiopoietin 2 and injected intravenously with 4T1 cancer cells. N=6. C) Quantification of surface lung nodules of mice treated with PBS or recombinant murine Angiopoietin 2 injected intravenously with 4T1 cancer cells. N=6. D) Representative images of the lungs of mice treated with either PBS or recombinant murine Angiopoietin 2 and injected intravenously with 4T1 cancer cells. Scale bar=25  $\mu$ m. E) Tumor volume measurements over time in orthotopic tumors with sham or UUO and either treated with IgG or anti-Angiopoietin 2. Two-way Anova with Tukey's multiple comparison test was used. F) Quantification of the metastatic area of the lungs of the indicated groups. N=8 per group. One-Way Anova was used. G) Representative images of lungs of mice with either sham or UUO treated with IgG. Scale bar=25  $\mu$ m. H) Quantification of the number of surface lung nodules in the indicated groups treated with IgG. N=8 per group. I) Representative images of lungs of mice with either sham or UUO treated with anti-Angiopoietin 2. Scale bar=25  $\mu$ m. J) Quantification of the number of surface lung nodules in the indicated groups treated with anti-Angiopoietin 2. N=8 per group. Data are represented as the mean  $\pm$ SEM using Student's T-test unless otherwise noted. \* $p < 0.05$ , \*\* $p < 0.01$ , \*\*\*\* $p < 0.0001$ . ns, not significant.

## Summary of Results

Herein we set out to determine the role of the fibrotic environment in the determination of breast cancer metastatic organotropism. By showing the significant similarities between the fibrotic lung and kidney for factors previously associated with the pre-metastatic niche and organotropism we developed a way to test the contribution of these factors on metastatic tropism. As expected the fibrotic environment in a tropic organ enhanced metastasis to that organ. However, despite previous evidence implicating the growth factors in the control of metastatic spread we did not see any metastasis to the fibrotic kidney. None the less the fibrotic kidney did enhance metastatic spread to the lungs. This led us to hypothesize that there was an alternative organ specific alteration that occurred due to the secretion of pro-tumorigenic fibrotic factors into circulation. We identified Angiopoietin 2 as a cytokine that is found to be upregulated in the circulation of fibrotic kidney disease. Previous research has also shown that Angiopoietin 2 is upregulated in patients with breast cancer and is prognostic of decreased disease free survival. By treating mice with Angiopoietin 2 we observed an organ specific vascular response leading to increased vessel permeability in the lungs, and a converse reaction in the kidneys. Further analysis revealed that there is an organ specific vascular response mediated by the expression of the tight junction protein Claudin-5. Finally, by treating tumor bearing mice that had fibrotic kidney damage with recombinant murine Angiopoietin 2 we showed that the enhanced metastatic phenotype could be enhanced, and it could be rescued by treating tumor bearing mice with kidney damage with anti-Angiopoietin 2. Together, our results show for the first time that organotropism is due to an organ specific vascular response to increased levels of circulating cytokines.



## Chapter 8: Summary and Discussion

The recognition that primary tumors have specific tropism for metastatic spread has long been an area of research (Fidler 2003) in the hopes of determining the mechanisms that control metastasis. The ultimate goal being the development of therapies aimed at treating and preventing metastasis. Given the fact that modern therapies are all but unable to treat metastatic disease and the poor prognosis associated with the diagnosis, this continues to be a high priority in cancer research. Since Virchow, Paget and Ewing (Talmadge and Fidler 2010) first began the study of metastatic disease the predominant focus of research has been to ask why cancer has tropism for specific organs. Given the failure of this approach to determine the mechanistic control of organotropism we choose to approach this issue from an alternative viewpoint. In this study we focused on not only asking why cancer spreads to the tropic organ, but also why it does not spread to non-organotropic organs. By developing a pro-tumorigenic environment in both a tropic and non-organotropic organ for two commonly used breast cancer metastasis models, we were able to elucidate the contribution that this environment plays in directing metastatic spread. This also allowed us to identify that an organ-specific vascular response to increased pro-tumorigenic cytokines may in fact be a key determining mechanism in organotropism of metastatic disease. Although it is considered common medical knowledge that organs have different structural vascular mechanics (Junqier Histology), the finding that organ-specific vasculature responds differently to the same cytokines, is a novel finding and may pave the way for the research and development of organ-specific therapies not only for cancer related diagnosis but also for organ specific pathologies.

*The Unusual Suspects; Organotropism is not determined by previously published factors complicit in the pre-metastatic niche*

While it has commonly been published that the tumor microenvironment, the pre-metastatic niche and the fibrotic environment are considered similar (Arwert, Hoste and Watt 2012), the ability of this environment to direct metastasis has not been truly tested. If these environments are all biochemically and biophysically similar, then the induction of fibrosis should enhance metastatic spread regardless of the organ of damage. Although some research has been done to show that the fibrotic environment can enhance metastasis (Erlner 2016), this has only been done in organs that are already tropic for that primary tumor. While this is relevant research, it does not fundamentally test the ability of the known pro-tumorigenic fibrotic factors to actually direct metastasis. If the fibrotic factors are the determinants of organotropism then regardless of location, when significantly upregulated, metastasis should spread to that organ. However, we clearly show here that that is not the case. This finding indicates that while these pro-tumorigenic fibrotic factors are able to enhance metastasis they are insufficient in directing organotropism. This indicates that alternative factors are the source of the mechanism of organotropism. While our model of surgically induced kidney fibrosis and chemically induced lung fibrosis do show increases in fibrotic factors it is important to note that the induction methods may elicit different fibrotic development. The surgically induced fibrosis causes an increase in shear stress in the proximal tubules due to an increase in pressure from un-excreted filtrate. This increase in continued shear stresses leads to proximal tubule damage and the chronic release of fibrotic factors ultimately leading to kidney fibrosis. While the chemical induction in the lungs is a response to the DNA damage agent bleomycin leading to an increase in epithelial cells releasing pro-fibrotic factors. It is possible that the different methods of induction elicit different responses. Nonetheless, we clearly show that the factors implicitly believed to be the controlling factors for organotropism are upregulated in both our lung and kidney fibrosis models. Given that the kidney fibrotic environment could not re-route metastasis we

concluded that alternative factors must be responsible for the control of organotropism. This result would indicate a paradigm shift as it clearly indicates that the pre-metastatic niche, that is significantly similar to the fibrotic environment is not sufficient to direct metastatic spread. While this indicates that the fibrotic factors are not responsible for directing organotropism, it does not mean that they are not responsible for the enhancement of metastasis. In fact, our findings profoundly support previous studies showing that these factors are pro-tumorigenic for metastatic enhancement.

*The seed grows where you want, you just have to put it there.*

In addition to the pre-metastatic niche being implicated in the determination of organotropism, the currently held belief for organotropism is that disseminated cancer cells only grow in specific organs based on Paget's seed and soil hypothesis. However, previous publications have shown that murine cancer cell lines that are known to be organotropic for specific organs can grow in non-organotropic organs. The key example of this would be the growth of 4T1 or B16-F1 cells in the kidneys of mice injected under hydrostatic pressure (Li and Liu 2011), and 4T1 cells directly injected into either the renal capsule or the cortex (Daniel Guimarães Tiezzi 2013). In these experiments a mammary fat pad cancer cell line that does not typically metastasize or colonize the kidney successfully grew in the kidneys. Physiologically, the only key system that is bypassed by these experiments is the vascular system. In the hydrostatic model they cause systemic vascular permeabilization by mechanistically overloading the osmotic pressure within the vessels. The direct injection models bypass the vascular system by simply being directed into the parenchymal perivascular spaces. Regardless of the method, the important point here is that these cell lines successfully grew in the kidneys when the vascular system is not an obstacle. By the

process of elimination, it is clear that the vasculature is an essential barrier to metastatic growth. However, the endothelial layer is a barrier to extravasation systemically, not just in the kidneys. In the lungs circulating cancer cells must also extravasate. Yet, under conditions where the primary tumor is grown orthotopically or injected intravenously under normal hemostatic pressures these cancer cells only grow in the lungs and other tropic organs. This indicates that the vasculature of different organs may behave differently depending on the organ. Observations supporting this is that lung fibrosis and kidney fibrosis release different levels of circulating Angiopoietin-2. While previous studies have shown that there is less Angiopoietin-2 expressed in the lungs as compared to the kidneys at basal non-pathological levels (Gale and Yancopoulos 2002), our results indicate that this is also true in the pathological state as well. Additionally, our Illumina array study comparing fibrotic lungs to healthy lungs showed that Angiopoietin 2 expression decreased significantly in the fibrotic lungs. There are many possible reasons for this and they are most likely related to the specific functions of the two organs. The lungs most likely have lower basal levels of Angiopoietin 2 as increased pulmonary vascular permeability would not be conducive to the organism as a whole and is generally restricted to tip cells in the lungs (Feltch 2012). Conversely, changes in vascular permeability in the kidneys under the control of Angiopoietin 2 might be useful for angiogenesis and also for the increased permeability of molecules required for reabsorption into circulation. Interestingly, a recent paper studying cerebral cavernous malformations found that increased levels of Angiopoietin 2 show a decrease in Claudin 5 expression in the brain (Zhou 2016). Given that breast cancer is known to metastasize to the brain, this indicates that Angiopoietin 2 has a similar vascular permeability mechanistic effect on both the lungs and brain lending further evidence to the organ specific responses to Angiopoietin 2. This further evidences a differential response to the same cytokine under similar pathological conditions. We induced fibrosis in both lung

and kidneys, and yet the lungs showed a different vascular response than did the kidneys, despite the fact that pro-tumorigenic factors were increased in both organs.

The organ-specific vascular response was further evidenced by the differences in vessel permeability as observed when mice were treated with Angiotensin 2 and FITC-Dextran and the response of the organ-specific cell lines. Similar to publications showing that increased circulating Angiotensin 2 induces pulmonary edema and increased lung vascular permeability (Parikh and Sukhatme 2006) we also noted the same, but no such change in the kidney. This was mirrored in the *in vitro* studies. When taken together with the evidence that increased expression of Angiotensin 2 is correlated with a poor disease-free prognosis in breast cancer patients, this indicates that the fibrotic cytokine Angiotensin 2 specifically causes vessel leakage in the lungs, but not in the kidneys.

While Angiotensin 2 is only one of many pro-tumorigenic cytokines released into circulation it is the observation that it elicits an organ-specific response that is most important. The next step in this area of research would be to test the vascular effects of injecting mice with pro-tumorigenic factors such as TGF $\beta$ , TNF $\alpha$  etc. Given that many of these cytokines are upregulated in the circulation of patients with tumors, it may be that the organ vascular response is what determines organotropism by vessel permeability. Taken a step further it may also be that the endothelial vessel response is specific in other mechanistic properties as well. For example, the expression of ICAM1 and VCAM1 by endothelial cells induced by the increased presence of pro-tumorigenic factors in circulation is a key mechanism for the binding of lymphocytes to endothelial cells for diapedesis. Given that we show that endothelial cells can respond differently, it is plausible that different organ endothelial cells may express different membrane receptors when exposed to pro-tumorigenic cytokines that better enable the binding of circulating tumor cells to the endothelial lumen and increase

their ability to cross into the perivascular space (Nolan 2013). Our finding also highlights the need to determine the specific cytokines that are released by differing primary tumors. If all primary tumors released the same cytokine profile, then one would surmise, based on our findings, that they would all have similar organotropism. However, it is known that that is not the case (Drandoff 2004). Therefore, we would surmise that different primary tumors, and possibly even tumors with different genetic mutations would have a different circulating cytokine profile. This differing circulating cytokine profile may therefore affect only some organs in a manner that makes them more susceptible to metastatic spread.

#### *It is all tight junctions all the time*

An area of study that is woefully under researched is the tight junctions that exist between endothelial cells. To date only Claudin-5 has been identified as a tight junction claudin involved in endothelial cells. The remaining proteins involved in the tight junctions of the endothelial cells have not been pursued in depth. Given that tight junctions are a key complex in the formation of the vascular barrier and cell-cell contacts, this is an area that requires more focus. Furthermore, similar to the claudin heterogeneity found in epithelial cells, this is likely an organ-specific difference that will be key in determining organ responses to circulating cytokines in both normal and pathological states (Nolan 2013). Given the endothelial mouse models that exist today, this area of research is more accessible than it was previously. The development of Tie-1, Tie-2, and CDH5 Cre mice tagged with a fluorescent promoter would allow the visualization and or Fluorescent Activated Cell Sorting sorting of these cells from specific organs to determine by both qPCR and protein staining the expression of the different proteins involved in tight junction complex formation (Nolan 2013). While we identified an organ-specific response for the

endothelial Claudin-5 tight junction complex, it is unlikely that this is the only claudin, or JAM implicate in the formation of endothelial tight junctions. Identification of the proteins that are differently required in each organ will open the door for possible organ-specific therapies. A good example of this would be with the blood-brain barrier. The main issue behind treating cerebral pathologies is that the blood-brain barrier is often impenetrable by drugs injected intravenously. The determination of the specific tight junction proteins involved in this barrier may allow for the momentary increase in cerebral vessel permeability with co-treatment of drugs typically unable to cross the blood-brain barrier. This will also allow for the development of new therapies and determination of adverse effects. For example, in the mice we treated with anti-Angiopoietin 2 we noted that there was a decrease in metastatic lung disease. Given our research into the kidney we could hypothesize that there would be limited to no negative renal effects. Given that currently there are trials for anti-Angiopoietin 2 therapy for cancer patients, this is an important finding.

In addition to cancer, this also holds vital findings for other systemic pathologies. As previously mentioned, patients with sepsis are commonly affected by pulmonary issues, including but not limited to pulmonary edema. Basic science research has linked this to excess Angiopoietin 2 in circulation. Furthermore, a less well studied pathology known as uremic lung also results in both alveolar and pleural pulmonary edema. Uremic lung occurs in patients who have either acute or chronic renal damage. It was noted that in the 1940s, during World War II, patients with kidney damage often required ventilators due to breathing issues. This was originally believed to be related to hypervolemia, and thought to resolve with the advent of dialysis. However, this was not the case and uremic lung still possess an issue for patients with renal damage today. In both these cases, the excess of circulating Angiopoietin 2 occurred in an unrelated organ and yet significantly adversely affected the



lungs. By focusing research on which cytokines affect which organs in what specific manners we can begin to develop focused therapies to combat organ specific disease.

### *Multiple factors affecting organotropism*

While our research has shown that the previous factors implicated in the pre-metastatic niche and fibrotic environment are able to enhance metastasis, they are not able to direct organotropism as previously believed. Furthermore, we implicate the vasculature in organotropism and show that organ-specific vascular responses to circulating cytokines may illicit organ-specific responses. Our research, taken in the context of previous publications, indicates that metastatic organotropism is likely a process that is based on the following three fundamental factors:

- 1) Primary tumor releases multiple subpopulations of circulating tumors cells that have differing ability to cross organ-specific endothelial barriers.
- 2) Primary tumor releases specific cytokine signature that systemically travel through circulation but affect different organ vasculature in different manners causing organ-specific alterations in endothelial behavior making specific organs susceptible to metastasis.
- 3) Tumor secreted cytokines affect different organ environments in different manners enhancing metastatic potential.

## References

1. (2015). "Reorganized text." JAMA Otolaryngol Head Neck Surg **141**(5): 428.
2. Aird, W. C. (2012). "Endothelial cell heterogeneity." Cold Spring Harb Perspect Med **2**(1): a006429.
3. Anderson, J. M. and C. M. Van Itallie (2009). "Physiology and function of the tight junction." Cold Spring Harb Perspect Biol **1**(2): a002584.
4. Angelow, S., R. Ahlstrom and A. S. Yu (2008). "Biology of claudins." Am J Physiol Renal Physiol **295**(4): F867-876.
5. Antonio, H. M., L. R. Mandarano, A. A. Coelho, M. G. Tiezzi, J. M. Andrade and D. G. Tiezzi (2013). "Mouse renal 4T1 cell engraftment as a model to study the influence of hypoxia in breast cancer progression." Acta Cir Bras **28**(2): 142-147.
6. Appleton & Lange
7. Armulik, A., G. Genove and C. Betsholtz (2011). "Pericytes: developmental, physiological, and pathological perspectives, problems, and promises." Dev Cell **21**(2): 193-215.
8. Arshad, F., L. Wang, C. Sy, S. Avraham and H. K. Avraham (2010). "Blood-brain barrier integrity and breast cancer metastasis to the brain." Patholog Res Int **2011**: 920509.
9. Arwert, E. N., E. Hoste and F. M. Watt (2012). "Epithelial stem cells, wound healing and cancer." Nat Rev Cancer **12**(3): 170-180.
10. Aslakson, C. J. and F. R. Miller (1992). "Selective events in the metastatic process defined by analysis of the sequential dissemination of subpopulations of a mouse mammary tumor." Cancer Res **52**(6): 1399-1405.

11. Avraham, H. K., S. Jiang, Y. Fu, H. Nakshatri, H. Ovadia and S. Avraham (2014). "Angiopoietin-2 mediates blood-brain barrier impairment and colonization of triple-negative breast cancer cells in brain." J Pathol **232**(3): 369-381.
12. Balda, M. S. and J. M. Anderson (1993). "Two classes of tight junctions are revealed by ZO-1 isoforms." Am J Physiol **264**(4 Pt 1): C918-924.
13. Barton, W. A., D. Tzvetkova-Robev, E. P. Miranda, M. V. Kolev, K. R. Rajashankar, J. P. Himanen and D. B. Nikolov (2006). "Crystal structures of the Tie2 receptor ectodomain and the angiopoietin-2-Tie2 complex." Nat Struct Mol Biol **13**(6): 524-532.
14. Bauer, H., J. Zweimueller-Mayer, P. Steinbacher, A. Lametschwandtner and H. C. Bauer (2010). "The dual role of zonula occludens (ZO) proteins." J Biomed Biotechnol **2010**: 402593.
15. Bazzoni, G. and E. Dejana (2004). "Endothelial cell-to-cell junctions: molecular organization and role in vascular homeostasis." Physiol Rev **84**(3): 869-901.
16. Bleyer, A. and H. G. Welch (2012). "Effect of three decades of screening mammography on breast-cancer incidence." N Engl J Med **367**(21): 1998-2005.
17. Bogdanovic, E., V. P. Nguyen and D. J. Dumont (2006). "Activation of Tie2 by angiopoietin-1 and angiopoietin-2 results in their release and receptor internalization." J Cell Sci **119**(Pt 17): 3551-3560.
18. Bos, P. D., X. H. Zhang, C. Nadal, W. Shu, R. R. Gomis, D. X. Nguyen, A. J. Minn, M. J. van de Vijver, W. L. Gerald, J. A. Foekens and J. Massague (2009). "Genes that mediate breast cancer metastasis to the brain." Nature **459**(7249): 1005-1009.
19. Bugianesi, E., N. Leone, E. Vanni, G. Marchesini, F. Brunello, P. Carucci, A. Musso, P. De Paolis, L. Capussotti, M. Salizzoni and M. Rizzetto (2002). "Expanding the

- natural history of nonalcoholic steatohepatitis: from cryptogenic cirrhosis to hepatocellular carcinoma." Gastroenterology **123**(1): 134-140.
20. Camire, R. B., H. J. Beaulac, S. A. Brule, A. I. McGregor, E. E. Lauria and C. L. Willis (2014). "Biphasic modulation of paracellular claudin-5 expression in mouse brain endothelial cells is mediated through the phosphoinositide-3-kinase/AKT pathway." J Pharmacol Exp Ther **351**(3): 654-662.
21. Chen, W., R. Sharma, A. N. Rizzo, J. H. Siegler, J. G. Garcia and J. R. Jacobson (2014). "Role of claudin-5 in the attenuation of murine acute lung injury by simvastatin." Am J Respir Cell Mol Biol **50**(2): 328-336.
22. Chevalier, R. L., M. S. Forbes and B. A. Thornhill (2009). "Ureteral obstruction as a model of renal interstitial fibrosis and obstructive nephropathy." Kidney Int **75**(11): 1145-1152.
23. Church, D., S. Elsayed, O. Reid, B. Winston and R. Lindsay (2006). "Burn wound infections." Clin Microbiol Rev **19**(2): 403-434.
24. Cox, T. R., A. Gartland and J. T. Eler (2016). "Lysyl Oxidase, a Targetable Secreted Molecule Involved in Cancer Metastasis." Cancer Res **76**(2): 188-192.
25. Cox, T. R., D. Bird, A. M. Baker, H. E. Barker, M. W. Ho, G. Lang and J. T. Eler (2013). "LOX-mediated collagen crosslinking is responsible for fibrosis-enhanced metastasis." Cancer Res **73**(6): 1721-1732.
26. Dranoff, G. (2004). "Cytokines in cancer pathogenesis and cancer therapy." Nat Rev Cancer **4**(1): 11-22.
27. Dvorak, H. F. (2015). "Tumors: wounds that do not heal-redux." Cancer Immunol Res **3**(1): 1-11.
28. Escudero-Esparza, A., W. G. Jiang and T. A. Martin (2012). "Claudin-5 participates in the regulation of endothelial cell motility." Mol Cell Biochem **362**(1-2): 71-85.

29. Ewing, J. (1919). Neoplastic diseases : a text-book on tumors. Philadelphia, W.B. Saunders Company.
30. Fagiani, E. and G. Christofori (2013). "Angiopoietins in angiogenesis." Cancer Lett **328**(1): 18-26.
31. Felcht, M., R. Luck, A. Schering, P. Seidel, K. Srivastava, J. Hu, A. Bartol, Y. Kienast, C. Vettel, E. K. Loos, S. Kutschera, S. Bartels, S. Appak, E. Besemfelder, D. Terhardt, E. Chavakis, T. Wieland, C. Klein, M. Thomas, A. Uemura, S. Goerd and H. G. Augustin (2012). "Angiopoietin-2 differentially regulates angiogenesis through TIE2 and integrin signaling." J Clin Invest **122**(6): 1991-2005.
32. Fidler, I. J. (1970). "Metastasis: quantitative analysis of distribution and fate of tumor emboli labeled with 125 I-5-iodo-2'-deoxyuridine." J Natl Cancer Inst **45**(4): 773-782.
33. Fidler, I. J. (2003). "The pathogenesis of cancer metastasis: the 'seed and soil' hypothesis revisited." Nat Rev Cancer **3**(6): 453-458.
34. Fidler, I. J. and I. R. Hart (1982). "Biological diversity in metastatic neoplasms: origins and implications." Science **217**(4564): 998-1003.
35. Fiedler, U., M. Scharpfenecker, S. Koidl, A. Hegen, V. Grunow, J. M. Schmidt, W. Kriz, G. Thurston and H. G. Augustin (2004). "The Tie-2 ligand angiopoietin-2 is stored in and rapidly released upon stimulation from endothelial cell Weibel-Palade bodies." Blood **103**(11): 4150-4156.
36. Folkman, J. (1971). "Tumor angiogenesis: therapeutic implications." N Engl J Med **285**(21): 1182-1186.
37. Francia, G., W. Cruz-Munoz, S. Man, P. Xu and R. S. Kerbel (2011). "Mouse models of advanced spontaneous metastasis for experimental therapeutics." Nat Rev Cancer **11**(2): 135-141.

38. Frisch, S. M., M. Schaller and B. Cieply (2013). "Mechanisms that link the oncogenic epithelial-mesenchymal transition to suppression of anoikis." J Cell Sci **126**(Pt 1): 21-29.
39. Gale, N. W., G. Thurston, S. F. Hackett, R. Renard, Q. Wang, J. McClain, C. Martin, C. Witte, M. H. Witte, D. Jackson, C. Suri, P. A. Campochiaro, S. J. Wiegand and G. D. Yancopoulos (2002). "Angiopoietin-2 is required for postnatal angiogenesis and lymphatic patterning, and only the latter role is rescued by Angiopoietin-1." Dev Cell **3**(3): 411-423.
40. Gilmore, A. P. (2005). "Anoikis." Cell Death Differ **12 Suppl 2**: 1473-1477.
41. Gordon, B. L. (2010). Breast cancer recurrence and advanced disease : comprehensive expert guidance. Durham NC, Duke University Press.
42. Gray, H., Standring, S., Ellis, H., & Berkovitz, B. K. (2005). Gray's anatomy: The anatomical basis of clinical practice. Edinburgh: Elsevier Churchill Livingstone.
43. Gulubova, M. V. (2002). "Expression of cell adhesion molecules, their ligands and tumour necrosis factor alpha in the liver of patients with metastatic gastrointestinal carcinomas." Histochem J **34**(1-2): 67-77.
44. Gunasinghe, N. P., A. Wells, E. W. Thompson and H. J. Hugo (2012). "Mesenchymal-epithelial transition (MET) as a mechanism for metastatic colonisation in breast cancer." Cancer Metastasis Rev **31**(3-4): 469-478.
45. Gurtner, G. C., S. Werner, Y. Barrandon and M. T. Longaker (2008). "Wound repair and regeneration." Nature **453**(7193): 314-321.
46. Hart, I. R. and I. J. Fidler (1980). "Role of organ selectivity in the determination of metastatic patterns of B16 melanoma." Cancer Res **40**(7): 2281-2287.
47. Hertig, A. T. Angiogenesis in the early human chorion and in the primary placenta of the macaque monkey.

48. Hu, B., M. J. Jarzynka, P. Guo, Y. Imanishi, D. D. Schlaepfer and S. Y. Cheng (2006). "Angiopoietin 2 induces glioma cell invasion by stimulating matrix metalloprotease 2 expression through the alphavbeta1 integrin and focal adhesion kinase signaling pathway." Cancer Res **66**(2): 775-783.
49. Hung, C., G. Linn, Y. H. Chow, A. Kobayashi, K. Mittelsteadt, W. A. Altemeier, S. A. Gharib, L. M. Schnapp and J. S. Duffield (2013). "Role of lung pericytes and resident fibroblasts in the pathogenesis of pulmonary fibrosis." Am J Respir Crit Care Med **188**(7): 820-830.
50. Hunter, J. (2007). "A treatise on the blood, inflammation, and gun-shot wounds. 1794." Clin Orthop Relat Res **458**: 27-34.
51. Joosse, S. A., T. M. Gorges and K. Pantel (2015). "Biology, detection, and clinical implications of circulating tumor cells." EMBO Mol Med **7**(1): 1-11.
52. Junqueira, L. C. U. a., J. Carneiro and A. N. Contopoulos Basic histology. A Concise medical library for practitioner and student. Los Altos, Calif.
53. Kampfer, H., J. Pfeilschifter and S. Frank (2001). "Expressional regulation of angiopoietin-1 and -2 and the tie-1 and -2 receptor tyrosine kinases during cutaneous wound healing: a comparative study of normal and impaired repair." Lab Invest **81**(3): 361-373.
54. Kanada, M., J. Zhang, L. Yan, T. Sakurai and S. Terakawa (2014). "Endothelial cell-initiated extravasation of cancer cells visualized in zebrafish." PeerJ **2**: e688.
55. Karnati, H. K., M. Panigrahi, N. A. Shaik, N. H. Greig, S. A. Bagadi, M. A. Kamal and N. Kapalavayi (2014). "Down regulated expression of Claudin-1 and Claudin-5 and up regulation of beta-catenin: association with human glioma progression." CNS Neurol Disord Drug Targets **13**(8): 1413-1426.



56. Keskin, D., J. Kim, V. G. Cooke, C. C. Wu, H. Sugimoto, C. Gu, M. De Palma, R. Kalluri and V. S. LeBleu (2015). "Targeting vascular pericytes in hypoxic tumors increases lung metastasis via angiopoietin-2." Cell Rep **10**(7): 1066-1081.
57. Knudson, A. G. (2000). Genetic mechanisms of cancer development. *Genetics in Medicine Genet Med*, 2(1), 48-48. doi:10.1097/00125817-200001000-00019
58. Kobayashi, H., K. C. Boelte and P. C. Lin (2007). "Endothelial cell adhesion molecules and cancer progression." Curr Med Chem **14**(4): 377-386.
59. Krause, G., L. Winkler, S. L. Mueller, R. F. Haseloff, J. Piontek and I. E. Blasig (2008). "Structure and function of claudins." Biochim Biophys Acta **1778**(3): 631-645.
60. Lange Medical Books/McGraw Hill
61. Langley, R. R. and I. J. Fidler (2011). "The seed and soil hypothesis revisited--the role of tumor-stroma interactions in metastasis to different organs." Int J Cancer **128**(11): 2527-2535.
62. Langley, R. R., K. M. Ramirez, R. Z. Tsan, M. Van Arsdall, M. B. Nilsson and I. J. Fidler (2003). "Tissue-specific microvascular endothelial cell lines from H-2K(b)-tsA58 mice for studies of angiogenesis and metastasis." Cancer Res **63**(11): 2971-2976.
63. Li, J. and M. R. King (2012). "Adhesion receptors as therapeutic targets for circulating tumor cells." Front Oncol **2**: 79.
64. Li, J., Q. Yao and D. Liu (2011). "Hydrodynamic cell delivery for simultaneous establishment of tumor growth in mouse lung, liver and kidney." Cancer Biol Ther **12**(8): 737-741.
65. Liu, D. and P. J. Hornsby (2007). "Fibroblast stimulation of blood vessel development and cancer cell invasion in a subrenal capsule xenograft model: stress-induced premature senescence does not increase effect." Neoplasia **9**(5): 418-426.

66. Lorusso, G. and C. Ruegg (2012). "New insights into the mechanisms of organ-specific breast cancer metastasis." Semin Cancer Biol **22**(3): 226-233.
67. Lye, M. F., A. S. Fanning, Y. Su, J. M. Anderson and A. Lavie (2010). "Insights into regulated ligand binding sites from the structure of ZO-1 Src homology 3-guanylate kinase module." J Biol Chem **285**(18): 13907-13917.
68. M. S. Balda, J. M. Anderson 1993 Two classes of tight junctions are revealed by ZO-1 isoforms American Journal of Physiology - Cell Physiology Apr, 264 (4) C918-C924
69. Marusyk, A. and K. Polyak (2010). "Tumor heterogeneity: causes and consequences." Biochim Biophys Acta **1805**(1): 105-117.
70. McGraw Hill: 11 volumes.
71. Mehlen, P. and A. Puisieux (2006). "Metastasis: a question of life or death." Nat Rev Cancer **6**(6): 449-458.
72. Mishiro, K., M. Ishiguro, Y. Suzuki, K. Tsuruma, M. Shimazawa and H. Hara (2013). "Tissue plasminogen activator prevents restoration of tight junction proteins through upregulation of angiopoietin-2." Curr Neurovasc Res **10**(1): 39-48.
73. Moeller, A., S. E. Gilpin, K. Ask, G. Cox, D. Cook, J. Gauldie, P. J. Margetts, L. Farkas, J. Dobranowski, C. Boylan, P. M. O'Byrne, R. M. Strieter and M. Kolb (2009). "Circulating fibrocytes are an indicator of poor prognosis in idiopathic pulmonary fibrosis." Am J Respir Crit Care Med **179**(7): 588-594.
74. Morita, K., H. Sasaki, M. Furuse and S. Tsukita (1999). "Endothelial claudin: claudin-5/TMVCF constitutes tight junction strands in endothelial cells." J Cell Biol **147**(1): 185-194.
75. National Cancer Institute. About Cancer. (n.d.). Retrieved August 07, 2016, from <http://www.cancer.gov/about-cancer>

76. Netland, P. A. and B. R. Zetter (1985). "Metastatic potential of B16 melanoma cells after in vitro selection for organ-specific adherence." J Cell Biol **101**(3): 720-724.
77. New York, Lange Medical Publications
78. Nishida, N., H. Yano, T. Nishida, T. Kamura and M. Kojiro (2006). "Angiogenesis in cancer." Vasc Health Risk Manag **2**(3): 213-219.
79. Noble, M. (1999). "Production and growth of conditionally immortal cell lines from the H-2KbtsA58 transgenic mouse." Methods Mol Biol **97**: 139-158.
80. Norwalk, Conn.
81. Nowell, P. C. (1976). "The clonal evolution of tumor cell populations." Science **194**(4260): 23-28.
82. Ohta, H., S. Chiba, M. Ebina, M. Furuse and T. Nukiwa (2012). "Altered expression of tight junction molecules in alveolar septa in lung injury and fibrosis." Am J Physiol Lung Cell Mol Physiol **302**(2): L193-205.
83. Ouban, A., & Ahmed, A. (2012). The Claudins family: Structure and function in normal and pathologic conditions. Atlas of Genetics and Cytogenetics in Oncology and Haematology, (12). doi:10.4267/2042/48373
84. Paget, S. (1989). "The distribution of secondary growths in cancer of the breast. 1889." Cancer Metastasis Rev **8**(2): 98-101.
85. Parikh, S. M., T. Mammoto, A. Schultz, H. T. Yuan, D. Christiani, S. A. Karumanchi and V. P. Sukhatme (2006). "Excess circulating angiopoietin-2 may contribute to pulmonary vascular leak in sepsis in humans." PLoS Med **3**(3): e46.
86. Peinado, H., S. Lavotshkin and D. Lyden (2011). "The secreted factors responsible for pre-metastatic niche formation: old sayings and new thoughts." Semin Cancer Biol **21**(2): 139-146.

87. Pepper, J. W., C. Scott Findlay, R. Kassen, S. L. Spencer and C. C. Maley (2009). "Cancer research meets evolutionary biology." Evol Appl **2**(1): 62-70.
88. Polosukhin, V. V., A. L. Degryse, D. C. Newcomb, B. R. Jones, L. B. Ware, J. W. Lee, J. E. Loyd, T. S. Blackwell and W. E. Lawson (2012). "Intratracheal bleomycin causes airway remodeling and airflow obstruction in mice." Exp Lung Res **38**(3): 135-146.
89. Psaila, B., R. N. Kaplan, E. R. Port and D. Lyden (2006). "Priming the 'soil' for breast cancer metastasis: the pre-metastatic niche." Breast Dis **26**: 65-74.
90. Pulaski, B. A. and S. Ostrand-Rosenberg (2001). "Mouse 4T1 breast tumor model." Curr Protoc Immunol **Chapter 20**: Unit 20 22.
91. Ramakrishna, R. and R. Rostomily (2013). "Seed, soil, and beyond: The basic biology of brain metastasis." Surg Neurol Int **4**(Suppl 4): S256-264.
92. Reymond, N., B. B. d'Agua and A. J. Ridley (2013). "Crossing the endothelial barrier during metastasis." Nat Rev Cancer **13**(12): 858-870.
93. Rock, J. R., C. E. Barkauskas, M. J. Cronic, Y. Xue, J. R. Harris, J. Liang, P. W. Noble and B. L. Hogan (2011). "Multiple stromal populations contribute to pulmonary fibrosis without evidence for epithelial to mesenchymal transition." Proc Natl Acad Sci U S A **108**(52): E1475-1483.
94. Rondaij, M. G., R. Bierings, A. Kragt, J. A. van Mourik and J. Voorberg (2006). "Dynamics and plasticity of Weibel-Palade bodies in endothelial cells." Arterioscler Thromb Vasc Biol **26**(5): 1002-1007.
95. Shibue, T. and R. A. Weinberg (2011). "Metastatic colonization: settlement, adaptation and propagation of tumor cells in a foreign tissue environment." Semin Cancer Biol **21**(2): 99-106.

96. Siemann, D. W. (2011). "The unique characteristics of tumor vasculature and preclinical evidence for its selective disruption by Tumor-Vascular Disrupting Agents." Cancer Treat Rev **37**(1): 63-74.
97. Srivastava, K., J. Hu, C. Korn, S. Savant, M. Teichert, S. S. Kapel, M. Jugold, E. Besemfelder, M. Thomas, M. Pasparakis and H. G. Augustin (2014). "Postsurgical adjuvant tumor therapy by combining anti-angiopoietin-2 and metronomic chemotherapy limits metastatic growth." Cancer Cell **26**(6): 880-895.
98. Steed, E., M. S. Balda and K. Matter (2010). "Dynamics and functions of tight junctions." Trends Cell Biol **20**(3): 142-149.
99. Stoletov, K., H. Kato, E. Zardoujian, J. Kelber, J. Yang, S. Shattil and R. Klemke (2010). "Visualizing extravasation dynamics of metastatic tumor cells." J Cell Sci **123**(Pt 13): 2332-2341.
100. Syrjala, S. O., R. Tuuminen, A. I. Nykanen, A. Raissadati, A. Dashkevich, M. A. Keranen, R. Arnaudova, R. Krebs, C. C. Leow, P. Saharinen, K. Alitalo and K. B. Lemstrom (2014). "Angiopoietin-2 inhibition prevents transplant ischemia-reperfusion injury and chronic rejection in rat cardiac allografts." Am J Transplant **14**(5): 1096-1108.
101. Talmadge, J. E. and I. J. Fidler (2010). "AACR centennial series: the biology of cancer metastasis: historical perspective." Cancer Res **70**(14): 5649-5669.
102. Talmadge, J. E., S. R. Wolman and I. J. Fidler (1982). "Evidence for the clonal origin of spontaneous metastases." Science **217**(4557): 361-363.
103. Tornavaca, O., M. Chia, N. Dufton, L. O. Almagro, D. E. Conway, A. M. Randi, M. A. Schwartz, K. Matter and M. S. Balda (2015). "ZO-1 controls endothelial adherens junctions, cell-cell tension, angiogenesis, and barrier formation." J Cell Biol **208**(6): 821-838.

104. Valentijn, K. M., J. E. Sadler, J. A. Valentijn, J. Voorberg and J. Eikenboom (2011). "Functional architecture of Weibel-Palade bodies." Blood **117**(19): 5033-5043.
105. Van Itallie, C. M. and J. M. Anderson (2014). "Architecture of tight junctions and principles of molecular composition." Semin Cell Dev Biol **36**: 157-165.
106. Weiss, N., F. Miller, S. Cazaubon and P. O. Couraud (2009). "The blood-brain barrier in brain homeostasis and neurological diseases." Biochim Biophys Acta **1788**(4): 842-857.
107. Winkler, E. A., R. D. Bell and B. V. Zlokovic (2011). "Central nervous system pericytes in health and disease." Nat Neurosci **14**(11): 1398-1405.
108. Wittchen, E. S. (2009). "Endothelial signaling in paracellular and transcellular leukocyte transmigration." Front Biosci (Landmark Ed) **14**: 2522-2545.
109. Wohlfart, S., S. Gelperina and J. Kreuter (2012). "Transport of drugs across the blood-brain barrier by nanoparticles." J Control Release **161**(2): 264-273.
110. Yu, A. S., K. M. McCarthy, S. A. Francis, J. M. McCormack, J. Lai, R. A. Rogers, R. D. Lynch and E. E. Schneeberger (2005). "Knockdown of occludin expression leads to diverse phenotypic alterations in epithelial cells." Am J Physiol Cell Physiol **288**(6): C1231-1241.
111. Zeisberg, M. and E. G. Neilson (2009). "Biomarkers for epithelial-mesenchymal transitions." J Clin Invest **119**(6): 1429-1437.
112. Zihni, C., C. Mills, K. Matter and M. S. Balda (2016). "Tight junctions: from simple barriers to multifunctional molecular gates." Nat Rev Mol Cell Biol **17**(9): 564-580.

**Vita**

Eliot Sananikone Fletcher was born in Sydney, Australia on May 29<sup>th</sup>, 1983 to Dr. Roland Fletcher and Ouma Sananikone. After completing Cranbrook High School he moved to Boston in 2001 and completed a Bachelors in Medical Anthropology. He then went on to complete two master degrees at Boston University in Healthy Law and International Health. After completion of the masters degrees Eliot worked for Children's Hospital Boston coordinating studies on the genetics of Thalassemia. He then began working for Dr. Ronald DePinho as a laboratory technician. In 2012 he entered The University of Texas Graduate School of Biomedical Sciences at Houston.

Permanent address:

19 Beach St. PH

New York, NY

10013